

AN INVESTIGATION OF THE EARLY ORBITS
IN THE UNIVERSITY OF MANITOBA CYCLOTRON

A Thesis
Submitted to the Faculty of Graduate Studies
University of Manitoba

In Partial Fulfillment
of the Requirements for the Degree
Master of Science

by
John A. Fannon April 1963



PREFACE

The work to be described was carried out at the University of Manitoba in the months between September, 1962 and April, 1963.

I am indebted to Dr. K. G. Standing for many helpful discussions and for his interest and direction during these past months. I would like to express my sincere thanks.

I would also like to thank Dr. B. G. Whitmore for laboratory facilities at the University here, and the University Authorities for providing me with a Graduate Fellowship.

Finally I am grateful to Mr. T. J. White of the Engineering Department for his assistance with the computer work.

TABLE OF CONTENTS

Preface	ii
Abstract	v
<u>1. General Introduction</u>	1
<u>2. Radial Instability in a Non-uniform Electric Field</u>	
2.1. Introduction	8
2.2. Motion of the Virtual Centre of Curvature	10
2.3. Instability in the Electric Field	17
2.4. Magnitude of the Drift	29
2.5. Treatment of Phase	33
2.6. An example	39
2.7. Summary	42
<u>3. Radial Instability in a Magnetic Flutter Field</u>	
3.1. Introduction	43
3.2. Two-Sector Flutter Field	46
3.3. A Vectorial Approach	51
3.4. Second Harmonic Flutter Field (Two Hills and Two Valleys)	55
3.5. Orbits of Large Radius	58
3.6. Conditions for Stability	62
3.7. Addendum	71

<u>4. The Vertical Motion</u>	
4.1. Introduction	72
4.2. The Wilson Region	77
4.3. The Rose-Cohen Region	77
4.4. Axial Focussing at Larger Radii	91
4.5. Use of Grids	96
4.6. Electric Field at a Grid Slit	98
4.7. Transition Effects - Grid to No Grid	104
<u>5. Computer Program and Results</u>	
5.1. Introduction	109
5.2. The Computer Program	109
5.3. Results for Uniform Magnetic Field	112
5.4. Magnetic Flutter Field Calculation	119
5.5. Results with the Magnetic Flutter Field Present	120
<u>Conclusions</u>	123
<u>References</u>	127

ABSTRACT

The non-uniform electric field in the University of Manitoba Cyclotron gives rise to a radial instability during the first few revolutions of the ion beam. A simple theory has been developed to investigate this instability in terms of the drift of orbit centres of the ions in the beam. It has been found that the addition of a second harmonic magnetic flutter field diminishes the drift of orbit centres. If the flutter field is given a suitable radial variation, the maximum strength required to eliminate the drift is shown to be about 1500 gauss.

The effect of the non-uniform electric field on the axial motion of the ion beam has also been examined. It is found that very few modifications need be made in the conclusions of Rose, Cohen and Wilson for a conventional cyclotron.

The behavior of the ion beam at grids inserted in the dee openings has been studied in the light of the theory developed earlier. It has been found that there can be a certain amount of radial defocussing at the grid slits and in the region where the grid ends. Methods for reducing this defocussing have been discussed.

To my Parents.

CHAPTER I
GENERAL INTRODUCTION

The idea of using an azimuthally dependent magnetic field to produce axial focussing in the cyclotron, was first put forward by L. H. Thomas⁽¹⁾ in 1938. However, it was not until twelve years later that the implications were fully realized.* In 1958, the first full scale cyclotron embodying Thomas' principles was built at Delft and, since then, a number of such machines have been completed and are now in operation. The machines have been given the name 'Sector-focussed Cyclotrons' because the azimuthal field variation, or "flutter", is put into the cyclotron in the form of sectors of alternately high and low magnetic field intensity. The regions of high intensity are called hills, regions of low intensity are called valleys. (Fig. 1)

Thomas was able to show that if the magnetic field were given an azimuthal dependence, axial focussing of the ion beam would be produced. Later it was shown by Kerst and Laslett that if the flutter field were given a spiral characteristic, (Fig. 2) two more focussing effects come into play. A detailed treatment of these azimuthal focussing forces can be found in any good book on cyclotrons⁽²⁾. Suffice to say that these forces are independent of any radial gradient of the magnetic field.

In the simple theory of the cyclotron, the angular velocity $w = v/r$ of the ions is given by

*when an electron model was constructed at Berkeley.

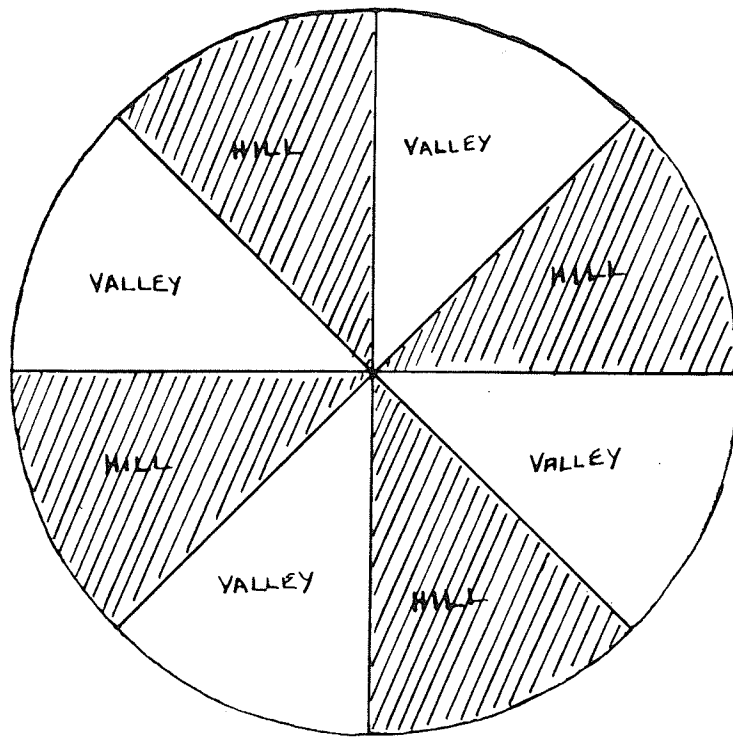


Fig. 1. Four sector Magnetic Flutter Field (Radial Ridge)
Diagram shows top view of the pole face.

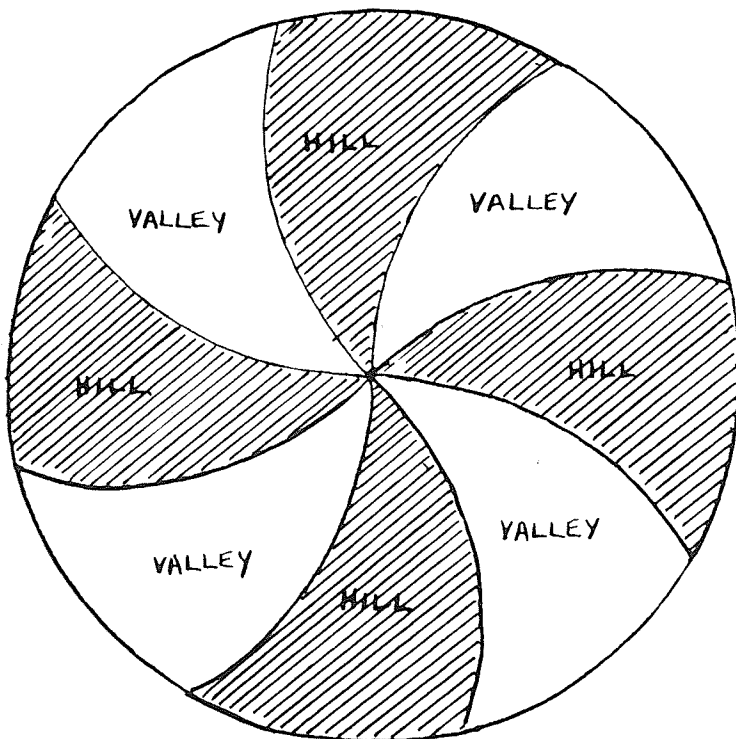


Fig. 2. Four sector Magnetic Flutter Field (Spiral Ridge)
Diagram shows top view of pole face.

$$Bev = mv^2/r \quad \text{with the usual nomenclature}$$

then $\omega = Be/m$

The frequency of the accelerating system must always be equal to the angular velocity of the ion in order to remain in phase with the ion, and to ensure its continuous acceleration. It might be thought that for a constant magnetic field, the angular velocity of the ion is constant at all radii. However in practice this cannot be so in a conventional cyclotron. There are two reasons:-

a) as the energy of the ion increases, the mass of the ion increases relativistically. If ω were to be kept constant the magnetic field B would have to increase proportionally. This requirement conflicts with:-

b) the necessity to decrease the magnetic field with radius to provide axial magnetic focussing. A radially increasing magnetic field would lead to a catastrophic defocussing of the ion beam.

These conflicting requirements led to the rejection of the idea of keeping the frequency of the accelerating potential constant. Synchro-cyclotrons and synchrotrons were developed for high energy acceleration of ions. These machines have the disadvantage that they can only accelerate groups of ions, not a continuous beam.

The discovery of azimuthal focussing forces has revived the idea of continuous acceleration of ions to *higher* energies. A radially increasing magnetic field is used to compensate for the relativistic effect, while the azimuthal field variation takes care of the axial focussing. Such machines are isochronous

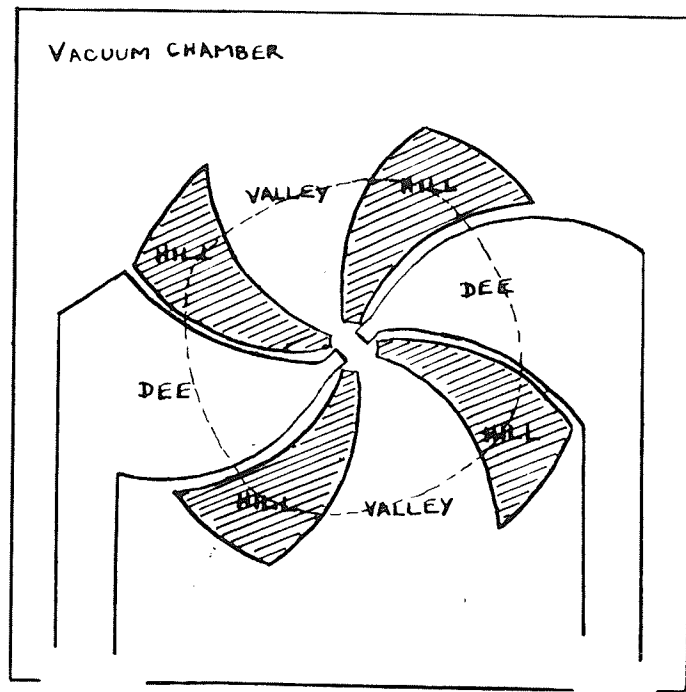


Fig 3. Median Plane of the Manitoba Cyclotron showing a Typical Orbit (dotted).

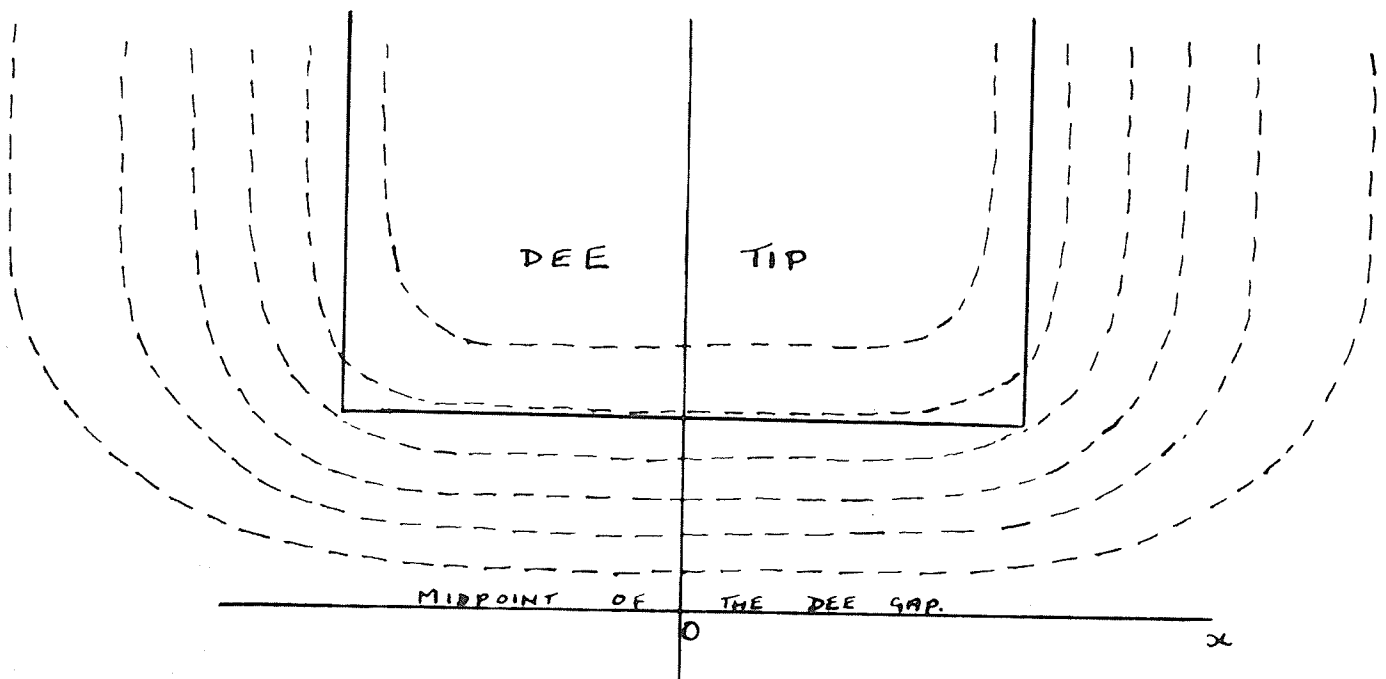


Fig 4. Equipotentials at a dee tip in the University of Manitoba Cyclotron.

as an ion performs a revolution in the same time at all energies. The frequency of the accelerating potential can now remain constant.

The cyclotron at present under construction at the University of Manitoba is designed with spiral sectors and thus utilises all three azimuthal focussing effects. The cyclotron is modelled after the machine now running at the University of California (Los Angeles)⁽³⁾, and has an unusual feature in its acceleration system - its dees are only about 45° wide instead of the more usual 180° . The reason for adopting this smaller angular width is that the dees can now be fitted nicely between the hills. (Fig. 3). The hills can thus be made much closer together, sharpening the transition from hill to valley with a consequent improvement of the axial focussing. A disadvantage is that there is a smaller energy gain per revolution, though this is offset to some extent by the fact that the dee capacitance is smaller, and the dees can carry a larger voltage for a given power.

The unorthodox dee shape does give rise, however, to a rather complicated electric field near the centre of the cyclotron. The field is shown schematically in Fig. 4. It is seen that the field is approximately uniform at small radii and also at fairly large radii where the flutter begins to become appreciable. In between, the equipotentials curl around the dee "corner" and produce an inhomogeneous field. In a conventional

cyclotron, the field at the centre is practically uniform, the only inhomogeneities which may occur are those due to a slight falling off of potential along the dee edge. These are hardly comparable to the inhomogeneities met with in the Manitoba cyclotron. The motion of ions in such fields has yet to be investigated.

It is the purpose of this thesis to describe the behavior of ions during their early revolutions in the Manitoba cyclotron. The problem naturally resolves itself into two parts, the radial and axial motion of the ions being treated separately. In the first part of the thesis, the radial motion will be discussed. It will be seen that in a non-uniform electric field there is an inherent instability which causes the centres of curvature of the orbits of ions in the field to tend to drift. The extent of the instability will be investigated and a means to repair this defect discussed. The second part of the problem involves the axial or vertical motion of the ion. The axial motion of ions in a conventional cyclotron has been well described by Wilson,⁽⁵⁾ Rose⁽⁴⁾ and Cohen⁽⁶⁾ who treated ions moving in fairly uniform electric fields. It is of prime importance to know whether or not their conclusions need be modified to include the non-uniform electric fields. The use of grids to produce extra axial focussing must be examined. It has been found that grids do provide adequate axial focussing near the cyclotron centre, but ^{sometimes} do this at the expense of radial focussing. The

extent of this defect must also be examined.

Finally, a computer program will be described with which orbits can be computed from a given set of starting conditions. This program has been used to check the conclusions drawn from the theory put forward in the earlier part of the thesis. The results of computations will be given.

CHAPTER 2

RADIAL INSTABILITY IN A NON-UNIFORM ELECTRIC FIELD

2.1 Introduction.

The problem of what happens to the ion beam in a non-uniform electric field is best approached by examining the motion of the centres of curvature of the orbits of ions in the beam. For, if a given set of ions having the same energy and phase also have their orbit centres close together, then the ions themselves are bunched together, and will tend to remain so. If the orbit centres are separated, the ions will rapidly disperse. Thus a bunching of orbit centres implies a strong ion beam.

The centre of curvature of the orbit of an ion moving in the cyclotron does not however exhibit a uniform motion in a given direction. Owing to local variations of the electric and magnetic fields, the orbit centre usually hops around quite violently. To investigate the general trend of the motion, it is necessary to consider some sort of average centre of curvature. It is found that if we average the centre of curvature over one revolution, the motion of this average centre gives a good indication of what the orbit is doing. The concept of an average centre of curvature is most useful when we are examining the results of orbit computations.

However, if we wish to investigate the motion of the centres of curvature of orbits analytically, the concept of an

average centre of curvature becomes a cumbersome one to use. It is much more convenient to talk about what shall be called a virtual centre of curvature. This is the centre of curvature of the ion orbit in a pure magnetic field B_0 which may or may not coincide with the actual field B . We can imagine it as the centre of curvature which the ion orbit would assume in the field B_0 , if the electric field were suddenly switched off.

The average centre of curvature and the virtual centre of curvature are to be regarded as complementary concepts, each useful in its own context. The virtual centre approximates quite well with the average centre, since the ion spends part of its time in a pure magnetic field inside the dees. The concept of a virtual centre of curvature becomes even more useful in the next chapter, when we shall consider the effect of a magnetic flutter field on the centre of curvature of the ion orbit.

Together with a virtual centre of curvature, we must define a virtual radius of curvature. This is the radius of curvature of the ion orbit in the pure magnetic field B_0 . For an ion moving at velocity v in the electric and magnetic fields, the virtual radius of curvature ρ is given in magnitude by the well known relation

$$B_0 e v = \frac{m v^2}{\rho}$$

or

$$\rho = \frac{v}{B_0 e / m}.$$

The direction of ρ is along the inward normal to the ion path, i.e., in the direction of $\underline{v} \times \underline{B}_0$.

So ρ is defined in magnitude and direction by the relationship

$$\rho = \frac{\underline{v} \times \underline{B}_0}{B_0^2 e/m} \dots \dots \dots .2.1.$$

2.2. Motion of the Virtual Centre of Curvature

Throughout this and the following chapter, the discussion will be confined to motion in the median plane. The axial motion of the ions is considered later. Consider an ion moving in a magnetic field \underline{B} (the actual field in the cyclotron) and velocity \underline{v} . The electric field is \underline{E} (Fig. 1) Suppose, at some instant, the ion is at a point P distance \underline{r} from some fixed origin O. The virtual centre of curvature of the orbit of the ion will be at C, a distance \underline{R} from O.

The virtual radius of curvature $\rho = \overrightarrow{PC}$ and is given by

$$\rho = \frac{\underline{v} \times \underline{B}_0}{B_0^2 e/m}$$

Now in Fig. 1, the distance of C from the origin $\overrightarrow{OC} = \underline{R}$ and is given by

$$\underline{R} = \underline{r} + \rho \dots \dots \dots .2.2.$$

Differentiating this with respect to time,

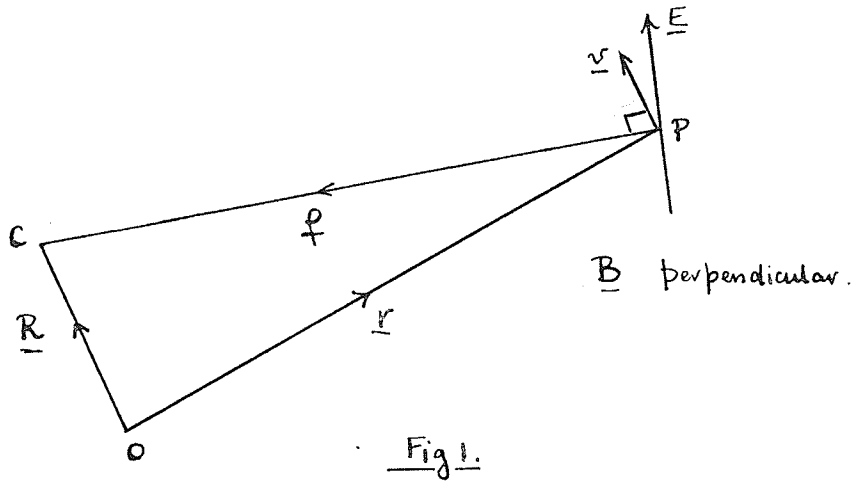
$$\begin{aligned} \frac{dR}{dt} &= \frac{dr}{dt} + \frac{d\rho}{dt} \\ &= \underline{v} + \frac{1}{B_0^2 e/m} \frac{d\underline{v}}{dt} \times \underline{B}_0 \end{aligned}$$

Since $\underline{v} = \frac{d\underline{r}}{dt}$ and \underline{B}_0 is time independent.

Now $\frac{d\underline{v}}{dt} = \underline{f}$, the acceleration of the ion in the electric and magnetic fields.

\underline{f} is given by the Lorentz relation.

$$\underline{f} = \frac{e}{m} \underline{E} + \underline{v} \times \underline{B} \frac{e}{m} \dots \dots \dots 2.3.$$



Substituting for \underline{f} ,

$$\frac{d\underline{R}}{dt} = \underline{v} + \frac{\underline{E} \times \underline{B}_0}{B_0^2} + \frac{(\underline{v} \times \underline{B}) \times \underline{B}_0}{B_0^2}$$

Now since we are considering motion in the median plane \underline{B} and \underline{B}_0 are perpendicular to \underline{v}

$$\text{Thus } (\underline{v} \times \underline{B}) \times \underline{B}_0 = -\underline{v} B B_0.$$

Finally
$$\frac{dR}{dt} = \frac{\underline{E} \times \underline{B}_0}{B_0^2} + \frac{v (B_0 - B)}{B_0} \dots \dots \dots 2.4$$

If $B = B_0$ this reduces to

$$\frac{dR}{dt} = \frac{\underline{E} \times \underline{B}_0}{B_0^2} \dots \dots \dots 2.5.$$

For a uniform magnetic field in the cyclotron, B_0 and B can be taken to be the same, i.e., in the median plane with magnetic field B_0 , the virtual radius of curvature is in a direction perpendicular to \underline{E} and of magnitude $\frac{E}{B_0}$.

For the Manitoba cyclotron E is of magnitude 2×10^6 V/m while $B \approx 2$ Wb/m². Then the speed of the virtual centre of curvature is 10^6 m/sec. In this cyclotron an ion takes about $1/50 \times 10^{-6}$ second to describe one half of a revolution. In this time, the virtual centre of curvature would move something like 2 cms.

The velocity of the virtual centre of curvature of an ion orbit thus depends on the values of the electric and magnetic field in which it is moving. However the physical significance of the formula derived is not at all clear. To bring out a better physical picture two simple examples will be given.

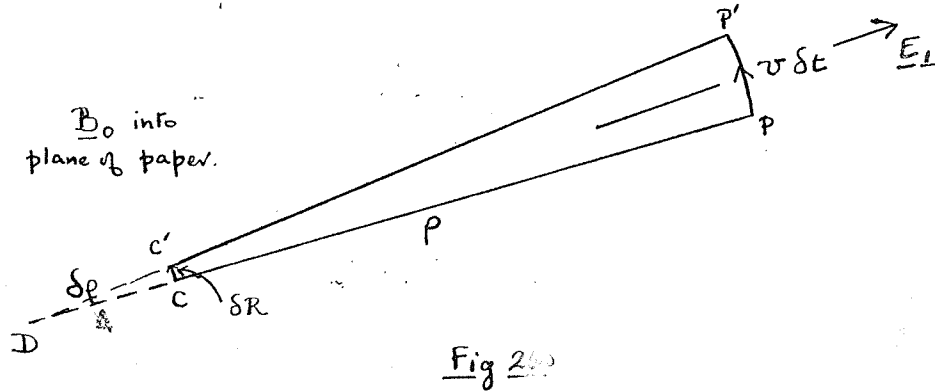
For the first example, consider the effect of an electric field \underline{E}_1 acting in the median plane in a direction normal to the path of the ion. A magnetic field B_0 is acting perpendi-

cular to the plane of motion. The electric field acting on the ion produces a force on the ion normal to the path of the ion. The magnetic field also produces a force on the ion normal to its path. The electric field E_{\perp} thus has an effect on the ion exactly equivalent to an increase or decrease of the magnetic field.

Consider an ion P moving in an orbit centre C , radius ρ at velocity \underline{v} in a uniform magnetic field \underline{B}_0 which is perpendicular to the plane of the motion. (Fig.2). Apply an electric field E_{\perp} along the outward normal to the ion path. Suppose the electric field is applied for a short time only. Consider what happens to the centre of curvature of the ion during this short time δt .

In fig. 2, the centre of curvature of the ion orbit just before the electric field is applied is at C . When the electric field is applied, the orbit centre jumps to D . During the whole time the electric field is present, the ion moves in orbit around the new centre of curvature. When finally the electric field is switched off again, the ion will be at P' , say, the orbit radius will return to its original value with the centre of curvature now at C' . The centre of curvature in the pure magnetic field (which is the virtual centre of curvature) has been moved from C to C' in time δt by the application of the electric field. The velocity at which the virtual

centre moved while the electric field was present can easily be derived.



In time δt (Fig.2) the ion moves from P to P' and the virtual centre from C to C'.

Let $CC' = \delta R$ say. If $\delta \rho$ is the increase in radius due to the electric field then

$$\frac{\delta R}{v \delta t} = \frac{\delta \rho}{\rho + \delta \rho}$$

where $\rho = CP = C'P'$ and $PP' = v \delta t$.

Now ρ is the radius of curvature before the electric field is applied.

Thus

$$B_0 e v = \frac{m v^2}{\rho}$$

$$\rho = \frac{v}{B_0 e / m}$$

When the electric field is present, the net force along the inward normal in the combined electric and magnetic fields is

$$B_0 e v - e E_{\perp} = \frac{mv^2}{\rho + \delta\rho}$$

$$\therefore \rho + \delta\rho = \frac{v}{e/mB'_0} \quad \text{where } B'_0 = B_0 - \frac{E_{\perp}}{v}$$

Thus the velocity of the virtual centre of curvature, $u_{||}$ is given by

$$\begin{aligned} u_{||} &= \frac{\delta R}{\delta t} = v \frac{v}{e/m} \left(\frac{1}{B'_0} - \frac{1}{B_0} \right) \frac{B'_0}{v} \frac{e}{m} \\ &= v \left(1 - \frac{B'_0}{B_0} \right) = \frac{v E_{\perp}}{v B_0} \end{aligned}$$

i.e.
$$u_{||} = \frac{E_{\perp}}{B_0} \dots \dots \dots 2.6.$$

a result reported by Spitzer⁽¹¹⁾.

So the velocity of the virtual centre of curvature of the ion orbit is of magnitude $\frac{E_{\perp}}{B_0}$. The direction is parallel to the ion path. This is in the direction $\underline{E}_{\perp} \times \underline{B}_0$

For the second example, consider the effect of an electric field in the median plane acting parallel to the path of the ion. Assume as before that the ion is at the point P (Fig.3) travelling with a velocity \underline{v} in a magnetic field B_0 . Suppose that an electric field $E_{||}$ is suddenly applied at P parallel to the path of the ion. The instantaneous acceleration

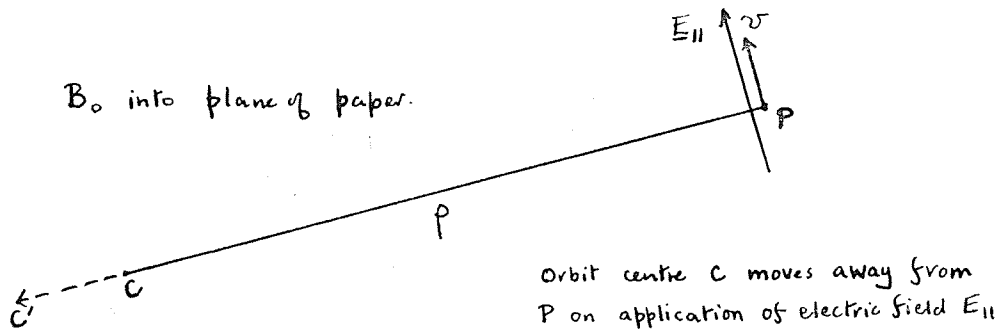


Fig 3.

of the ion parallel to its path is given by

$$f_{11} = \frac{e}{m} E_{11} \dots \dots \dots 2.7.$$

The radius of the orbit is given by $\rho = \frac{v}{B_0 e/m}$. The action of

E_{11} is to change the velocity of the ion and thus change the radius of the orbit. The centre of curvature of the orbit is ~~identical~~ with the virtual centre here as the force on the ion due to E_{11} is along the ion's path not normal to it. The velocity of the virtual centre will be equal to the rate of change of orbital radius. This may be obtained by differentiating the expression for ρ .

$$\frac{d\rho}{dt} = \frac{1}{B_0 e/m} \frac{dv}{dt}$$

But $\frac{dv}{dt} = f_{11} = \frac{e}{m} E_{11}$

So $\frac{d\rho}{dt} = \frac{E_{11}}{B_0}$

So the velocity of the virtual centre of curvature u_{\perp} is given by

$$u_{\perp} = \frac{E_{\perp 1}}{B_0} \dots \dots \dots 2.8.$$

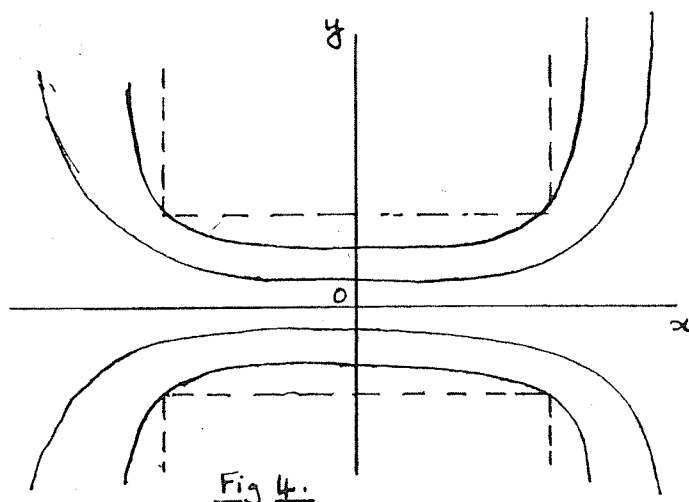
The direction of u_{\perp} is away from the ion if $E_{\perp 1}$ is such that the ion is accelerated. The direction of u_{\perp} is thus in the direction of $\underline{E} \times \underline{B}_0$ (see 11)

2.3. Instability in the Electric Field.

The action of the electric field on the ion beam in the University of Manitoba cyclotron can now be investigated. To do this, the relative motion of the virtual centres of curvature of the orbits of two ions will be considered. The ions considered have the same energy and phase and initially they are fairly close together. Typically, for a pair of ions, one at the centre of the ion beam and one at the edge, their separation might be of the order of 3-5 mm. In this and all subsequent discussion we shall use the term "orbit centre" instead of the cumbersome expression "virtual centre of curvature of the ion orbit". Unless otherwise indicated, only virtual centres of curvature will be considered.

In Fig. 4, the bold lines indicate the general shape of the equipotentials for the electric field between the tips of the dees in the University of Manitoba cyclotron. The broken lines show the dee edges. An analytic expression for the shape

of these equipotentials is too complicated to be of any use. Any calculations done on the field are best performed on a computer.



Let us set up a system of cartesian coordinate axes, taking the centre of the cyclotron O (Fig. 4) as the origin. The Ox axis is drawn parallel to the dee edge. The Oy axis is perpendicular to the Ox axis across the dee gap. The Oz axis is perpendicular to both, and points out of the plane of the paper.

For an ion moving at velocity \underline{v} through an electric field \underline{E} and in a magnetic field \underline{B}_0 , the velocity \underline{u} of the orbit centre is given by $\underline{u} = \frac{\underline{E} \times \underline{B}_0}{B_0^2}$ as derived

in the last section. Let the components of \underline{u} in the Ox, Oy directions be U_x , U_y respectively. Then, expanding the cross-product, and remembering that \underline{B}_0 points into the plane of the paper, we arrive at expressions for U_x and U_y

$$U_x = \frac{-E_y}{B_0} \qquad U_y = \frac{E_x}{B_0} \dots\dots\dots 2.9.$$

E_x , E_y are the components of the electric field in the X, Y directions.

Referring to Fig. 4 again, consider the behavior of an ion whose orbit centre is initially at the origin, O. As the ion describes a revolution, it will be moving in an electric field for some part of its path, and during the time the ion moves through the electric field, the orbit centre will have a velocity in some direction away from O. However, from the symmetry of the electric field, it can be seen that to first order, motion of the orbit centre in a given direction when the ion is at some point in its path is counteracted by motion in the opposite direction half a revolution later. For example, the velocity of the orbit centre as the ion crosses the positive Ox axis is in the direction of negative Ox. However, when the ion crosses the negative Ox axis one half revolution later, the velocity of the orbit centre is directed along the positive Ox axis. Thus to a first order approximation (neglecting the motion of the orbit centre during the revolution) it can be seen that there will be no net motion of an orbit which is centred at the origin. This is true whatever the phase of the ion, but the energy gain will be different for different phases.

Consider now an ion whose orbit centre is somewhere on

the X-axis. We will assume that the ion is in phase with the accelerating potential, off-centred orbits whose ions are out of phase with the accelerating potential will be treated later. From the symmetry of Fig. 4, it can be seen that, as the ion describes a revolution in the electric field, there is no resultant motion of the orbit centre in the Y-direction. For the Y-velocity of the orbit centre, when the ion is at some point in the first quadrant of the field, is matched by an equal velocity in the opposite direction when the ion is at the corresponding point in the fourth quadrant. This can be seen from the directions of the X-component of the electric field in the first and fourth quadrants. Similarly, the Y-velocity of the orbit centre when the ion is at a point in the second quadrant is matched by an equal but opposite velocity when the ion is at the corresponding point in the third quadrant.

In like manner, we can consider the case of an ion whose orbit centre is on the Y axis. By matching X-velocities in the first and second quadrants and in the third and fourth quadrants it can be shown that there is no net motion of the orbit centre in the X-direction.

The complete motion of an orbit centre on the X-axis will now be examined. As before, it will be assumed that the ion corresponding to this orbit centre is in phase with the accelerating potential. It has been shown above that for such an orbit centre, there is no net motion in the Y- direction

over one revolution of the ion. It remains, therefore to consider the motion of the orbit centre in the X- direction.

Consider a pair of equipotentials ϕ_1 , ϕ_2 in the peak electric field (Fig. 5). Suppose that these equipotentials are very close together, having an infinitesimal potential difference $\Delta\phi$. Suppose an ion P, in phase with the accelerating potential and having an orbit centre at C, somewhere on the X axis, crosses the pair of equipotentials at time t. Let us see what happens to the orbit centre.

It has been shown that the X-velocity of the orbit centre when the ion is somewhere in the electric field is given by $U_x = \frac{-E_y}{B_0}$, where E_y is the Y-component of the electric field acting on the ion at that point. In the case given above, E_y will be the electric field at the point at which the ion crosses the pair of equipotentials, at point A in Fig. 5, say.

If the ion P crosses the pair of equipotentials in a time δt , then the motion of the orbit centre in the X direction will be

$$\delta x = \frac{-E_y}{B_0} \delta t$$

Now at point A in Fig. 5, suppose the normal to the equipotentials makes an angle α to the Oy direction. Let the distance between the equipotentials at A along the normal be d_a . Then the electric field at A is

$$\mathcal{E} = \frac{\Delta\phi}{d_a} \quad \text{along the inward normal}$$

not taking into account the time variation of the electric field, while the component in the Y-direction will be

$$\mathcal{E}_y = \mathcal{E} \cos \alpha = \frac{\Delta \phi}{d_a} \cos \alpha$$

But we must take into account the time variation of the field to obtain the field seen by the ion at time t.

This is

$$\begin{aligned} E_y &= \mathcal{E}_y \cos \omega t \\ &= \frac{\Delta \phi}{d_a} \cos \omega t \cos \alpha \end{aligned}$$

Now suppose the path of the ion through the equipotential pair is of length S_a

Then $\delta t = \frac{S_a}{v}$ where v is the velocity of

the ion.

But the direction of S makes an angle ωt with the Oy direction since S_a is normal to the radius vector CP. Thus the angle between d_a and S_a is $(\omega t - \alpha)$ and so

$$S_a = \frac{d_a}{\cos(\omega t - \alpha)}$$

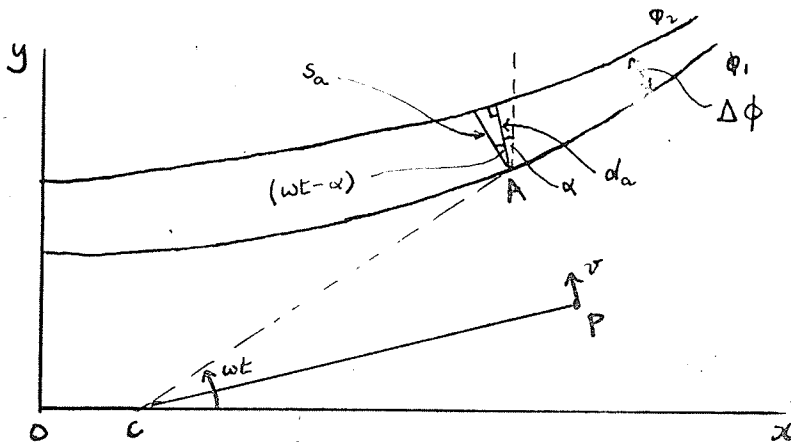


Fig 5.

So finally
$$\delta x = -\frac{\Delta\phi}{vB_0} \frac{\cos \omega t \cos \alpha}{\cos(\omega t - \alpha)}$$

i.e.,
$$\delta x = -\frac{\Delta\phi}{vB_0} \frac{1}{1 + \tan \omega t \tan \alpha} \dots \dots \dots .2.10.$$

Similarly, if we consider an ion Q whose orbit centre D is somewhere on the Y axis, (Fig. 6) then the motion of D in the Y direction as Q passes across the equipotential pair at time t is given by

$$\delta y = -\frac{\Delta\phi}{vB_0} \frac{\cos \omega t \sin \alpha}{\cos(\omega t - \alpha)}$$

i.e.,
$$\delta y = -\frac{\Delta\phi}{vB_0} \frac{1}{\tan \omega t + \cot \alpha} \dots \dots \dots .2.11.$$

the negative sign is due to the X-component of the electric field being in the negative X-direction (Fig. 6). At time t = 0, the radius vector of the ion is parallel to the OX axis.

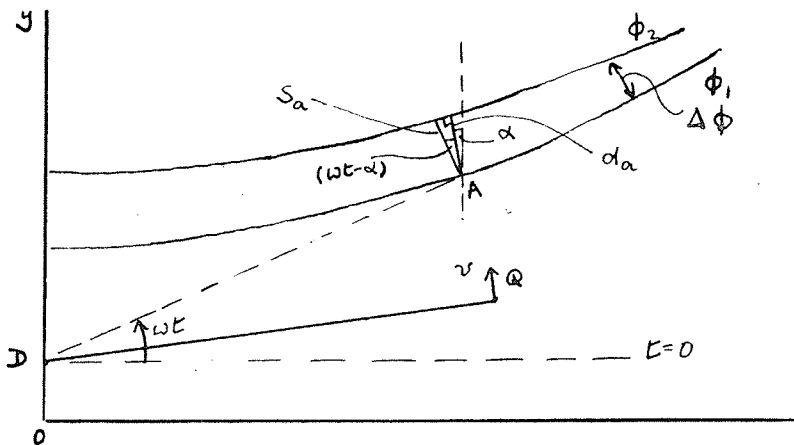
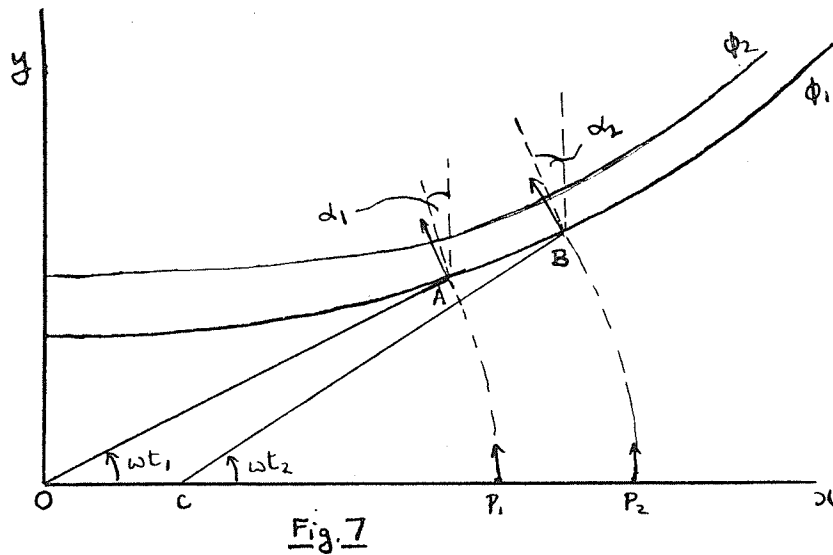


Fig 6.

α

The expressions derived above show the motion of the orbit centre over a small portion of the orbit of an ion. We wish to know, however, what happens to the orbit centre over a whole revolution of the ion. To do this let us compare what happens to the orbit centres of two ions as each passes through the pair of equipotentials. For the first case, one of the ions has its orbit centre at the origin while the other has its orbit centre somewhere on the X-axis. We know that on the average, over a revolution, the orbit centre at the origin remains at the origin, so from this comparison we can say something about what happens to the orbit centre on the X-axis over one revolution.



Let the ions be P_1 and P_2 with the same energy and phase. Let the orbit centre of P_1 be at the origin while the orbit centre of P_2 is somewhere on the X-axis, at C say. Suppose that they cross the Ox axis at time $t = 0$, i.e., they

are in phase with the accelerating potential (Fig. 7). It can be seen from Fig. 7, that due to the separation of the ions, the ion P_1 will cross the given pair of equipotentials at a time t_1 , earlier than the time t_2 at which P_2 crosses them.

Also, the point A at which P_1 crosses the equipotentials is ~~lower~~ ^{at a smaller y} than the point B at which P_2 crosses them. This is due to the shape of the equipotentials. The normal to the equipotentials at A makes a smaller angle α_1 with the Oy direction than does the normal at B which makes an angle α_2 .

As P_1 crosses the equipotentials, the orbit centre moves a distance δx_1 , given by

$$\delta x_1 = \frac{-\Delta\phi}{vB_0} \frac{1}{1 + \tan wt_1 \tan \alpha_1}$$

As P_2 crosses the equipotentials, its orbit centre moves a distance δx_2 given by

$$\delta x_2 = \frac{-\Delta\phi}{vB_0} \frac{1}{1 + \tan wt_2 \tan \alpha_2}$$

The motion of the orbit centre of P_2 relative to the orbit centre of P_1 is just $\delta x_2 - \delta x_1$ and equals

$$\frac{\Delta\phi}{vB_0} \left(\frac{1}{1 + \tan wt_1 \tan \alpha_1} - \frac{1}{1 + \tan wt_2 \tan \alpha_2} \right)$$

But $wt_1 < wt_2$ so $\tan wt_1 < \tan wt_2$

and $\alpha_1 < \alpha_2$ so $\tan \alpha_1 < \tan \alpha_2$

So $\delta x_2 - \delta x_1$ is positive. This means that the orbit centre of P_2 moves along the Ox axis away from the orbit centre of P_1 .

In the second quadrant of the electric field, the roles of the ions are reversed. However, the direction of the Y-component of the electric field is also reversed, so $\delta x_2 - \delta x_1$ remains positive. A similar analysis in the third and fourth quadrants shows that throughout the motion $\delta x_2 - \delta x_1$ remains positive. The same treatment can be applied to any pair of equipotentials in the field with the same results. So throughout the revolution, the orbit centre of P_2 moves away from the orbit centre of P_1 along the Ox axis. But over a revolution, the orbit centre of P_1 remains at the origin. Thus we can say that an orbit centre on the Ox axis will tend to drift away from the origin down the Ox axis as its ion moves in the electric field.

The discussion of the motion of an orbit centre on the Y-axis is very similar. The situation is depicted in Fig. 8. As before, P_1 is the ion whose orbit centre is at the origin, while P_2 is the ion whose orbit centre is at D on the Y-axis. The ions P_1 and P_2 have the same energy and phase. At time $t = 0$, P_1 is crossing the X-axis, while P_2 is at a point such that its radius vector is parallel to the Ox axis, as shown in Fig. 8. It can be seen from the diagram that P_2 crosses the pair of equipotentials earlier than does P_1 . However, due to the shape of the equipotentials and the separation of the orbit centres, P_1 crosses the equipotentials at a point ^{with smaller y} ~~lower~~ ^{that for} P_2 .

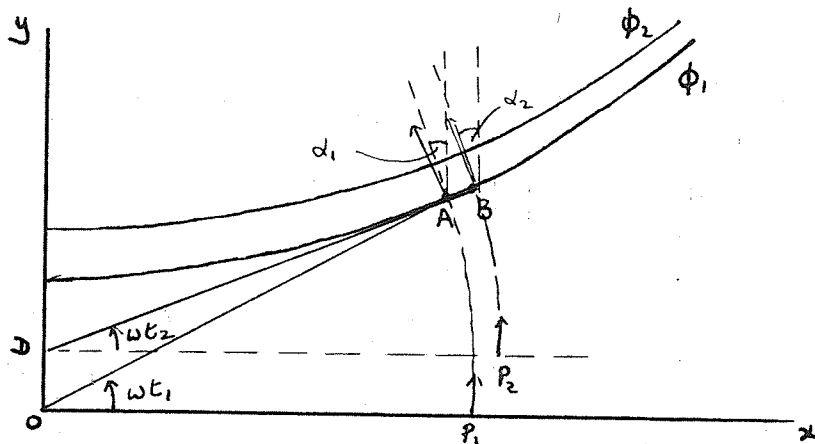


Fig. 8

Thus, with the same nomenclature as before,

$$\begin{aligned} \omega t_2 &< \omega t_1 \\ \alpha_2 &> \alpha_1 \end{aligned}$$

Now

$$\delta y_1 = -\frac{\Delta\phi}{vB_0} \frac{1}{\cot \alpha_1 + \tan \omega t_1}$$

$$\delta y_2 = -\frac{\Delta\phi}{vB_0} \frac{1}{\cot \alpha_2 + \tan \omega t_2}$$

Thus the motion of the orbit centre of P_2 relative to that of P_1 is

$$\delta y_2 - \delta y_1 = \frac{\Delta\phi}{vB_0} \left(\frac{1}{\cot \alpha_1 + \tan \omega t_1} - \frac{1}{\cot \alpha_2 + \tan \omega t_2} \right)$$

but

$$\begin{aligned} \tan \omega t_2 &< \tan \omega t_1 \\ \cot \alpha_2 &< \cot \alpha_1 \end{aligned}$$

Thus $\delta y_2 - \delta y_1$ is negative. This means that the orbit centre of P_2 moves towards the orbit centre of P_1 . Consideration of the direction of the X-component of the electric field, and of the roles of the two ions in each of the other three quadrants, shows that over the whole revolution $\delta y_2 - \delta y_1$ is negative. Also the same treatment can be applied to any pair of equipotentials in the field, with the same results. So the orbit centre of P_2 moves towards the orbit centre of P_1 along the Oy axis. But over a revolution, the orbit centre of P_1 remains at the origin. Thus we can say that an orbit centre on the Oy axis will tend to drift towards the origin along the Oy axis, as its ion moves in the electric field.

Considerations of symmetry show that orbit centres on the X-axis on either side of the origin will move away from the origin. Orbit centres on the Y axis on either side of the origin will move towards the origin. Orbit centres off the axes will experience a motion towards the origin in the Y-direction and away from the origin in the X-direction. The general direction of the orbit centre drifts is shown in Fig. 9.

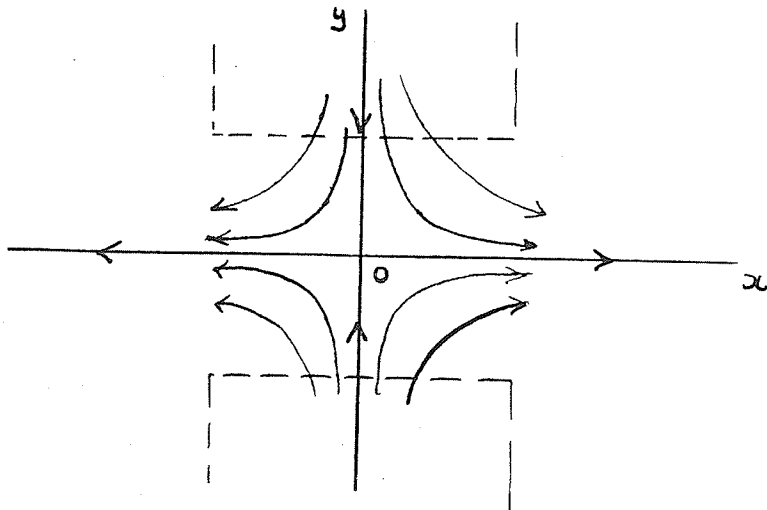


Fig 9. Directions of Orbit Centre Drifts.

2.4. Magnitude of the Drift.

The general direction of the drift of orbit centres in the electric field of the University of Manitoba cyclotron, has been established. It now remains to obtain some idea of the magnitude of the drift. We will examine first the motion on the X-axis.

Consider the ions P_1 , P_2 as before, where the orbit centre of P_1 is at the origin, while that of P_2 is at point C on the X-axis (Fig. 10). P_1 and P_2 have the same energy and phase. At time $t = 0$ they cross the Ox axis together, in phase with the accelerating potential and with the separation of their orbit centres a distance x_0 . The diagram (Fig. 10) depicts the situation a time t later when the ions are at P_1' , P_2' and the separation of their orbit centres is x .

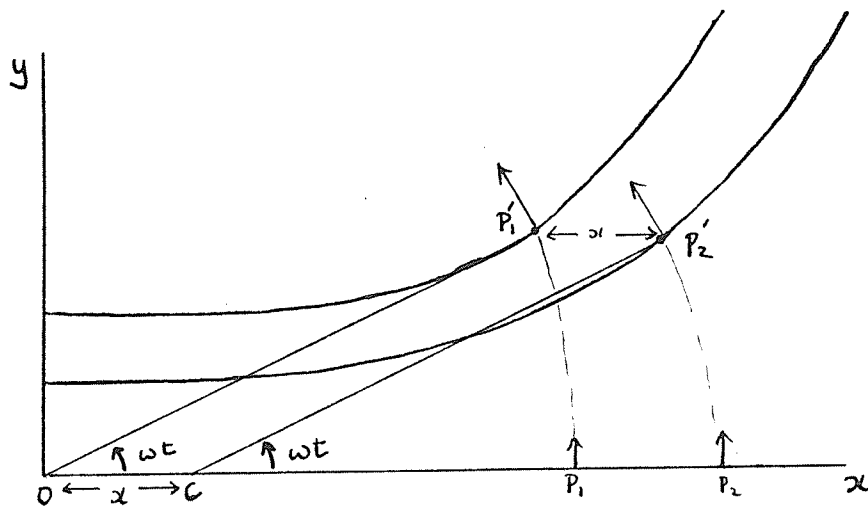


Fig 10

At time t , the X-velocities of the orbit centres of P_1' , P_2' are given by equation (2.9).

$$U_{x1} = \frac{-E_{y1}}{B_0} \quad U_{x2} = \frac{-E_{y2}}{B_0}$$

Where E_{y1} , E_{y2} are the Y-components of the electric field seen by the ions at P_1' , P_2' respectively.

The relative velocity U_x , of the orbit centre of P_2 with respect to the orbit centre of P_1 is thus

$$U_x = U_{x2} - U_{x1} = \frac{E_{y1}}{B_0} - \frac{E_{y2}}{B_0}$$

and since the separation of the orbit centres at time t is x , then $U_x = \frac{dx}{dt}$

Now in time t , the radius vectors OP_1 , OP_2 of P_1 , P_2 turn through an equal angle ωt . Also since P_1 , P_2 are of the same energy, the radii of their orbits are the same. Thus in Fig.10, the separation of the ions at time t is equal to the separation of the orbit centres.

i.e., the distance $P_1 P_2 = x$.

Now at time t ,

$E_y = \mathcal{E}_y \cos \omega t$ where \mathcal{E}_y is a function of x and y only. If P_1' is the point (X, Y) then P_2' is the point $(X \neq x, Y)$.

$$\text{Thus } E_{y1} = \mathcal{E}_y(X, Y) \cos \omega t$$

$$E_{y2} = \mathcal{E}_y(X \neq x, Y) \cos \omega t$$

$$\text{Thus } E_{y1} - E_{y2} = \left[\mathcal{E}_y(X, Y) - \mathcal{E}_y(X \neq x, Y) \right] \cos \omega t.$$

If the separation of orbit centres is small we can expand the quantity in square brackets using Taylor's expansion.

Thus to first order

$$E_{y1} - E_{y2} = -x \left(\frac{\partial E_y}{\partial x} \right)_{X,Y} \cos \omega t.$$

where the partial derivative is evaluated at (X,Y)

So
$$U_x = \frac{dx}{dt} = \frac{-x}{B_0} \left(\frac{\partial E_y}{\partial x} \right)_{XY} \cos \omega t.$$

$$\frac{dx}{x} = - \frac{1}{B_0} \left(\frac{\partial E_y}{\partial x} \right)_{X,Y} \cos \omega t \, dt. \dots \dots \dots .2.12.$$

$\frac{dx}{x}$ is the fractional displacement of the orbit centre over the time dt. If the coefficient of dt in the right hand side of this equation is small, then the fractional displacement over one revolution of the ion can be obtained by direct integration.

Thus if x_0 is the initial position of the orbit centre at the beginning of the revolution and during the revolution the displacement is Δx , then

$$\frac{\Delta x}{x_0} = - \int_{P_1} \frac{1}{B_0} \left(\frac{\partial E_y}{\partial x} \right)_{XY} \cos \omega t \, dt. \dots \dots \dots .2.13$$

the integration is along the path of P_1 for one revolution. This integral depends on the radius of the orbit of the ion since this determines the field through which the ion moves.

So we can put

$$\frac{\Delta x}{x_0} = \lambda(\rho) \dots \dots \dots .2.14.$$

where $\lambda(\rho)$ is some function of the radius. We shall refer to this relationship again in the next chapter.

The validity of the expression depends upon $\lambda(\rho)$ being small. In practice $\lambda(\rho)$ is fairly small, its maximum value not rising above 0.4. Even at the maximum value, equation 2.14 is valid to within 6% error.

A more accurate treatment is the direct integration of both sides of 2.13 over one revolution. This results in

$$\log \left\{ \frac{x_0 + x}{x_0} \right\} = - \int_{P_1} \frac{1}{B_0} \left(\frac{\partial E_y}{\partial x} \right) \cos \omega t \, dt \dots 2.15.$$

For the electric field considered, $\frac{\partial E_y}{\partial x}$ is predominantly negative so the integrals in equations 2.13, 2.15 have negative values. Thus $\lambda(\rho)$ is positive and the orbit centre of P_2 moves away from the origin.

A similar analysis can be carried out to investigate the motion of an orbit centre on the y axis. A similar expression is obtained.

$$\log \frac{y_0 + y}{y_0} = \int_{P_1} \frac{1}{B_0} \left(\frac{\partial E_x}{\partial y} \right) \cos \omega t \, dt \dots 2.16$$

Where the integration is carried out over the path of P_1 as before. In the electric field considered, $\frac{\partial E_x}{\partial y}$ is predominantly negative, so the right hand side of equation 2.16 is negative. Thus the orbit centre of P_2 moves towards the origin on the y-axis.

Furthermore, if we express the field components in terms of the potential function ϕ then

$$\begin{aligned} E_x &= -\frac{\partial \phi}{\partial x} & \text{and} & & E_y &= -\frac{\partial \phi}{\partial y} \\ \text{Thus } \frac{\partial E_x}{\partial y} &= \frac{\partial E_y}{\partial x} = -\frac{\partial^2 \phi}{\partial x \partial y} \dots \dots \dots 2.17 \end{aligned}$$

The equality of $\frac{\partial \epsilon_x}{\partial y}$ and $\frac{\partial \epsilon_y}{\partial x}$ together with the equations 2.15 and 2.16, brings out quite nicely the fact that the magnitude of the drift is the same on each axis, but one is directed towards the origin and the other away from the origin.

We can develop an approximate relationship for the y-direction as we did for the x-direction. This is

$$\frac{\Delta y}{y_0} = - \lambda (\rho) \dots \dots \dots .2.18$$

by virtue of 2.17.

2.5. Treatment of Phase.

The discussion so far has been with reference to orbit centres of ions which are in phase with the accelerating potential. The treatment will now be extended so as to include out of phase ions.

Consider two ions of equal energy whose orbit centres are at the origin. Let one of the ions, P, be in phase with the accelerating potential while the other P' is out of phase by an angle θ . Suppose that in the first quadrant of the electric field, the out of phase ion lags the accelerating potential. Let us compare the electric field seen by each ion as each passes through corresponding points in all four quadrants.

(Fig. 11)

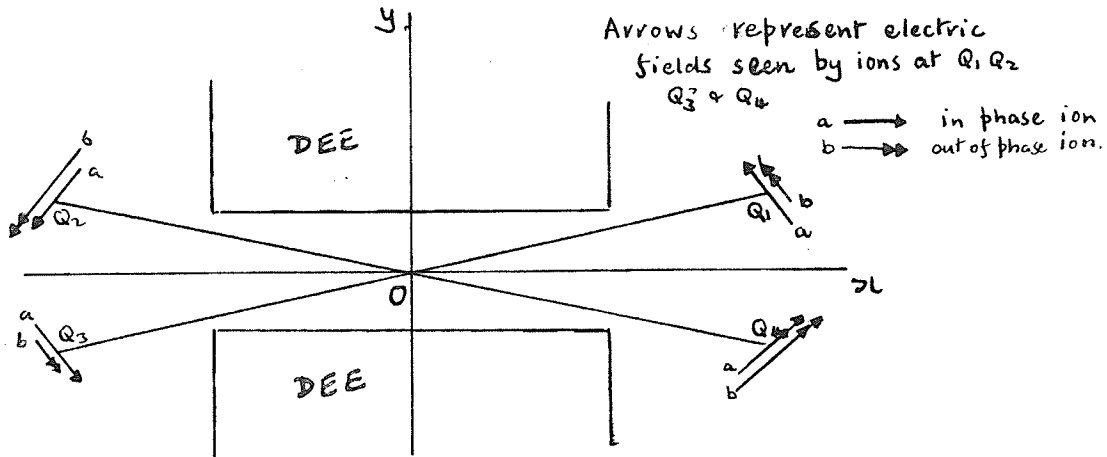


Fig 11.

Let the corresponding points in the four quadrants be Q1, Q2, Q3, Q4 as in Fig. 11. The peak value of the electric field has the same magnitude for each, i.e., $E(x,y)$ while the directions are as shown.

If the in phase ion passes through Q1, at time t , the field seen by the ion will be $E(x,y) \cos \omega t$ while the out of phase ion will only see a field $E(x,y) \cos (\omega t - \theta)$ when it passes through Q1. However, in the second quadrant, the electric field is increasing with time, so the out of phase ion, which passes through Q2 later, sees the greater field. The fields seen by the in phase and the out of phase ions will be $E(x,y) \cos \omega t$, $E(x,y) \cos (\omega t - \theta)$. In the third quadrant the field is decreasing with time and the situation is the same as in the first quadrant. Similarly the situation in the second and fourth quadrants is the same.

Considering first the motion of the orbit centre of each ion over a revolution, it is noticed that in the first

and third quadrants the x and y components of the electric field seen by each ion are equal and opposite. The same goes for the second and fourth quadrants. Thus there is no net motion of the orbit centre of either ion over a revolution. So an orbit centre at the origin remains at the origin, regardless of the phase of ion. This was stated at the beginning of section 2.3 but not proved.

Next consider the rate of radial increase of each ion.

This is given by
$$\frac{dp}{dt} = \frac{E_{11}}{B_0}$$

Where E_{11} is the component of the electric field tangential to the path of the ion. (See the second example in section 2.2.)

For the first quadrant at the point Q_1 , the rate of radial increase is

$$\frac{dp}{dt} = \frac{E_{11}}{B_0} (x,y) \cos \omega t$$

for the in phase ion. 2.19

$$\frac{dp}{dt} = \frac{E_{11}}{B_0} (x,y) \cos (\omega t \neq \theta) 2.20$$

for the out of phase ion.

For the whole revolution, we must consider the contributions from all four quadrants. In the second quadrant, the out of phase ion sees the greater electric field and the $\cos(\omega t \neq \theta)$ must be replaced by a factor $\cos(\omega t - \theta)$ in equation 2.20. The net contributions from all four quadrants give the rate of radial increase as

$$\frac{dp}{dt} = 4 \frac{E_{11}}{B_0} (x,y) \cos \omega t 2.21.$$

for the in phase ion,
and

$$\frac{dp}{dt} = 2 \frac{E_{11}}{B_0} (x,y) [\cos (wt - \theta) + \cos (wt + \theta)]$$

i.e.,
$$\frac{dp}{dt} = 4 \frac{E_{11}}{B_0} (x,y) \cos wt \cos \theta \dots \dots \dots 2.22$$

for the out of phase ion.

If the total increase in radius over a revolution is required, then this is obtained by integrating 2.21 and 2.22 over one quarter of a revolution, since we have considered contributions from all four quadrants simultaneously.

It is easily seen from 2.21 and 2.22 that the out of phase ion is less readily accelerated than the in phase ion. Thus the ions will move apart. However, there will be no drifting apart of the orbit centres. These will remain at the origin. This gives us an insight as to the treatment of ions which are out of phase, and whose orbit centres are not at the origin. Just as an in phase ion was compared to one whose orbit centre was at the origin, so then an out of phase ion must be compared with an ion out of phase by the same amount, and whose orbit centre is at the origin.

The relative velocity of drift of orbit centres in the x-direction for a pair of ions at a given time t has been shown to be

$$U_x = \frac{E_y - E_y'}{B_0}$$

where E_y is the y-component of the electric field, seen at time t

by the ion whose orbit is centred at the origin, and E_y' is the y-component of the electric field seen at time t by the ion whose orbit is centred on the x axis.

If the ions are each out of phase by an angle θ with the accelerating potential then

$$E_y = \mathcal{E}_y \cos (wt - \theta)$$

$$E_y' = \mathcal{E}'_y \cos (wt - \theta)$$

in some quadrant.

Thus the relative velocity at time t is given by

$$U_x = \frac{\mathcal{E}_y - \mathcal{E}'_y}{B_0} \cos (wt - \theta)$$

compare this with the corresponding expression obtained for ions in phase with the accelerating potential. This

$$U_x = \frac{\mathcal{E}_y - \mathcal{E}'_y}{B_0} \cos wt$$

At first sight the expressions seem different but this is not the whole story. Ions which are out of phase are also less readily accelerated. Thus they take a greater number of revolutions to increase their radius by a given amount than do ions in phase. So the amount of drift over a given increase in radius would be a better way of comparing the in phase and out of phase ions.

For an in phase ion, the rate of increase in radius is

$$\frac{dp}{dt} = \frac{\mathcal{E}_{\parallel}}{B_0} \cos wt$$

While for the quadrant concerned, the rate of radial increase for the out of phase ion is

$$\frac{dp}{dt} = \frac{\mathcal{E}_{\parallel}}{B_0} \cos (wt - \theta)$$

Thus the amount of drift per unit radial increase is $\frac{dx}{dp}$

and is given by

$$\frac{dx}{dp} = \frac{\epsilon_y - \epsilon'_y}{\epsilon_{\parallel}} \quad \text{for an in phase ion,}$$

with exactly the same expression for an out of phase ion. So, for an orbit centre on the Ox axis, the amount by which it drifts along the Ox axis over a given radial increment of the orbit is independent of the phase of the ion. The same is true for the drift along the y axis of an orbit centre there.

The situation is not totally unchanged, however. For an orbit centre on the Ox or Oy axis there will be a resultant motion perpendicular to that axis if the ion is out of phase with the accelerating potential. To see this, consider Fig. 12.

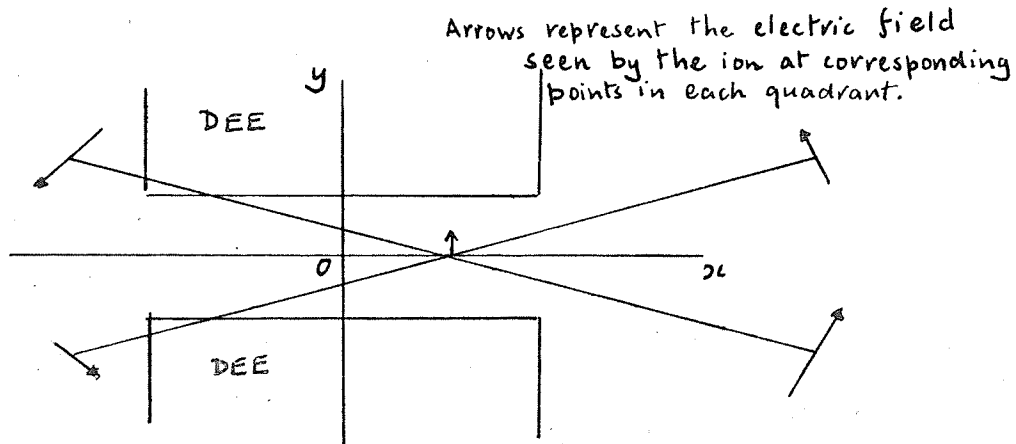


Fig 12.

If the ion is lagging the potential, it will see a greater potential in the first quadrant than it will in the fourth. Also, it will see a greater potential in the third quadrant than it will in the second. Since the orbit of the ion is not centred, the potentials in quadrants one and three, and the potentials in quadrants two and four do not match. There is thus a net motion of the orbit centre in the negative y-direction as shown. Similarly, an orbit centre on the y-axis, besides its normal drift along the y-axis also exhibits a tendency to move in the positive x-direction. The effect of the ion lagging the accelerating potential is a clockwise precession of the orbit centres about the origin. Similarly, the effect of an ion leading the accelerating potential is an anti-clockwise precession. This precession will not alter the instability of the orbit centres very much. It will tend to make the situation neither better nor worse. Therefore, it can be neglected in the discussion that is to follow in the next chapter.

2.6. An Example.

Before proceeding further with the discussion, it would be well to apply the analysis of section 2.4 to some simple field to give an idea of the orders of magnitude expected, and to demonstrate the method.

The function chosen for the shape of the equipotential lines is

$$\phi = \frac{A \sin \theta}{r}$$

expressed in polar coordinates r, θ where A is a constant.

This function is a fairly simple one to handle and it is consistent with Laplace's equation for a symmetric field about the median plane. By the usual manipulation of partial derivatives,

$\left(\frac{\partial \phi_y}{\partial x}\right)_y$ can be expressed in terms of polar coordinates.

Thus

$$\frac{\partial \phi_y}{\partial x} = \left(\frac{\phi_{\theta\theta}}{r^2} + \frac{\phi_r}{r} - \phi_{rr} \right) \sin \theta \cos \theta + \left(\frac{\phi_\theta}{r^2} - \frac{\phi_{r\theta}}{r} \right) (\cos^2 \theta - \sin^2 \theta).$$

where subscripts θ, r denote partial differentiation with respect to θ, r .

The differentials required are

$$\phi_r = \frac{-A \sin \theta}{r^2}, \quad \phi_\theta = \frac{A \cos \theta}{r}, \quad \phi_{r\theta} = \frac{-A \cos \theta}{r^2}$$

$$\phi_{rr} = \frac{2A \sin \theta}{r^3}, \quad \phi_{\theta\theta} = \frac{-A \sin \theta}{r}$$

from which

$$\frac{\partial \phi_y}{\partial x} = \frac{2A}{r^3} (\cos^3 \theta - 3 \cos \theta \sin^2 \theta).$$

The integral in equation 2.15 thus becomes

$$\log \frac{x_0 + \Delta x}{x_0} = - \int_P \frac{1}{B_0} \frac{2A}{r^3} (\cos^3 \theta - 3 \cos \theta \sin^2 \theta) \cos \omega t \, dt.$$

integrated over the path of P. Now when P is at the point (r, θ) at time t , then the angle $\theta = \omega t$. Thus, substituting in the equation we get

$$\log \frac{x_0 + x}{x_0} = - \frac{2A}{B_0 \omega r^3} \int_P (\cos^4 \theta - 3 \cos^2 \theta \sin^2 \theta) \, d\theta.$$

Next suppose that the ion enters the dee where $\theta = \alpha$ (Fig. 13.)

Where the ion is in the dee, there is no electric field present.

So to integrate over the whole path of P, we only need to integrate at constant r from $\theta = 0$ to $\theta = \alpha$ and then multiply by 4.

Thus

$$\begin{aligned} \log \frac{x_0 \pm \Delta x}{x_0} &= \frac{-8 A}{B_0 \omega r^3} (\sin \theta \cos^3 \theta) \Big|_0^\alpha \\ &= \frac{-8 A}{B_0 \omega r^3} \times .31 \end{aligned}$$

if α is taken as in (Fig. 13).

The value of α results from the geometry of the dee and the radius of the orbit. To obtain α we have assumed $r = 2.5''$, and the half length of the dee is $2''$. The gap between the dees is also $2''$.

We can now determine A

$$\text{At } \theta = \alpha \quad \phi = V_0 = \frac{A \sin^2 \alpha}{r}$$

Thus $A = \frac{5V_0 r}{3}$ for the value of α given.

$$\text{i.e., } \log \frac{x_0 \pm \Delta x}{x_0} = \frac{-1}{B_0 \omega} \frac{40V_0}{r^2} \times 0.31$$

For the Manitoba cyclotron, $B_0 = 2 \text{ Wb/m}^2$, $\omega = 2 \times 10^8 \text{ /sec.}$
 $V_0 = 42 \times 10^3 \text{ volts}$ and $r = 2.5''$ or $\frac{2.5}{40} \text{ m approx.}$

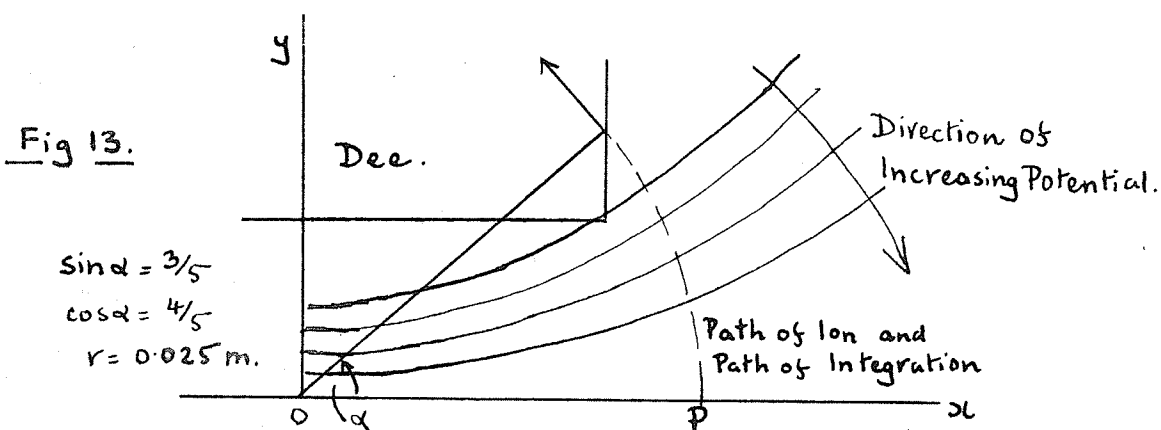
$$\text{So } \log \frac{x_0 \pm \Delta x}{x_0} = -0.11$$

or to small error

$$\Delta x = -0.11 x_0$$

Similarly $\Delta y = 0.11 y_0$.

Note that for this arrangement, there is defocussing in the y-direction and focussing in the x direction. This is because for this field, the potentials are higher towards the origin. The ion, in effect, is moving round in a decelerating field. (Fig. 13)



2.7 Summary.

It has been shown in this chapter, that in the non-uniform electric field of the University of Manitoba cyclotron, there is an instability which causes the drifting of orbit centres of ions moving in the field. It has been found that the orbit centres tend to drift towards the origin along one axis of symmetry and tend to drift away from the origin along the other axis of symmetry. The amount by which an orbit centre drifts during one revolution of the ion depends on the radius of the orbit of the ion and on the distance of the orbit centre from the origin.

Chapter 3.

RADIAL INSTABILITY IN A MAGNETIC FLUTTER FIELD.

3.1 Introduction.

At the beginning of the last chapter, an expression was derived for the velocity of the orbit centre of an ion moving in an electric field \underline{E} and a magnetic field \underline{B} . The expression was

$$\frac{d\mathbf{R}}{dt} = \frac{\underline{E} \times \underline{B}_0}{B_0^2} + \underline{v} \left(\frac{B_0 - B}{B_0} \right)$$

The remainder of that chapter was devoted to the discussion of what happened when the electric field was that of the University of Manitoba cyclotron and the magnetic field in which the ion moved was equal to B_0 . In this chapter we shall extend the investigation so as to include magnetic fields not equal to B_0 . Since B_0 is a uniform magnetic field, we can regard the difference between it and the magnetic field B as a superimposed flutter field ΔB . If we have

$$\Delta B = B - B_0 \tag{3.1}$$

then ΔB will be positive for a hill and negative for a valley. The expression for the velocity of the orbit centre now becomes

$$\frac{d\mathbf{R}}{dt} = \frac{\underline{E} \times \underline{B}_0}{B_0^2} - \underline{v} \frac{\Delta B}{B_0} \tag{3.2}$$

The instantaneous velocity of the orbit centre of an ion moving in an electric and magnetic field is made up of two parts.

One contribution is due to the electric field and the other is due to the magnetic field. Each contribution is a vector quantity, and it can be seen that the vectors never point in the same direction. So we could never reduce the instantaneous velocity of the orbit centre to zero by, say, a judicious choice of magnetic flutter field. However, it could be arranged that the average value of the velocity of the orbit centre over one revolution of the ion was made equal to zero.

This could be done by ensuring that the average value of $\frac{\mathbf{E} \times \mathbf{B}_0}{B_0^2}$ over a revolution was equal to the average value of

$\frac{v \Delta \mathbf{B}}{B_0}$ over a revolution. Now the average value of $\frac{\mathbf{E} \times \mathbf{B}_0}{B_0^2}$

represents the rate of drift of the orbit centre due to the non-uniform electric field and was discussed in the last chapter. It can be seen, therefore, that the flutter field is also going to give rise to a drift of orbit centres and we must arrange that this drift runs counter to that produced by the electric field.

Since the terms due to the electric and magnetic fields in equation 3.2 are independent, we can forget about the electric field for the time being and consider the drift of orbit centres in the flutter field. We are then required to find a flutter field that will produce a drift of orbit centres equal in magnitude but opposite in direction to that produced by the electric field. Then, when this flutter field is superposed on the electric field, the net drift will be zero, and we

will have stability of orbit centres.

The magnetic flutter field required must have the following characteristics:

- (a) it must be symmetric about the x and y axes. This indicates that a sector flutter of sorts is called for.
- (b) the field must produce equal and opposite drifts of orbit centres along axes perpendicular to each other. These axes may be the x and y axes. If they are not, the flutter field can always be rotated as a whole, to bring the axes in line with the x and y axes.

The simplest flutter field that satisfies the first requirement is a two hill second harmonic flutter field. It has been shown* that such a flutter field does produce radial instability of ion orbits and this is what we are looking for. An examination of the motion of orbit centres in this flutter field would seem to be a good approach to the problem. It will become clear later on that a two sector flutter does not satisfy the second requirement. The simplest field that satisfies all the requirements is a second harmonic flutter composed of a set of two hill sectors and two valley sectors placed at right angles to each other. The analysis of this flutter field is made much simpler, if the motion of orbits in a two sector flutter is considered first.

* See Reference 2.

3.2. Two-Sector Flutter Field.

If we consider an ion moving in a magnetic flutter field alone, the expression for the velocity of its orbit centre becomes

$$\frac{dR}{dt} = - \frac{v}{B_0} \frac{\Delta B}{B_0} \quad 3.3.$$

If ΔB is positive, i.e., the flutter field is a hill, then it is seen that the orbit centre moves antiparallel to the path of the ion in the flutter field. If ΔB is negative, i.e., the flutter field is a valley, then the orbit centre moves parallel to the path of the ion in the field. The physical significance is made clearer if we consider a simple example.

Suppose an ion P is moving at a velocity v in a uniform magnetic field B_0 (Fig. 1). Let the centre of curvature of its orbit be at c . While the ion moves in the magnetic field B_0 , c represents the orbit centre or virtual centre of curvature. Suppose that the ion enters a region of higher magnetic field B . This region is in effect a superimposed flutter field of magnitude $\Delta B = B - B_0$. As the ion moves in this flutter field, its orbit will have a smaller radius of curvature since the flutter field is a hill. The centre of curvature of the orbit will jump from c to the point D , say, as soon as the ion enters the flutter field. If the flutter field is uniform, the centre of curvature of the orbit will

remain at D all the while the ion moves in the flutter field. When the ion leaves the flutter field and enters the original field B_0 again, the radius of curvature will resume its original value. The centre of curvature will not jump back to c, however, as the radius vector is in a different direction. The centre of curvature will thus jump to c'. The action of the flutter field is to displace the centre of curvature of the orbit.

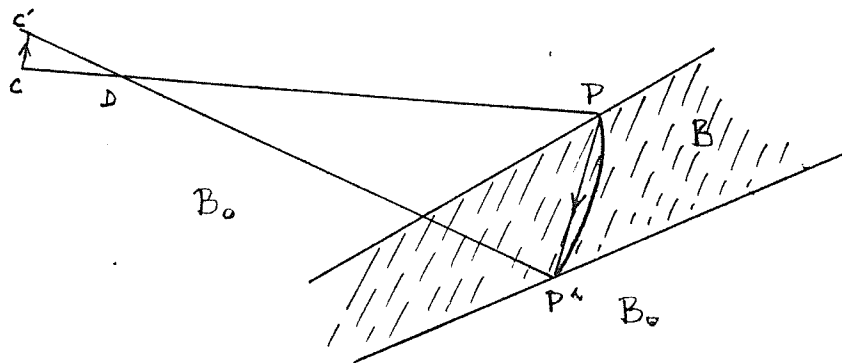


Fig 1.

It is seen from Fig. 1, that as the ion moves in the flutter field from P to P' say, its orbit centre moves from c to c'. As the ion moves about D, so also does its orbit centre c. The orbit centre thus moves antiparallel to the path of the ion in the flutter field. The velocity at which the orbit centre moves can easily be shown to be equal to $v \frac{\Delta B}{B_0}$ as given in equation 3.3. The situation is very similar to the example cited in the last chapter where the ion moved round in an electric field E_{\perp} which always acted normal to its path. In

fact the flutter field could well be treated in terms of an equivalent electric field. This field would act along the inward normal for a positive ΔB and along the outward normal for a negative ΔB .

The path of the ion through the flutter field thus gives an indication of what is happening to the orbit centre. In Fig. 1, since the resultant path of the ion through the flutter field is PP' the resultant path of the orbit centre will be antiparallel to this

$$cc' = \frac{\Delta B}{B_0} P'P \quad 3.4$$

This is a very convenient way of considering the path of the orbit centre.

We are now in a position to examine the motion of the orbit centre of an ion as the ion moves round in a two-sector flutter field. We will consider the net displacement of the orbit centre from different positions in the field, and over one revolution of the ion. The situation is depicted in Fig. 2 with the axes of symmetry of the flutter field along the x and y axes.

First consider an ion whose orbit centre is at the origin O. (Fig. 2s). Over one revolution of the ion the resultant paths of the ion in each sector are the vectors \vec{AB} and \vec{CD} . The path of the orbit centre will be antiparallel to the resultant of these. But, since the field is symmetric about the origin, the paths of the ion in each sector will be equal in length but oppositely directed. Hence the resultant of \vec{AB}

and \vec{CD} is zero. Thus, on the average an orbit centre at the origin will remain there.

Next consider an ion whose orbit centre is on the y-axis (Fig. 2b). Let the paths of the ion through each sector be \vec{AB} and \vec{CD} as before. Then it is seen from symmetry that the components of the vectors \vec{AB} and \vec{CD} cancel in the y direction and add up in the x direction. The direction of motion of the orbit centre is antiparallel to the resultant of \vec{AB} and \vec{CD} . Hence the net motion of the orbit centre over one revolution of the ion will be perpendicular to the y-axis and in the x-direction.

Similarly for an orbit centre on the x-axis, the net motion over one revolution of the ion will be in the y-direction, perpendicular to the x-axis.

For an orbit centre off the axes of symmetry, the ion will always spend more time in one of the sectors than in the other. Thus the motion of the orbit centre will be predominantly due to that sector. By direct geometric construction, or by consideration of the amount of time spent by the ion in each sector, the magnitude and direction of the displacement of the orbit centre can be found for any point in the field. We can thus think of the whole field as being mapped out by a set of flow lines, where the direction of the flowline at any

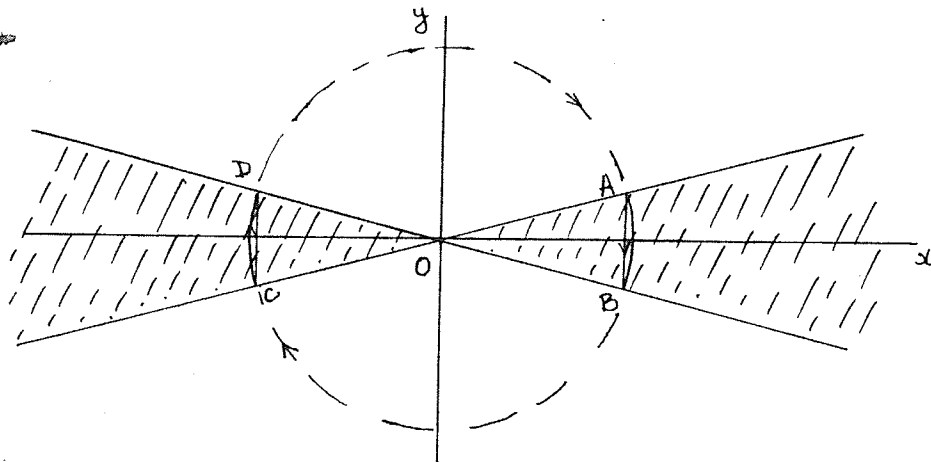


Fig 2(a)

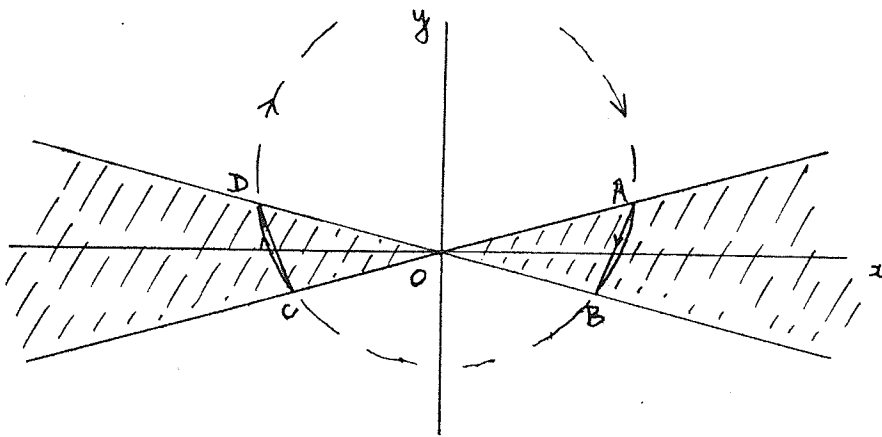
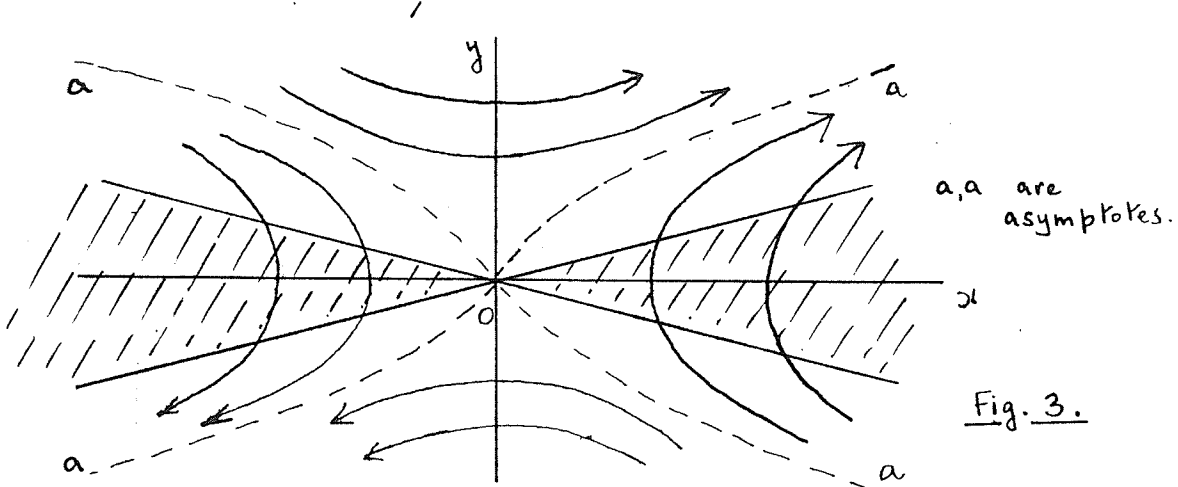


Fig. 2(b).

point in the field gives the direction of motion of the orbit centre at that point. It has been shown above that the orbit centres cross each axis of symmetry in a direction perpendicular to it, so the flowlines will be orthogonal to the axes of symmetry.

The flowlines for the whole field are shown in Fig.3. Note that in each quadrant there exists an asymptote (shown dotted), such that the orbit centres on one side move so as to cross the Ox axis eventually, while orbit centres on the other side of the asymptote move so as to cross the Oy axis eventually. At large distances, the flowlines run parallel to

the edges of the sectors.



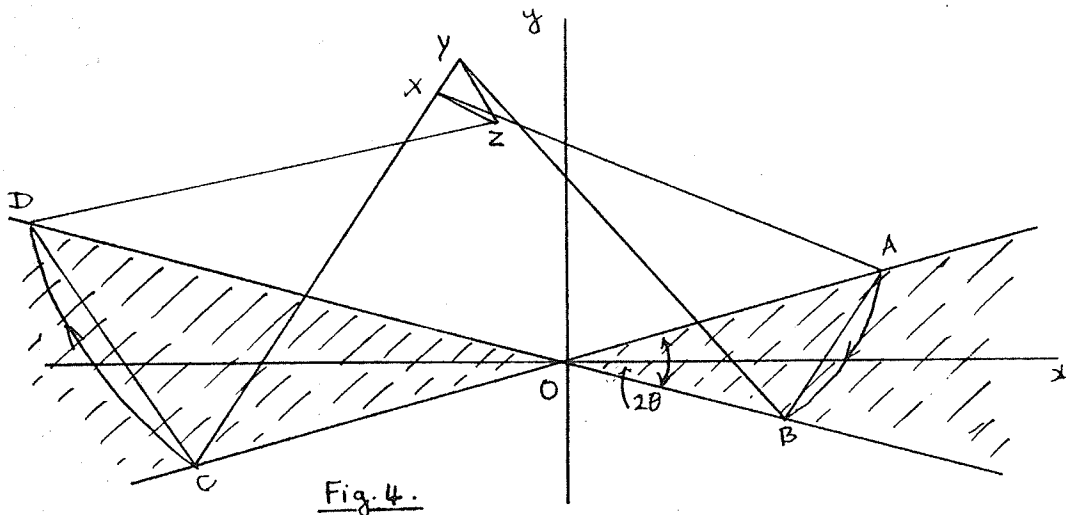
3.3. A Vectorial Approach.

The general character of the motion of the orbit centre was established qualitatively in the last section. Some of the results obtained can be derived in a more vigorous way using a vector approach to the problem.

In Fig. 4 (overleaf), let X be the orbit centre of an ion P as it travels in the field B_0 . The ion enters the first sector of the flutter field at A and leaves it at B . While it is travelling through the sector, the orbit centre moves from X to Y . There is no motion of the orbit centre while the ion is moving between the sectors. The ion enters the second sector at C and leaves it at D . Meanwhile the orbit centre moves from Y to Z . The net displacement of the orbit centre is \vec{XZ} .

A, B, C, D are the points at which the ion crosses the flutter field boundaries. Let OA, OB, OC, CD be represented by $\underline{a}, \underline{b}, \underline{c}, \underline{d}$ respectively. The magnitudes of these vectors

will be a, b, c, d .



From Fig. 4, $\vec{XZ} = \vec{XY} + \vec{YZ}$. 3.4

Now \vec{XY} is antiparallel to \vec{AB} , the direction of the path of the ion through the flutter field. In fact

$$\vec{XY} = \frac{\Delta B}{B_0} \vec{BA} \quad (\text{From equation 3.3})$$

Similarly $\vec{YZ} = \frac{\Delta B}{B_0} \vec{DC}$

Thus from equation 3.4,

$$\vec{XZ} = \frac{\Delta B}{B_0} (\vec{BA} + \vec{DC})$$

or expressing these vectors in terms of \underline{a} , \underline{b} , \underline{c} , and \underline{d}

$$\vec{XZ} = \frac{\Delta B}{B_0} ((\underline{a} + \underline{c}) - (\underline{b} + \underline{d})) \quad 3.5$$

We can go further by expressing \underline{a} , \underline{b} , \underline{c} and \underline{d} in terms of unit vectors \underline{i} , \underline{j} in the Ox and Oy directions. Then if 2θ is the angular width of each sector,

$$\underline{a} = a \cos \theta \underline{i} + a \sin \theta \underline{j} \quad \text{with like expressions for}$$

b, c, d.

If Δx and Δy are the components of the motion of the orbit centre over the whole revolution,

$$\vec{XZ} = \underline{i} \Delta x + \underline{j} \Delta y$$

It follows then that

$$\Delta x = \frac{\Delta B}{B_0} ((a - c) - (b - d)) \cos \theta$$

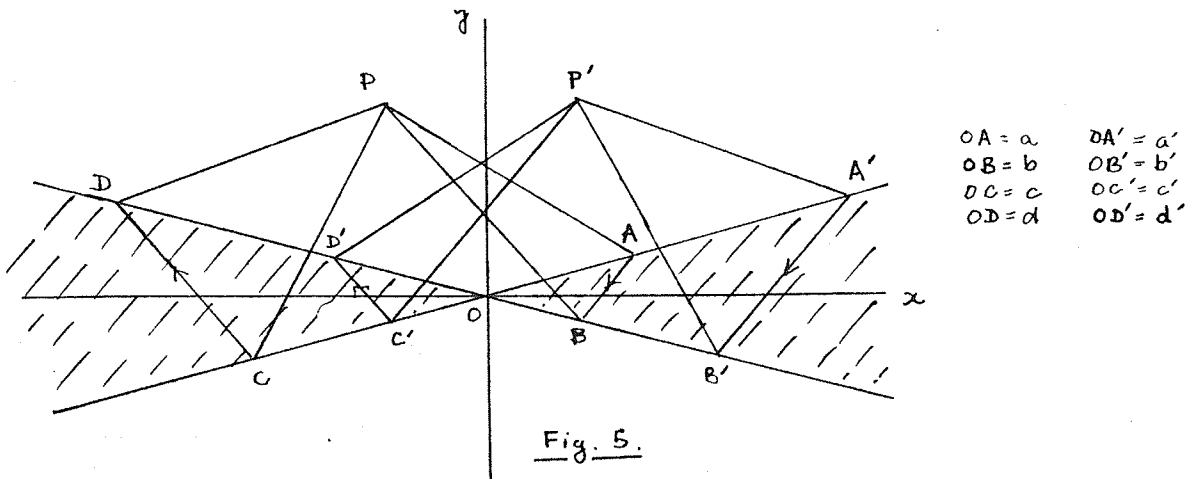
$$\Delta y = \frac{\Delta B}{B_0} ((a - c) + (b - d)) \sin \theta$$

The gradient of the path of the orbit centre is thus

$$\frac{\Delta y}{\Delta x} = \frac{(a - c) + (b - d)}{(a - c) - (b - d)} \tan \theta \quad 3.6$$

an expression solely in terms of the intercepts which the ion cuts off at the hill boundaries during its revolution. The value of $\frac{\Delta y}{\Delta x}$ at a point in the field represents the gradient

of the flow line at that point. It can now be shown quite easily that the flow lines are symmetric about the axes of symmetry.



Consider two points P, P' equidistant from the x-axis and mirror images in the y-axis. If the value of ΔB is small compared to that of B_0 , the orbit centre moves little during the revolution of the ion. We can neglect the motion of the orbit centre during the revolution as a first order approximation just as we did in the electric field case. The points at which the ion crosses the sector boundaries can be found by drawing a circle with radius equal to that of the orbit and with centre P or P'.

With P as centre the circle will cut the hill boundaries at ABCD while with P' as centre the circle will cut the hill boundaries at A'B'C'D'.

It is seen from the symmetry that the paths $\vec{AB} + \vec{CD}$ and $\vec{A'B'} + \vec{C'D'}$ are mirror images of one another, the only difference being a change in sign.

Hence the gradient at P $\left(\frac{\Delta y}{\Delta x} \right)_P$ is equal to the gradient at P', $\left(\frac{\Delta y}{\Delta x} \right)_{P'}$ but opposite to it in sign. It follows that the path of the orbit centre is symmetrical about the Cy axis. In particular, for an orbit centre on the y-axis, the points P, P' are identical and the gradient of the path is zero.

Thus the orbit centres on the y-axis move in a direction perpendicular to the y-axis over one revolution of their ions. The other axis of symmetry, the Ox axis, can be treated in like manner with similar results.

3.4. Second Harmonic Flutter Field (Two Hills and Two Valleys).

We can see that the drift of orbit centres produced by the two hill second harmonic flutter field is quite different across each axis of symmetry. The flow lines about the y-axis are flatter than those about the x-axis. Now in an electric field, the amount of drift is the same on each axis. Apart from the direction of the drift, we could not distinguish between the axes. As we wish to use the instability produced by the magnetic field to counteract the instability due to the electric field, we must seek a magnetic field whose flowlines are the same for each axis. The natural step is to introduce another pair of sectors similar to the first pair and placed orthogonal to them. The new sectors must be valleys or else complete stability would be produced! (cf. Reference 2). This pair of valleys is placed symmetrically about the Oy axis. The situation is as shown in Fig. 6.

This composite flutter field is treated in the same way as was the two hill flutter. An orbit centre on the Ox axis or Oy axis will move perpendicular to that axis as its ion describes a revolution. Also, the flowlines about each axis must be exactly the same since, apart from the sign of the flutter, there is nothing to distinguish between the pair of hills and the pair of valleys. The composite flutter field has two more axes of mirror symmetry than has the two hill flutter. These are the 45° axes OV, OW (Fig. 6.) Consider an ion whose orbit centre K is on the axis OV, say.

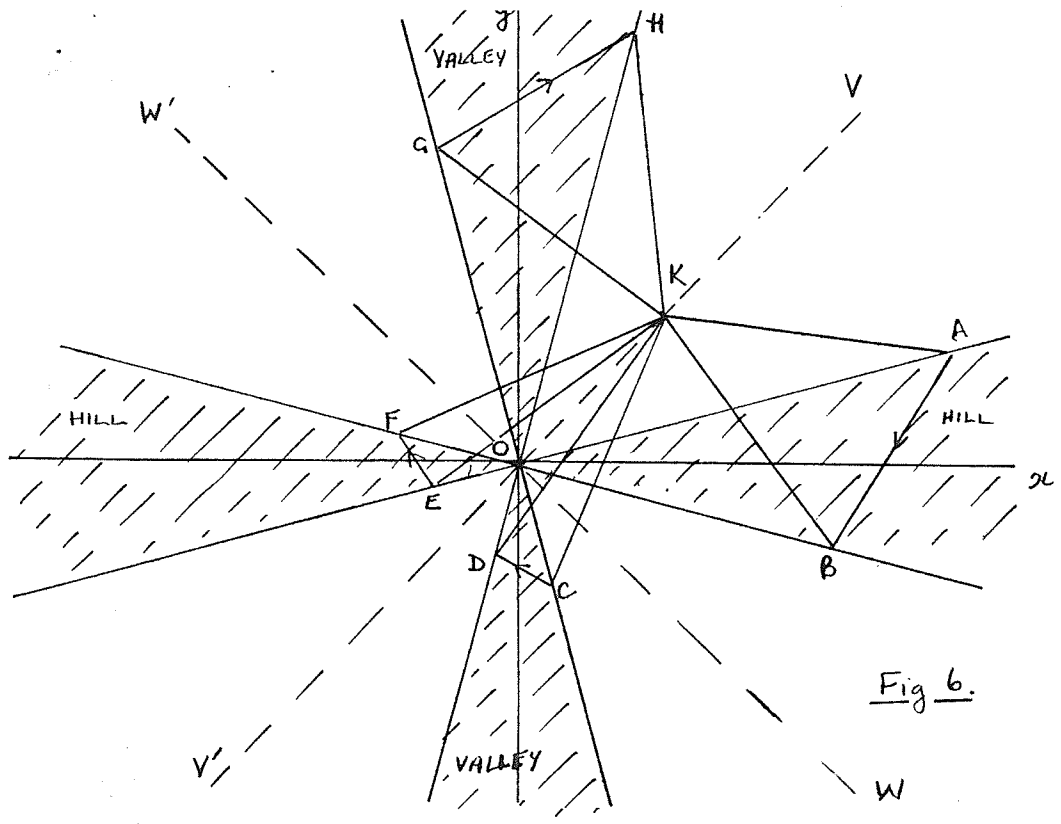


Fig 6.

Suppose that as the ion makes one revolution it crosses the sector boundaries at A, B, C, D, E, F, G, H.

\vec{AB} , \vec{EF} represent the paths of the ion through the hills.

\vec{CD} , \vec{GH} represent the paths of the ion through the valleys. The orbit centre suffers four displacements as the ion passes through the sectors and the net displacement is the resultant of these. When the ion passes through a hill, the orbit centre moves antiparallel to its path. When the ion passes through a valley, the orbit centre moves parallel to

its path. Since the fractional change in orbit radius is the same in magnitude for every sector, then the net displacement of the orbit centre over one revolution of the ion is

$$\frac{\Delta B}{B_0} (\vec{BA} + \vec{CD} + \vec{FE} + \vec{GH})$$

From the symmetry of Fig. 6, it is seen that the components of these vectors perpendicular to OV are in opposite directions and sum to zero. The components along OV add up to some finite amount. Since \vec{BA} and \vec{GH} are much larger than \vec{CD} and \vec{FE} , the net result is a vector pointing along OV away from O. Thus an orbit centre originally on the line OV tends to move away from O along OV. Similarly, it can be shown that the orbit centres on the lines OW, OW' tend to approach O along OW, OW'. Also, an orbit centre on OV' tends to move away from O along OV'.

The flow lines for a second harmonic flutter field with two hills and two valleys are as shown in Fig. 7. It is seen that there is a focussing effect along one 45° axis while there is a defocussing effect along the other 45° axis. Comparison with Fig. 9 of Chapter 2 shows that this is just what is required to balance the instability due to the electric field. The sectors must be rotated of course so that the focussing direction is the x-direction.

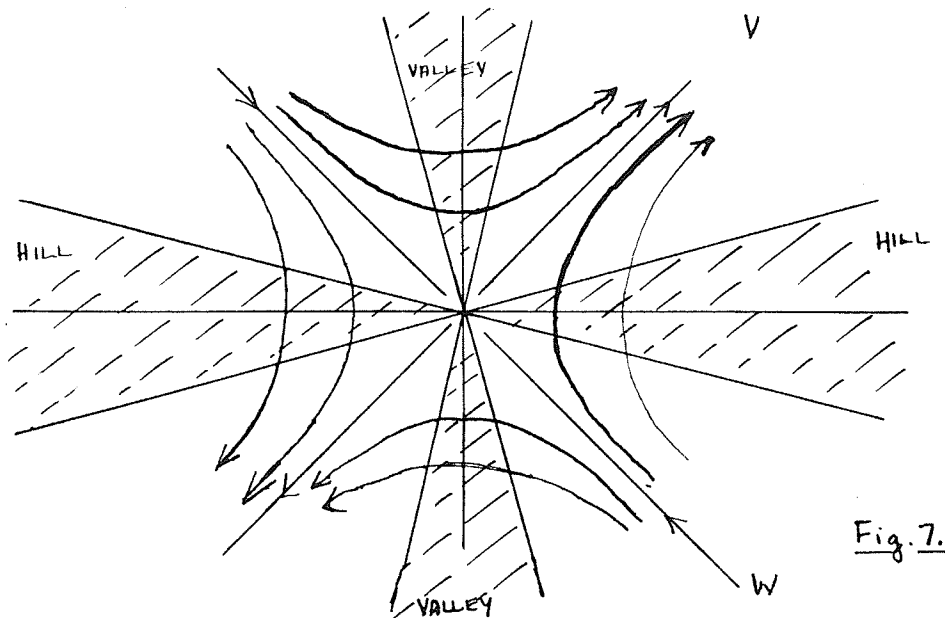


Fig. 7.

3.5 Orbits of Large Radius.

It seems then that the drift of orbit centres produced by the non-uniform electric field can be counteracted by inserting a symmetric second harmonic magnetic flutter field of suitable strength and composed of two hills and two valleys. However, before we proceed to calculate the size of the flutter field required, an important question must be settled. This is the effect of this flutter field on the subsequent motion of the ion.

At an orbit radius of about 10 cm, the electric field through which the ion moves is quite uniform once more. Also, the main flutter field is beginning to take over, and this will provide axial and radial stability. The second harmonic flutter field is not needed any more. If this flutter is cut off sharply, there will be defocussing effects as the ion passes across the boundary from flutter to no flutter. The flutter must be made to die away in such a way that no instabilities are produced.

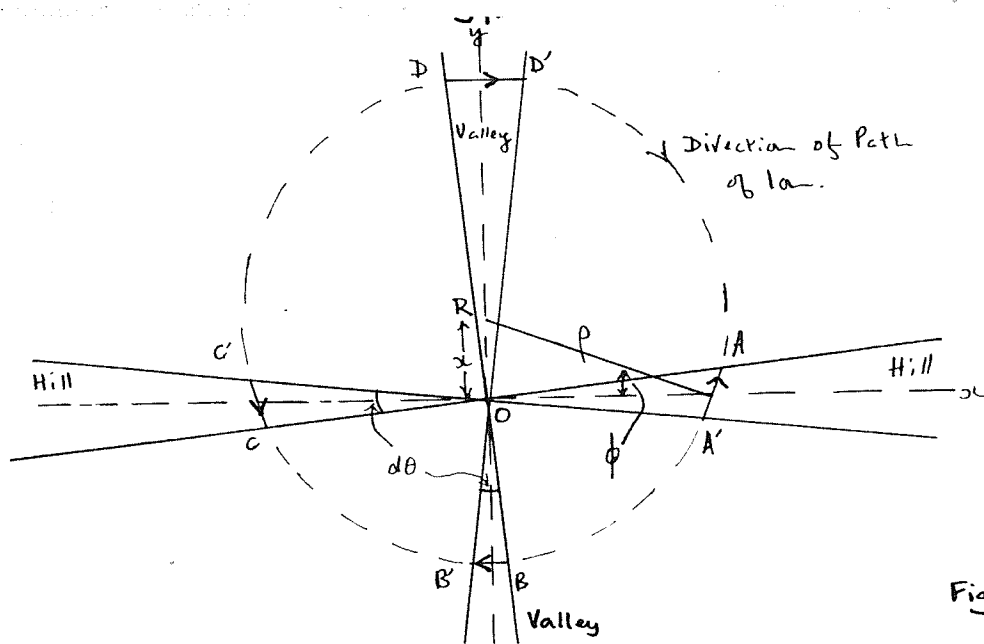


Fig 8.

In Fig. 8 is shown the path of an ion as it describes one revolution in the second harmonic flutter field. The ion moves in an orbit of radius ρ , and has its orbit centre at R. For simplicity, we assume that R is on one of the axes of symmetry, the Oy axis. We will consider first the case of a second harmonic flutter whose sectors have a very small angular width $d\theta$. The strength of the flutter is assumed to be radially dependent i.e., the variation of ΔB with distance r from the origin is given by

$$\Delta B = f(r) \quad \text{for a hill or valley.}$$

The diagram shows the ion moving round the field in a clockwise direction. It enters and leaves the hills at A, A' and C, C' while it enters and leaves the valleys at B, B' and D, D'. The arrows on the lines AA', BB', CC', DD', indicate the direction of the motion of the orbit centre at R as the ion moves through the sector in question.

The magnitude of the displacement of the orbit centre as the ion moves through a sector of the flutter field is a fraction $\frac{\Delta B}{E_0}$ of the path length of the ion through that sector.

From the symmetry of Fig. 3, it can be seen that there is no net displacement of the orbit centre in the y direction. This is because the path lengths AA' and BB' are equidistant from the origin (so they see the same flutter field), they are of equal length and they slope in opposite directions. Their components in the y-direction add up, however.

The net displacement of the orbit centre over one revolution of the ion is in the x-direction and is given by

$$\Delta x = \frac{\Delta B_1}{B_0} AA' \sin \phi + \frac{\Delta B_2}{B_0} CC' \sin \phi - \frac{\Delta B_3}{B_0} BB' + \frac{\Delta B_4}{B_0} DD'$$

this can be seen with reference to Fig. 3.

The first two terms of this expression are equal.

ΔB_1 is the flutter field at AA' etc.

ϕ is the angle which the directions AA' and CC' make with the Cy axis.

Now if h_1, h_2, h_3, h_4 are the widths of the sectors at AA', BB', CC' and DD' and r_1, r_2, r_3, r_4 are the distances of AA', BB', CC' and DD' from the origin, then

$$AA' = \frac{h_1}{\cos \phi} \quad CC' = \frac{h_3}{\cos \phi} \quad \text{and } h_1 = h_3$$

$$BB' = h_2 \quad DD' = h_4.$$

So

$$\Delta x = \frac{1}{B_0} (2 \Delta B_1 h_1 \tan \phi - \Delta B_2 h_2 + \Delta B_4 h_4)$$

Since the radius of the orbit ρ is assumed much larger than the distance x of the orbit centre from the origin, then approximately

$$r_1 = r_3 = \rho$$

$$r_2 = \rho - x \quad \tan \phi = x/r_1$$

$$r_4 = \rho + x$$

Also $h_1 = r_1 \delta\theta$, $h_2 = r_2 \delta\theta$, $h_3 = r_3 \delta\theta$ and $h_4 = r_4 \delta\theta$

Further, the flutter field has a radial dependence $\Delta B = f(r)$

$$\text{So } \Delta B_1 = \Delta B_3 = f(r_1) = f(\rho)$$

$$\Delta B_2 = f(r_2) = f(\rho - x) = f(\rho) - xf'(\rho)$$

$$\Delta B_4 = f(r_4) = f(\rho + x) = f(\rho) + xf'(\rho)$$

In these last two relationships, $f(r_2)$ and $f(r_4)$ have been expanded in a Taylor series to first order.

Substituting for all these quantities in the above expression for Δx , we get

$$\Delta x = \frac{\delta\theta}{B_0} \left[2xf(\rho) - (f(\rho) - xf'(\rho))x(\rho-x) + \frac{(f(\rho) + xf'(\rho))}{x(\rho+x)} \right]$$

which reduces to

$$\Delta x = 2x \frac{\delta\theta}{B_0} (2f(\rho) + \rho f'(\rho))$$

Δx will always be equal to zero if $2f(\rho) + \rho f'(\rho) = 0$ for all ρ .

Thus

$$f'(\rho) = \frac{-2}{\rho} f(\rho)$$

or $f(\rho) = \frac{A}{\rho^2}$ where A is a constant of integration.

So the required radial dependence of the flutter field ($f(r)$) is given by

$$f(r) = \frac{A}{r^2}$$

Note that this radial dependence does not involve the angular width of the sector. The radial dependence has been arrived at with the orbit centre on one of the axes of symmetry. It will be seen in the next section that for the same radial dependence, there is no motion on the 45° axis either. Since then a flutter field falling off radially as $1/r^2$ produces no motion of orbit centres displaced on all eight axes of symmetry about the origin it is safe to assume that the same radial dependence holds good ^{to first approximation} for an orbit displaced in any direction from the origin.

The result is important. It indicates that no matter what the flutter is at small radius, there will be no untoward effect on the subsequent motion of the ion as long as the flutter eventually dies away as $1/r^2$.

3.6 Conditions for Stability.

We have seen that when an ion beam moves in a non-uniform electric field, there is a drift of orbit centres towards the origin in the y-direction and away from the origin in the x-direction. It has also been shown that a four sector magnetic field suitably orientated produces effects so as to reverse the trend of these drifts. It remains to be seen then the size of the flutter required to balance the drifts due to the electric field and due to the flutter field. An orbit centre in such a combined field would remain in a fixed position on the average.

The flutter field arrangement is shown in Fig. 9. Preliminary calculations using a geometrical construction to trace the path of the orbit centre as the ion describes one revolution indicate that if the strength of the flutter field is uniform at all points on all four sectors, then the motion of the orbit centre is extremely small. For an orbit of 10 cm radius with orbit centre displaced 1 cm from the origin, the movement of the orbit centre over one revolution of the ion is about 0.25 mm for flutter field of 0.25 wb/m^2 (the hill and valley sectors being sixty degrees wide). This is a very large flutter.

The crux of the matter is that the motion of the orbit centre is a second order effect. It is the difference between two sets of small terms. In Fig. 9, the components of the paths a, a' add together against the components of paths b, b' .

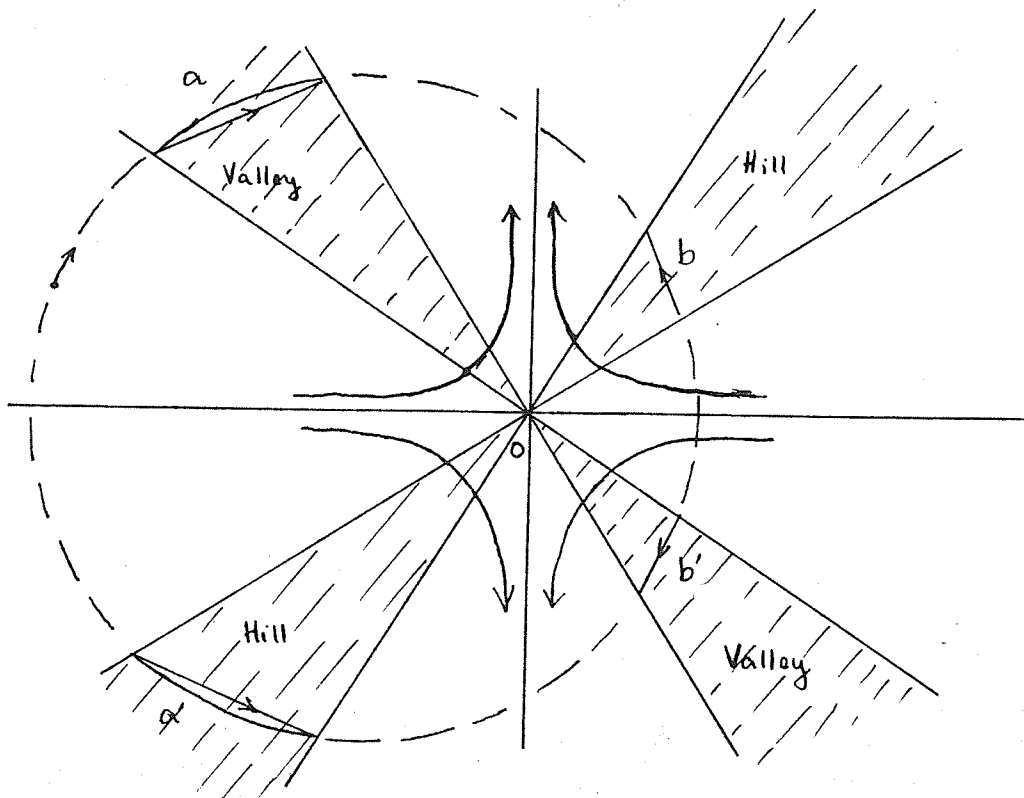


Fig. 9

It is noticed, however, that the paths b, b' are closer to the origin than a, a' . Thus if the flutter field is made to increase with radius, the motion of the orbit centre can be amplified. To keep the fourfold symmetry of the flutter field the radial dependence must be the same (in magnitude) for each sector. Thus the size of the flutter seen at a is the same as that at a' , while the flutter at b equals that at b' .

We can amplify the motion of orbit centres still more if we increase the angular width of the sectors. This can be done quite nicely if the flutter field is given an azimuthal variation of $\sin 2\theta$, i.e., for a point (r, θ) in the field, the strength of the flutter field is given by

$$\Delta B = f(r) \sin 2\theta .$$

The $\sin 2\theta$ term provides that the flutter should be a maximum on the 45° axes and zero on the Ox, Oy axes. If θ is measured from the Ox axis, the $\sin 2\theta$ also provides the correct sign. Thus we have a hill in the first and third quadrants and a valley in the second and fourth quadrants. This arrangement is correct only if the ion is travelling clockwise around the field. If the ion reversed its direction, the hills and valleys would have to be interchanged.

The kind of function $f(r)$ required for the radial dependence of the flutter field will now be derived. Since there is a uniform variation of the flutter at all points in the field, we must consider first the effect of an infinitesimal sector of width $d\theta$. Then we can consider the effect of the whole field simply by integrating over θ . To simplify the

analysis still further, we shall consider the nett effect of four of these infinitesimal sectors at once. Each of these sectors will have the same angular width $d\theta$, each will be in a different quadrant and each will be inclined at an angle θ to the x-axis. If we assume that the hills and valleys are correctly arranged to produce focussing in the x-direction of the orbit centres and defocussing in the y-direction, we can drop the sign of the flutter and consider magnitudes only.

Fig. 10 shows four infinitesimal sectors of angular width $d\theta$ and all inclined to the x-axis. They are labelled hills and valleys as shown and the ion whose orbit centre is at O, moves round the field in a clockwise direction. Its orbital path is shown dotted. The ion crosses the sectors at a, b, c, d and the small arrows in Fig. 10 show the direction in which the orbit centre moves as the ion passes through each sector. The diagram is completely symmetric about the x-axis. The ion paths at a, d make equal contributions to the motion of the orbit centre in the x-direction. So also do the ion paths at b, c. The contributions in the y-direction are equal and opposite so the nett effect is zero. Since a and d are completely equivalent and b and c also completely equivalent, then in future we can forget about c and d as long as we introduce a factor 2 into the calculations.

Let r_a, r_b be the distance from the origin at which the ion crosses the sectors a, b. Let h_a, h_b be the widths of the sectors at these points.

Then $h_a = r_a d\theta$
 $h_b = r_b d\theta$

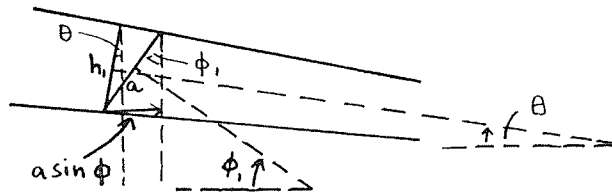
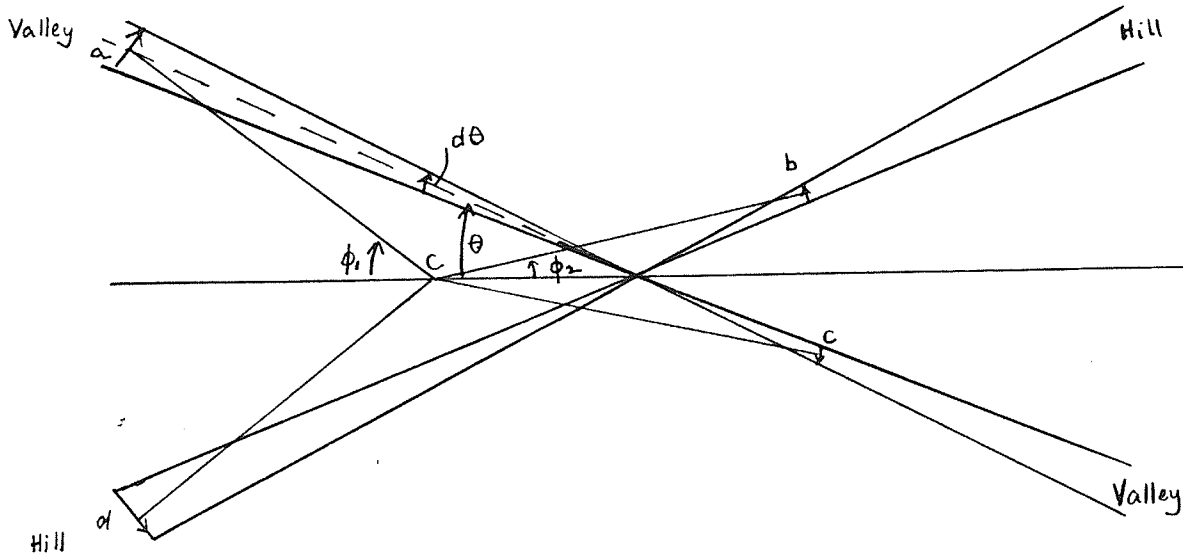


Fig 10.

From the inset in Fig. 10 it is seen that h_a is inclined at θ to the y-direction while a is inclined at ϕ_1 to the y direction. The angle between the two is $(\phi_1 - \theta)$

So $a = \frac{h_a}{\cos(\phi_1 - \theta)}$

and the component of a in the x-direction is $a \sin \phi_1$. To obtain the corresponding motion of orbit centre this must be multiplied by the fraction $\frac{\Delta B_a}{B_0}$. ΔB_a is the magnitude of the flutter at a and B_0 is the uniform magnetic field on which the flutter is superposed.

$\Delta B_a = f(r_a) \sin 2\theta$

since the sign of ΔB_a has already been taken into account when

we gave a direction to a.

Thus the motion of the orbit centre due to the flutter at a is

$$\frac{f(r_a) \sin 2\theta}{B_0} \quad \frac{h_a \sin \phi_1}{\cos(\phi_1 - \theta)}$$

The contribution due to a and d is thus $\frac{2 f(r_a) \sin 2\theta h_a \sin \phi_1}{B_0 \cos(\phi_1 - \theta)}$

Similarly the motion due to b and c is

$$\frac{2f(r_b) \sin 2\theta}{B_0} \quad \frac{h_b \sin \phi_2}{\cos(\phi_2 - \theta)}$$

The net displacement Δx of the orbit centre over one revolution of the ion thus becomes

$$\Delta x = \frac{2 \sin 2\theta d\theta}{B_0} \left[\frac{r_a \sin \phi_1}{\cos(\phi_1 - \theta)} f(r_a) - \frac{r_b \sin \phi_2}{\cos(\phi_2 - \theta)} f(r_b) \right]$$

Now suppose the orbit centre is originally a distance x from the origin. Then, from the simplified diagram of Fig. 11 it is seen that

$$\begin{aligned} \rho \sin \phi_1 &= r_a \sin \theta \\ \rho \cos \phi_1 &= r_a \cos \theta - x \end{aligned}$$

So that

$$\tan \phi_1 = \frac{r_a \sin \theta}{r_a \cos \theta - x}$$

and

$$r_a = \rho \left(1 - \frac{x^2 \sin^2 \theta}{\rho^2} \right)^{\frac{1}{2}} + x \cos \theta$$

or

$$r_a = \rho + x \left(\cos \theta - \frac{x \sin^2 \theta}{2\rho} \right) \quad \text{To first order approximately.}$$

This approximation is valid provided that $x \ll \rho$.

$$\tan \phi_2 = \frac{r_b \sin \theta}{r_b \cos \theta + x}$$

$$r_b = \rho - x \left(\cos \theta + \frac{x \sin^2 \theta}{2 \rho} \right)$$

Consider $\frac{\sin \phi_1}{\cos(\phi_1 - \theta)}$ Expanding we get $\frac{\tan \phi_1}{\cos \theta + \tan \phi_1 \sin \theta}$

Substitute for $\tan \phi_1$ and we get $\frac{r_a \sin \theta}{r_a - x \cos \theta} = \sin \theta \left(1 - \frac{x \cos \theta}{r_a} \right)^{-1}$

Since $\rho \gg x$, then r_a also $\gg x$ and we can expand by the binomial theorem

$$\text{Thus to first order } \frac{\sin \phi_1}{\cos(\phi_1 - \theta)} = \sin \theta \left(1 + \frac{x \cos \theta}{r_a} \right)$$

$$\text{and } \frac{\sin \phi_2}{\cos(\phi_2 - \theta)} = \sin \theta \left(1 - \frac{x \cos \theta}{r_b} \right)$$

Substitute in the expression for Δx and take out the factor $\sin \theta$.

$$\text{Then } \Delta x = \frac{2 \sin \theta \sin 2\theta d\theta}{B_0} \left[f(r_a)(r_a + x \cos \theta) - f(r_b)(r_b - x \cos \theta) \right]$$

$$\text{Now put } r_a = \rho + xK \quad \text{where } K = \cos \theta - \frac{x \sin^2 \theta}{2 \rho}$$

$$r_b = \rho - xL \quad \text{where } L = \cos \theta + \frac{x \sin^2 \theta}{2 \rho}$$

Expand $f(r_a)$, $f(r_b)$ in a Taylor series to first order.

Then

$$f(r_a) = f(\rho) + xK f'(\rho)$$

$$f(r_b) = f(\rho) - xL f'(\rho)$$

the primes denoting differentiation.

Now substitute into the expression for Δx , multiply out and rearrange. After a little work, the expression reduces to

$$\Delta x = \frac{2x(K+L) \sin \theta \sin 2\theta d\theta}{B_0} \left[\rho f'(\rho) + f(\rho) + x(K-L)f'(\rho) + \frac{2x \cos \theta f(\rho)}{K+L} + x \cos \theta \frac{(K-L)f'(\rho)}{K+L} \right]$$

Now $2\cos\theta = K + L$

$-\frac{x\sin^2\theta}{\rho} = K - L$

So

$$\Delta x = \frac{2x \sin^2 2\theta d\theta}{B_0} \left[2f(\rho) + \rho f'(\rho) - \frac{3x^2}{2} \frac{f'(\rho)}{\rho} \sin^2 \theta \right]$$

To obtain the motion of the orbit centre due to the whole flutter field we must integrate over the range $0 \rightarrow \pi/2$.

Since we considered four sectors at once, the range $0 \rightarrow \pi/2$ takes care of the whole field.

We know $\int_0^{\pi/2} \sin^2 2\theta d\theta = \frac{\pi}{4}$

and $\int_0^{\pi/2} \sin^2 \theta \sin^2 2\theta d\theta = \frac{\pi}{8}$

Then the total displacement over one revolution $(\Delta x)_T$ is given by

$$(\Delta x)_T = x \frac{\pi}{2B_0} \left[2f(\rho) + \rho f'(\rho) - \frac{3}{4} x^2 \frac{f'(\rho)}{\rho} \right]$$

The third term is small enough to be neglected so finally we get

$$\frac{(\Delta x)_T}{x} = \frac{\pi}{2B_0} \left[2f(\rho) + \rho f'(\rho) \right]$$

This is the fractional displacement of the orbit centre at radius ρ over one revolution. Suppose that at this radius the electric field produces a fractional displacement $\lambda(\rho)$ of the orbit centre over one revolution. Then if

$$\frac{\pi}{2B_0} \left[2f(\rho) + \rho f'(\rho) \right] = \lambda(\rho)$$

then the electric instability will be annulled.

Rearranging we get

$$f'(p) + \frac{2f(p)}{p} = \frac{2B_0}{\pi} \frac{\lambda(p)}{p}$$

Multiply throughout by p^2

$$p^2 f'(p) + 2p f(p) = \frac{2B_0}{\pi} p \lambda(p)$$

From which

$$f(p) = \frac{2B_0}{\pi p^2} \int p \lambda(p) dp + \frac{C}{p^2}$$

C is a constant to be determined.

This is the radial variation of the flutter field that is required to annul the electric instability. The form of the function depends very much on how λ varies with radius. Usually λ is very small at small radius, rises very rapidly to some maximum value then falls off slowly.

Computer calculations give values of λ at various radii. The maximum value of λ is about 0.4 occurring at a radius of 5cm. It is found that the flutter field required need not exceed about 1400 gauss. This is very encouraging.

There is one final point. If λ is put equal to zero, we obtain the radial dependence required for there to be no movement of the orbit centre. This is

$$f(p) = \frac{C}{p^2}$$

This is exactly the same function obtained in the last section when the orbit centre was on the axis of maximum flutter. So if this radial variation is used, there will be no motion of

orbit centres on any of the Ox , Oy or 45° axes. Thus we can safely say that there will be no motion at any point near the origin since the maximum instability occurs on these axes.

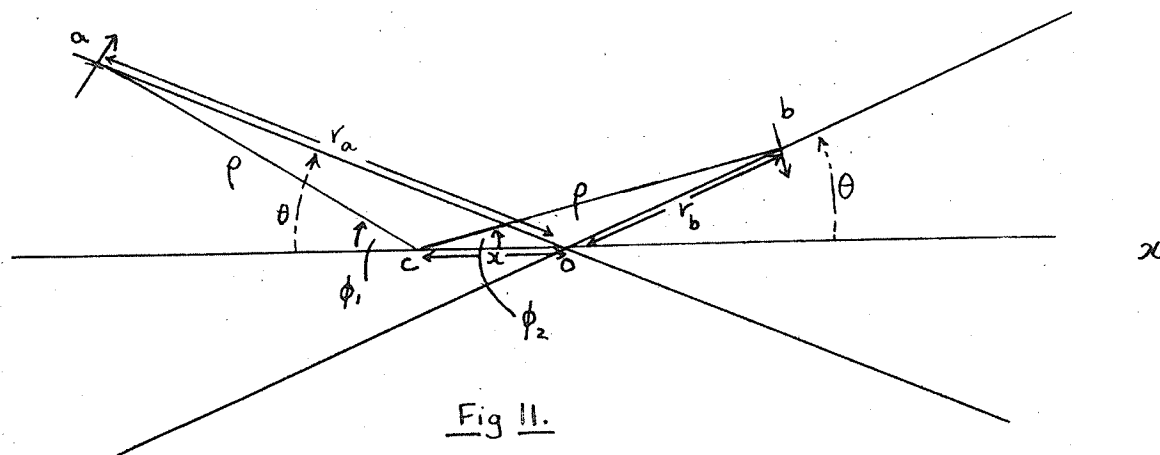


Fig II.

3.7. Addendum.

It is well-known that a second harmonic flutter field produces a radial instability of ion orbits in the cyclotron. The suggestion of using such a field to produce stability might therefore seem most surprising. It must be remembered however that in the University of Manitoba cyclotron there is already a radial instability due to the electric field. What we essentially want to do is to counteract this by an instability in the opposite direction. This can be done using a second harmonic flutter field suitably orientated. If this flutter field is given a suitable radial variation, the instability produced by the electric field can be eliminated.

CHAPTER 4

THE VERTICAL MOTION

4.1 Introduction.

The axial motion of ions under electric and magnetic fields in the cyclotron was investigated extensively by M. E. Rose⁽⁴⁾ in 1936. In his treatment of the electric field he considered the axial motion of an ion as it crossed the dee gap under two sets of conditions.

a) taking into account the time variation of the electric field but neglecting the change in velocity of the ion as it crossed the gap.

b) taking into account the change in velocity of the ion but neglecting the time variation of the electric field.

He thus divided the electric axial focussing into two parts - the "field variation" focussing corresponding to case (a) above and the "energy change" focussing corresponding to case (b). The physical significance of these terms is as follows.

The electric field lines across the dee gap point towards the median plane in the first half of the gap but point away from the median plane in the second half of the gap. (Fig. 1) Thus it would seem that when an ion crossed the gap the electric forces tending to drive it into the median plane experienced during the first half of the gap would be counteracted completely by forces in the opposite direction in the second half of the gap. This, however, is not the case. During the passage of the ion through the gap it is being continuously accelerated. So

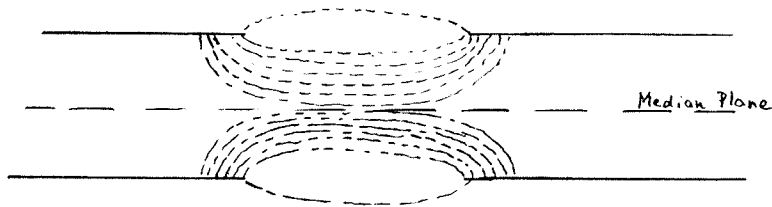


Fig 1. Electric Field in a Dees Gap.

it will spend less time in the second (defocussing) half of the gap than in the first. Therefore, there will be a resulting force on the ion which is always focussing. This is what Rose calls the "Energy Change" focussing.

Furthermore, the electric field is changing in time as the ion crosses the gap. If the ion crosses the gap slightly out of phase with the electric field the focussing and defocussing forces will be not quite equal. There will be a net force on the ion which will be focussing or defocussing, depending on whether the electric field is decreasing or increasing as the ion crosses the gap.

The results of Rose's analysis are as follows.

a) the electric focussing is only a differential effect being the difference between a focussing and defocussing deflexion.

b) Rose expressed the focussing effect in terms of $\Delta\alpha$, the deflexion of the ion in the lens. The expression for the field variation focussing was found to be

$$(\Delta\alpha)_{f.v.} = - \frac{e V_0 \sin\theta}{E} \frac{w}{v} z$$

where V_0 is the peak dee potential, θ is the angle by which the ion is out of phase with the accelerating potential, v and E are the velocity and energy of the ion, e is the charge on the ion, ω is the angular frequency of the accelerating potential and x is the distance of the ion from the median plane.

The deflexion $\Delta\alpha$ is towards the median plane for positive θ (a phase lag of the ion) and away from the median plane for negative θ (a phase lead of the ion). Thus the field variation forces are focussing only if the ion crosses the gap in a decreasing electric field.

Note that the magnitude of the field variation focussing is independent of the shape of the dees. Nothing would be gained by altering the shape of the dees, e.g., by having one dee higher than the other (Fig. 8).

c) Rose found that the deflexion due to the energy change always gave focussing and is dependent on the geometry of the dees. He obtained an expression for the ratio of the energy change and field variation contributions to the focussing

$$\text{viz } \frac{(\Delta\alpha)_{\text{en.ch.}}}{(\Delta\alpha)_{\text{f.v.}}} = b \left(\frac{eV_0}{E} \right)^{3/2} \frac{\cos^2 \theta}{\sin \theta}$$

where b is a constant depending on the geometry. For customary geometries, b is of the order of unity.

The expression is fairly small at appreciable energies indicating that the energy change term is a relatively minor

effect. The contribution due to the field variation is the most important. The contribution due to the energy change is more appreciable at smaller energies, but even at an energy of $10eV_0$ which is the smallest energy at which Rose's analysis still holds, the energy change term is still only of the order of one-thirtieth of the field variation term. Rose's analysis is not valid near the central region of the cyclotron where the energy of the ion is less than $10eV_0$.

Rose did not extend his analysis to the centre region of the cyclotron. This was done, however, by R.R. Wilson⁽⁵⁾ whose paper was published at the same time as was Rose's. Wilson investigated the energy change term only. He used analytical methods for ions whose orbit radii were greater than 10 cm, while he used a graphical method for smaller orbits. He was able to show that the energy change term increased as the energy of the ion decreased, and reached a maximum at an energy somewhat less than $10eV_0$. At still smaller energies there was a rapid decrease of the energy change term to zero.

Recently, Rose's work has been developed by B. L. Cohen⁽⁶⁾. Using an analytic expression for the electric field of the cyclotron at Oak Ridge National Laboratory, he has found a solution to Rose's basic equation which connected the energy change of the ion as it crossed the dee gap with the time variation of the electric field. Rose, in his analysis, split up the equation into two independent parts and evaluated them separately to obtain the field variation and energy change terms.

Cohen has shown that the energy change and field variation terms are not quite independent. He obtains a focussing formula which contains Rose's terms together with two second order correction terms which are defocussing and a first order correction term which may be defocussing or focussing. This first order term is a correction to Rose's field variation term. It is always less than the field variation term and of the same sign. Cohen's analysis is valid down to energies of about $10eV_0$. At this energy the ion has just about completed its third revolution out from the ion source and is starting on its fourth.

In the treatments of Rose, Cohen and Wilson, outlined above, one of the main assumptions was that the equipotentials between the dees were always parallel to the edges of the dees, throughout the length of the dees. This is not true in the Manitoba cyclotron. The aim of this chapter is to investigate what modifications, if any, must be made in order to generalise these treatments, to the field of the Manitoba cyclotron. The problem can be broken down into two parts. First we will consider ions whose energies are less than $10eV_0$, i.e., we will examine the vertical motion during the first three revolutions. This region we will call the Wilson region of the cyclotron, as Wilson's treatment, or some modification of it, will apply here. At energies greater than $10eV_0$, the Rose-Cohen analysis is valid. So the region of the cyclotron in which the ion moves with energies above $10eV_0$ will be called the Rose-Cohen region.

4.2. The Wilson Region.

Graph I of Chapter 5 shows the orbits of various ions computed for the Manitoba cyclotron at a dee voltage of 42 KV. The dee boundaries are also shown. It is seen that for the first three revolutions the ions enter and leave the dees across their horizontal boundaries. Thus, during the first three revolutions at least, the dees are "orthodox", that is, they are exactly the same as in a conventional cyclotron. Hence, Wilson's treatment need not be modified at all for the Manitoba cyclotron and his general conclusions about the behavior of the energy change term at low energies still apply.

4.3. The Rose-Cohen Region.

Referring again to Graph I of Chapter 5, it is seen that after the ion has described its first three revolutions, and its energy is large enough for the Rose-Cohen analysis to become valid, the ion still describes at least one more revolution within the horizontal dee boundaries. During this revolution, all the Rose-Cohen conditions as regards energy of the ion and uniformity of the field are valid. Therefore, their analysis holds to a good approximation. In subsequent revolutions, however, the ion crosses the boundaries of the dees which are perpendicular to the Ox axis and parallel to the Oy axis. The field in which the ion moves is not uniform any more.

At high energies, it is seen from Fig. 2 that the field lines start to become straight and parallel once more. The distance through which the ion travels between the dees becomes quite large, and the only appreciable electric fields seen by the ion are near the dee edges. In between, the ion travels in a virtually field-free region. The effect is as if a dummy dee were placed near each dee edge. The electric fields seen by the ion as it enters and leaves the dees are quite uniform and the Rose-Cohen theory can be applied. Thus we have a situation in which the Rose-Cohen theory is valid at low energies and also at high energies. It could be surmised that the theory is not going to change by very much at these intermediate energies, since nothing drastic happens to the field here.

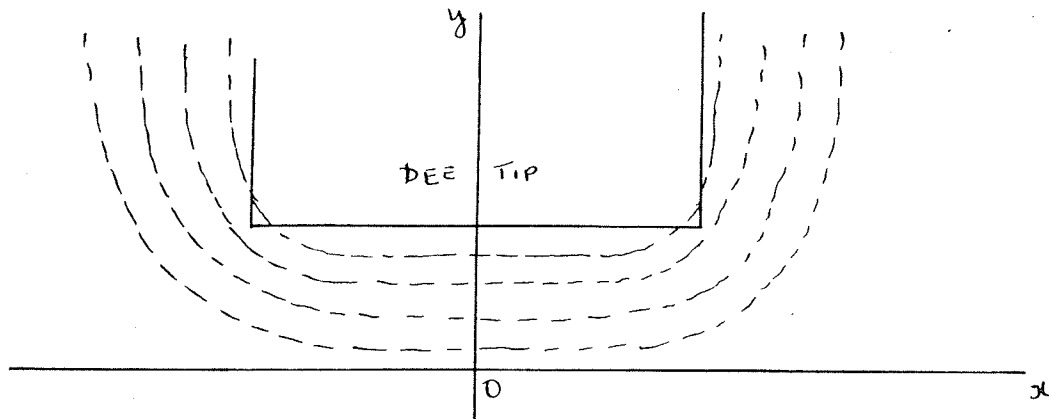


Fig 2. Equipotentials About a Dee Tip.

We will now examine the situation in greater detail, first giving the Rose-Cohen treatment for an ion moving across the dee gap in a uniform field. Later we will discuss what modifications must be made for the non-uniform field in the University of Manitoba cyclotron.

Consider an ion moving across the dee gap in a uniform electric field. The ion is moving in a direction parallel to the y-axis along the electric field lines. Since the field is uniform, the electric field lines will be straight and parallel. Suppose that at time t, the ion is at a point P (x,y,z) in the electric field. The point P is distance z from the median plane. The equation of motion for the ion in the axial direction is

$$m \frac{d^2 z}{dt^2} = - e \frac{\partial V_t}{\partial z}$$

where V_t is the potential at the point P at time t. Now if v is the velocity of the ion along its path then $v = \frac{dy}{dt}$ and

$$v \frac{d}{dy} = \frac{d}{dt}$$

So
$$\frac{d^2 z}{dt^2} = v \frac{d}{dy} \left(v \frac{dz}{dy} \right)$$

Here, we assume that at the energies concerned, the energy change focussing is much smaller than the field variation focussing. This is true as Rose and Cohen have shown that the energy change term rapidly dwindles away as the energy increases.

Hence we may neglect the change in velocity of the ion as it crosses the gap to a very good approximation. Thus we get

$$m \frac{d^2 z}{dy^2} = mv^2 \frac{d^2 z}{dy^2} = 2E \frac{d^2 z}{dy^2}$$

where E is the energy of the ion. The equation of motion becomes

$$\frac{d^2 z}{dy^2} = - \frac{e}{2E} \frac{\partial V_t}{\partial z} \quad \text{u.l.}$$

Now at time t , $V_t = V(x, y, z) \cos (wt + \theta)$ where $V(x, y, z)$ is the peak potential at the point P . The angle θ is the phase difference between the ion and the accelerating potential. If θ is positive, this represents an ion lagging the potential. Such an ion crosses the dee gap in a decreasing electric field. The focussing of the ion as it crosses the dee gap is determined by the deviation of its path as it crosses the gap. The gradient of the path of the ion is given by $\frac{dz}{dy}$, and the change in this quantity as the ion crosses the dee gap is the path deviation $\Delta\alpha$. Obviously, if $\Delta\alpha$ is negative, this implies a focussing effect.

$$\Delta\alpha = \left(\frac{dz}{dy} \right)_{y = \infty} - \left(\frac{dz}{dy} \right)_{y = -\infty}$$

Since at $y = \pm \infty$ the ion will be totally inside the dees and in zero electric field. We are thus required to integrate equation 4.1 between the limits $y = +\infty$ and $y = -\infty$.

$$\text{i.e. } \Delta\alpha = \int_{-\infty}^{\infty} \frac{d^2z}{dy^2} dy = - \frac{e}{Z E} \int_{-\infty}^{\infty} \frac{\partial V_t}{\partial z} dy.$$

$$\text{Now } \frac{\partial V_t}{\partial z} = \frac{\partial V}{\partial z} \cos (wt + \theta) = \frac{\partial V}{\partial z} (\cos wt \cos \theta - \sin wt \sin \theta)$$

Also, if the time is measured from the instant at which the ion crosses the midpoint of the dee gap, then $t = \frac{y}{v}$

Thus

$$\Delta\alpha = -\frac{e \cos \theta}{2E} \int_{-\infty}^{\infty} \frac{\partial V}{\partial z} \cos \left(\frac{\omega y}{v} \right) dy + \frac{e \sin \theta}{2E} \int_{-\infty}^{\infty} \frac{\partial V}{\partial z} \sin \left(\frac{\omega y}{v} \right) dy \quad 4.2.$$

The kernel of the first integral is antisymmetric since $\frac{\partial V}{\partial z}$ is antisymmetric across the dee gap and $\cos \frac{wy}{v}$ is symmetric.

The statement that $\frac{\partial V}{\partial z}$ is antisymmetric assumes that the dees are exactly alike. The value of the first integral is thus equal to zero. So we are left with

$$\Delta \alpha = \frac{e \sin \theta}{2E} \int_{-\infty}^{\infty} \frac{\partial V}{\partial z} \sin \frac{wy}{v} dy \quad 4.3$$

At the point P, Laplace's equation holds in three dimensions

$$\frac{\partial^2 V}{\partial x^2} + \frac{\partial^2 V}{\partial y^2} + \frac{\partial^2 V}{\partial z^2} = 0$$

However, since the field lines are straight and parallel to the y-axis, then there is no electric field component in the x-direction. Thus $\frac{\partial^2 V}{\partial x^2} = 0$ and we may write

$$\frac{\partial^2 V}{\partial y^2} + \frac{\partial^2 V}{\partial z^2} = 0 \quad 4.4$$

for the uniform electric field concerned. Furthermore, since the distance across the dee gap is small, then for finite values of $\frac{\partial V}{\partial z}$, $\frac{wy}{v}$ is small and we can set $\sin \frac{wy}{v}$ equal to $\frac{wy}{v}$ with small error.

Thus
$$\Delta \alpha = \frac{e \sin \theta}{2E} \int_{-\infty}^{\infty} \frac{w}{v} \frac{\partial V}{\partial z} y dy \quad 4.5$$

Integrating by parts we get

$$\int_{-\infty}^{\infty} \frac{\partial V}{\partial z} y dy = y \int_{-\infty}^{\infty} \frac{\partial V}{\partial z} dy - \int_{-\infty}^{\infty} dy \int_{-\infty}^y \frac{\partial V}{\partial z} dy$$

The first term is zero as the kernel is antisymmetric. The

second term may be evaluated by noting that

$$\frac{\partial}{\partial z} \left[\int_{-\infty}^{\infty} dy \int_{-\infty}^{\infty} \frac{\partial V}{\partial z} dy \right] = \int_{-\infty}^{\infty} dy \int_{-\infty}^{\infty} \frac{\partial^2 V}{\partial z^2} dy$$

which is equal to, by virtue of 4.4, $-\int_{-\infty}^{\infty} dy \int_{-\infty}^{\infty} \frac{\partial^2 V}{\partial y^2} dy$

i.e.

$$\frac{\partial}{\partial z} \left[\int_{-\infty}^{\infty} dy \int_{-\infty}^{\infty} \frac{\partial V}{\partial z} dy \right] = - \int_{-\infty}^{\infty} \frac{\partial V}{\partial y} dy = 2V_0 \quad 4.6$$

where V_0 is the peak potential on each dee. Note that the minus sign vanishes. This is because we are integrating across the dee from a high potential to a low potential and so

$$[V_{\infty} - V_{-\infty}] = -2V_0$$

Now we must multiply both sides of 4.6 by dz and integrate.

from $z = 0$ to z . Note that we are assuming $\frac{\partial}{\partial z} = \frac{d}{dz}$.

This is true with small error. Thus we get

$$\int_{-\infty}^{\infty} dy \int_{-\infty}^{\infty} \frac{\partial V}{\partial z} dy = 2V_0 z.$$

Finally we substitute into 4.5 to get Rose's focussing formula

$$\Delta \alpha = \frac{-eV_0}{E} \sin \theta \frac{\omega z}{v} \quad 4.7$$

Note that $\Delta \alpha$ is negative for a phase lag of the ion. (θ is positive.)

Now we must see where Rose's assumptions break down in the case of a non-uniform field. We will compare Rose's electric field with the field in the Manitoba cyclotron. Then we can see what modifications must be made so that Rose's treatment can be extended to the non-uniform field.

Rose assumed that the electric field in the dee gap was uniform and that the ion moved across the gap parallel to the electric field lines. He also assumed that the path of the ion in the dee gap was straight and that the width of the dee gap was small. Thus the ion spent only a short time in regions where the electric field was appreciable.

In the dee gap of the Manitoba cyclotron, the path of the ion is curved. So we must integrate over the ion path 's' rather than in the y-direction. To preserve consistency, we will measure the distance of an ion along its path as it crosses the dee gap from the point at which the path crosses the xz plane. The gradient of the path will now be $\frac{dz}{ds}$. However, we cannot now integrate from $s = -\infty$ to $s = +\infty$. This is physically misleading, as the ion will in practice cross an infinite number of subsequent dee gaps as s goes to infinity. What we really want to do is to integrate over that part of the path near the dee gap in question where the electric field is appreciable. For this reason we will take the limits $s = \pm a$, where $\pm a$ are the points on the path and inside the dee where the electric field has become infinitesimally different from zero. It must be emphasized that taking these new limits will not alter the value of the integrals in question - the new limits just make the operation more meaningful. Equation 4.2 now becomes

$$\Delta\alpha = - \frac{e \cos \theta}{2E} \int_{-a}^a \frac{\partial V}{\partial z} \cos \frac{ws}{v} ds + \frac{e \sin \theta}{2E} \int_{-a}^a \frac{\partial V}{\partial z} \sin \frac{ws}{v} ds \dots 4.3$$

Whatever the shape of the field between the dees, it still retains its essential symmetry. Thus $\frac{\partial V}{\partial z}$ as a function of s is antisymmetric. Hence the first integral is zero. We are left with

$$\Delta \alpha = \frac{e \sin \theta}{2E} \int_{-a}^a \frac{\partial V}{\partial z} \sin \frac{ws}{v} ds \quad 4.9$$

In the field we are considering, the ion will not be moving parallel to the field, nor will the electric field be uniform. The equipotentials will take the form of curved surfaces, and though Laplace's equation will still hold in three dimensions, the relation $\frac{\partial^2 V}{\partial s^2} + \frac{\partial^2 V}{\partial z^2}$ will not be equal to zero.

To treat this case, we must first make the simplifying assumption that the ion is moving orthogonal to the equipotentials, i.e., along the electric field lines. Afterwards we can modify the results obtained so as to include ions moving across the field lines.

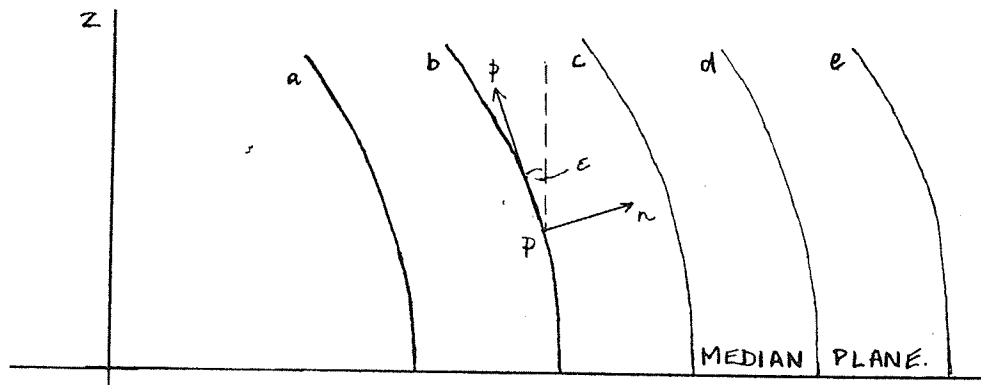


Fig. 3. Plane of the paper represents an equipotential surface through P. a, b, c, d, e, are sections of surfaces orthogonal to the equipotential surface. They represent the surfaces of the electric field in the vicinity of P.

The equipotentials form a family of curved surfaces surrounding each dee. We can construct a set of surfaces ortho-

gonal to them and these surfaces will contain the electric field directions. In Fig. 3, the plane of the paper represents the surface of an equipotential at the point P. The lines represent sections of surfaces out of the plane of the paper, orthogonal to the equipotential surface. These surfaces contain the electric field directions and since the ion is assumed to be moving parallel to the electric field and orthogonal to the equipotentials, then the path of the ion at P will be into the plane of the paper.

Accordingly, we can construct at P a set of orthogonal curvilinear coordinates P_s , P_n , P_p . P_s is taken tangential to the path of the ion at P, into the plane of the paper, P_n is along the outward normal to the electric field surface at P, and P_p is tangential to the field surface at P and perpendicular to P_s , P_n .

At P, Laplace's equation holds

$$\frac{\partial^2 V}{\partial s^2} + \frac{\partial^2 V}{\partial p^2} + \frac{\partial^2 V}{\partial n^2} = 0$$

Also, since P_n is along the normal to the surface, P_n is in an equipotential. Along P_n therefore, the potential V remains constant and $\frac{\partial^2 V}{\partial n^2} = 0$

$$\text{Thus } \frac{\partial^2 V}{\partial p^2} + \frac{\partial^2 V}{\partial s^2} = 0 \quad 4.10$$

Note that the P_p axis is not identified with the z-axis. This is why $\frac{\partial^2 V}{\partial s^2} + \frac{\partial^2 V}{\partial z^2}$ cannot equal zero except when P is on the

median plane. For points off the median plane, the Pp axis will be inclined to the z-axis at some angle ϵ which varies along the path of the ion. At the point P, the electric field in the z-direction will be

$$\frac{\partial V}{\partial z} = \frac{\partial V}{\partial p} \cos \epsilon \quad 4.11$$

$\cos \epsilon$ is a symmetric function of ϵ and $\frac{\partial V}{\partial p}$ is an antisymmetric function of ϵ . The general form of the function $\frac{\partial V}{\partial p}$ will be similar to that of $\frac{\partial V}{\partial z}$.

Indeed, the two are identical on the median plane. In equation 4.9 we can replace $\frac{\partial V}{\partial z}$ by $\frac{\partial V}{\partial p} \cos \epsilon$. We do not know how ϵ varies over the path of the ion. However, we know that it will be small and we can simplify the analysis by taking an average value $\overline{\cos \epsilon}$. Then 4.9 becomes

$$= \frac{e \sin \theta}{2E} \overline{\cos \epsilon} \int_{-a}^a \frac{\partial V}{\partial p} \sin \frac{ws}{v} ds. \quad 4.12$$

Now Rose was able to set $\sin \frac{ws}{v}$ equal to $\frac{ws}{v}$ since the dee gap was small. We cannot take a similar step here, however, since the dee gap in our case is large. In practice the angular width of the dee gap will be something like 120° . So the maximum value of $\frac{ws}{v}$ will be something like $\pi/3$ radians.

We can see what difference the function $\sin \frac{ws}{v}$ instead of $\frac{ws}{v}$ will make by comparing the functions

$$\frac{\partial V}{\partial p} \sin \frac{ws}{v} \quad \text{and} \quad \frac{\partial V}{\partial p} \frac{ws}{v}$$

over the range $-a < s < a$. The function $\frac{\partial V}{\partial p}$ is anti-symmetric

and is represented in Fig. 4 by the curve (a). The functions $\sin \frac{ws}{v}$ and $\frac{ws}{v}$ are also anti-symmetric, and are represented by

curves (b) and (c). The value of the integral $\int_{-a}^a \frac{\partial V}{\partial p} \sin \frac{ws}{v} ds$

is found by multiplying curve (a) by curve (b) and finding the area under the resulting curve. Similarly, the integral

$\int_{-a}^a \frac{\partial V}{\partial p} \frac{ws}{v} ds$ is found by multiplying curve (a) by curve (c) and

finding the area under the resulting curve. For values of $\frac{ws}{v}$

greater than $\pi/3$ and less than $-\pi/3$, the function $\frac{\partial V}{\partial p}$ will be

infinitesimally different from zero, so we can neglect the area under the curve beyond these limits, with very small error. It

can be seen straight away that the value of the integral

$\int_{-a}^a \frac{\partial V}{\partial p} \sin \frac{ws}{v} ds$ will be less than $\int_{-a}^a \frac{\partial V}{\partial p} \frac{ws}{v} ds$. The differ-

ence between the two is not determinable since we do not know

the form of the function $\frac{\partial V}{\partial p}$ explicitly. However, we can obtain

an estimate of the difference by comparing the areas enclosed

by the functions $\sin \frac{ws}{v}$ and $\frac{ws}{v}$ over the range $-\pi/3 < \frac{ws}{v} < \pi/3$.

It can easily be shown that $\int \sin \frac{ws}{v} ds = \frac{v}{w}$ over this range

whereas $\int \frac{ws}{v} ds = \frac{v}{w} \frac{\pi^2}{9} = 1.097 \frac{v}{w}$. Hence the function

$\sin \frac{ws}{v}$ will reduce the value of the integral somewhat but the amount by which it is reduced will be of the order of 10%. We can set

$$\int_{-a}^a \frac{\partial V}{\partial p} \sin \frac{ws}{v} ds = (1 - K) \int_{-a}^a \frac{\partial V}{\partial p} \frac{ws}{v} ds$$

where K is usually of the order of 10%. An upper limit for K (worst possible case) can be found by comparing $\sin \pi/3$ and $\pi/3$. There is a difference of about 21% between the two. This would represent the case of a rather exotic non-uniform field.

We can now proceed to integrate the integral

$$\int_{-a}^a \frac{\partial V}{\partial p} \frac{ws}{v} ds \text{ in a manner exactly the same as we did for the integral } \int_{-a}^a \frac{\partial V}{\partial z} \frac{wy}{v} dy. \text{ We get a very similar result}$$

$$\int_{-a}^a \frac{\partial V}{\partial p} \frac{ws}{v} ds = 2V_0 p \tag{4.13}$$

Here p will be the distance of the ion above the median plane measured in the surface containing the electric field directions. In our expression for $\Delta\alpha$ we now have a factor p and a factor $\overline{\cos \epsilon}$. Clearly $p \overline{\cos \epsilon}$ is going to represent some mean distance of the ion from the median plane. Let us put $p \overline{\cos \epsilon} = \bar{z}$ and so write

$$\Delta\alpha = -\frac{eV_0}{E} \sin \frac{w}{v} \bar{z} (1 - K) \tag{4.14}$$

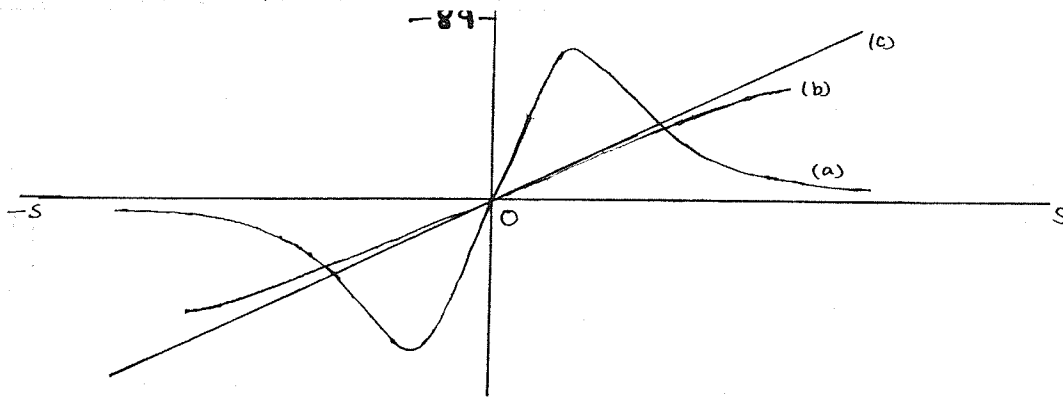


Fig 4

- a) Variation of $\frac{\partial V}{\partial p}$ with path length s .
 s is measured from the point at which the ion crosses midpoint of gap.
 b) Variation of $\sin \frac{\omega s}{v}$ with s .
 c) Variation of $\frac{\omega s}{v}$ with s .

Hitherto we have considered the path of the ion to be parallel to the electric field lines. We have seen earlier that this is definitely not the case. To see how the above conclusions must be modified, to accommodate the ion moving across the field lines, consider once more the case of Rose's uniform field with the ion travelling at an angle η to the field lines.

The velocity of the ion along the field lines is then $v \cos \eta$ and Rose's formula becomes

$$\Delta \alpha = \frac{-eV_0}{E} \frac{\sin \theta}{\cos^3 \eta} \frac{\omega z}{v} \quad 4.15$$

Note the occurrence of a $\cos^3 \eta$ factor instead of just a $\cos \eta$ factor as might be expected. This is because the factor E implies a v^2 term.

Thus it is seen that the amount of focussing is increased when the ion is not moving parallel to the field. Physically, this means that the ion takes longer to cross the dee gap and so the axial forces have a longer time in which to influence it.

For an ion in the non-uniform field of the University of Manitoba cyclotron, the angle between the path of the ion and the electric field is continuously varying. However, some idea of the extent of the effect may be obtained by integrating $\cos^3 \eta$ across the dee gap and finding the average value.

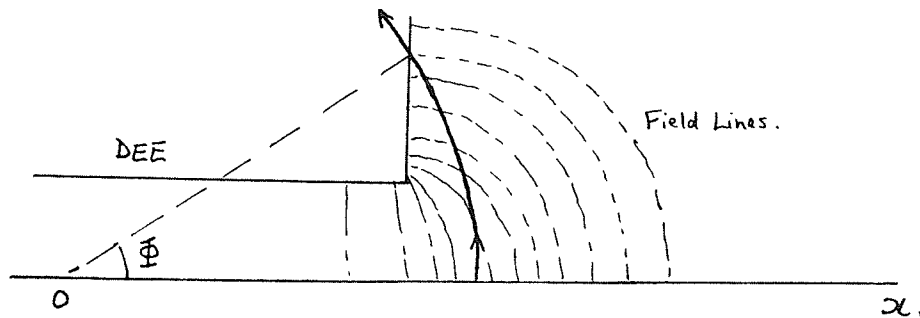


Fig 5 Path of Ion through Electric Field

Again we do not know how $\cos \eta$ varies throughout the path, but we can obtain an estimate of the order of magnitudes involved in the following way.

Consider the path of the ion from the time it crosses the x axis to the time it enters the dee (Fig. 5). Suppose that the edge of the dee at which it enters is parallel to the y-axis. Then the electric field there will be parallel to the x-axis whereas on the x-axis the electric field is perpendicular to the x-axis. Suppose the angular width of the path of the ion between the point at which it crosses the x-axis and the point at which it enters the dee is ϕ . Then as it crosses the x-axis, the ion is moving parallel to the field. However

when it enters the dee, the ion is moving at an angle $(\pi/2 - \Phi)$ to the field (see Fig. 5). If we assume that η varies uniformly as the ion traverses its path, then the value of η at an intermediate angle ϕ between 0 & Φ is given by

$$\eta = \phi \left(\frac{\pi}{2\Phi} - 1 \right)$$

The average value of $\cos^3 \eta$ over this half dee gap is given by

$$\langle \cos^3 \eta \rangle_{av} = \frac{1}{\Phi} \int_0^{\Phi} \cos^3 \left(\frac{\pi}{2\Phi} - 1 \right) \phi \, d\phi$$

which can be shown to be equal to $\frac{\cos \Phi}{\pi/2 - \Phi}$ ^{together with} ~~neglecting~~ terms

in $\cos^3 \Phi$

So the average value of $\cos^3 \eta = \frac{\cos \Phi}{\pi/2 - \Phi}$

For $\Phi = \pi/3$ $\langle \cos^3 \eta \rangle_{av} = 0.87$.

The final formula for $\Delta\alpha$ thus becomes

$$\Delta\alpha = \frac{-eV_0}{H} \frac{\sin\theta}{\langle \cos^3 \eta \rangle_{av}} \frac{wZ}{v} (1 - K) \quad 4.16$$

The effect of the $1 - K$ and $\cos^3 \eta$ terms is to counteract each other. Therefore the axial focussing ~~will~~ not be damaged much for the non-uniform field in the Manitoba cyclotron.

4.4. Axial Focussing at Larger Radii.

The first thing that must be made clear is that when we refer to orbits of large radius in this section, we mean orbit radii of 8-10 cm.

Rose has shown that the significance of the energy-change term decreases rapidly with energy. Furthermore, Cohen's second-order interaction terms contain an energy change term

which is always defocussing, and thus tends to cancel out Rose's energy change term. Hence it may be safely assumed that at the orbit radii in question, the ion has reached an energy large enough that the energy change contribution to the focusing is negligible. It remains then to consider the field variation contribution only.

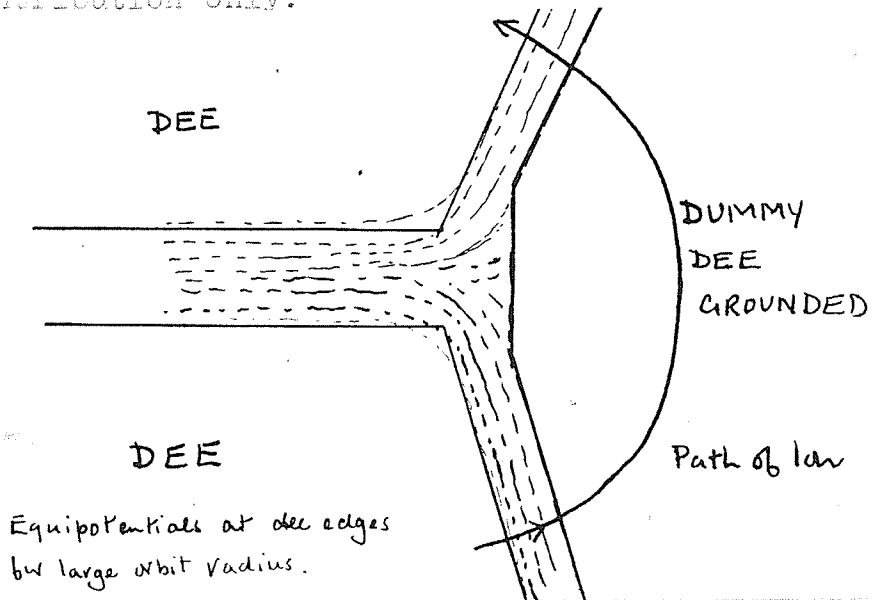


Fig 6.

When the ion has reached an orbit radius of the order of 8-10 cm, the path of the ion in the dee gap becomes quite large. The dees are widely separated at this radius and the ion travels between them in a virtually field free region, encountering an appreciable field only near the dee edges. These fields, being so close to the dee edges, are quite uniform, and the field lines may be regarded as straight and parallel to a good approximation. The overall effect is as if there were a grounded dummy dee placed in the dee gap near each dee edge (Fig. 6).

The electric fields in the gap between each dee and its dummy are uniform. The ion crosses each gap at some small angle of say η to these electric fields. Each dee, together with its dummy, constitutes an electric lens similar to that considered by Rose. To find out whether these lenses are focussing or defocussing, we must consider the rate of field variation across each gap.

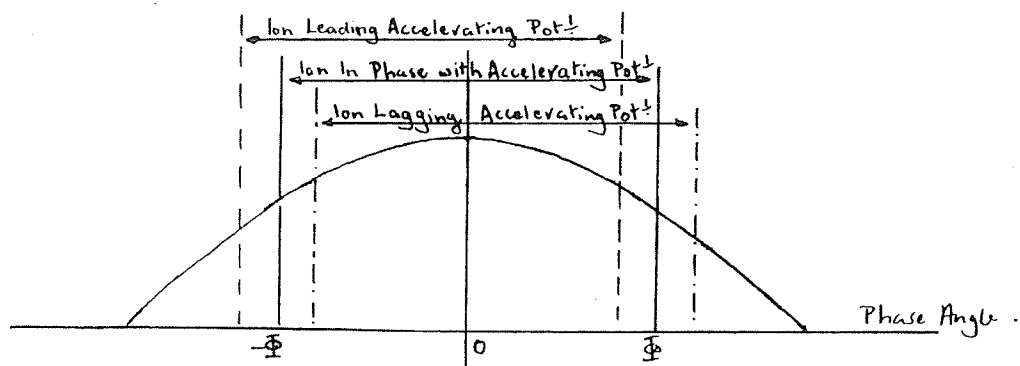


Fig. 7 cosine Variation of Electric Field.

Suppose that the angular distance between the edge of one dee and the edge of the other is 2Φ at the orbit radius concerned. Then each lens is at an angular distance of Φ from the Ox axis in Fig. 6. The diagram (Fig. 7) shows the cosine variation of the accelerating potential. An ion in phase with the accelerating potential will cross the Ox axis at maximum potential. Such an ion will pass through the first lens when $wt = -\Phi$ and through the second lens when $wt = +\Phi$. In each case the potential will have been reduced by a factor $\cos\Phi$.

As the ion passes through the first lens, it can be seen from Fig. 7 that the electric field is increasing. So the

first lens will be defocussing, i.e., divergent. After passing through the first lens, the ion coasts in a field free region until it meets the second lens. The electric field is decreasing as the ion passes through the second lens so this lens is focussing, i.e., convergent. As the ion passes through each lens, the rate of change of potential is the same, so the power of each lens will be the same in magnitude.

If an ion is leading the accelerating potential, it will pass through each lens earlier. It can be seen that the rate of change of potential as the ion passes through each lens is greater for the first lens than for the second. Hence the diverging power of the first lens will be greater than the converging power of the second. Similarly, if an ion is lagging, the accelerating potential, it will cross each lens later. Thus the converging power of the second lens will be greater than the diverging power of the first.

Rose's formula for the deviation $\Delta\alpha$ of the path of an ion as it passes through an electric lens can easily be extended to the case considered. The maximum potential difference between the dees considered by Rose was $2V_0$. The maximum potential difference between a dee and its dummy dee considered here is V_0 .

The deviation $\Delta\alpha$, of an ion as it passes through the first lens lagging the accelerating potential by angle θ is given by

$$\Delta\alpha_1 = \frac{eV_0}{2E} \frac{wz}{V\cos^3\eta} \sin(\Phi - \theta) \quad 4.17$$

Note that this is defocussing except if $\theta > \Phi$. This is because for small angles θ , the ion always passes through the first lens in an increasing field.

$\cos^3 \eta$ is the factor which takes into account the ion not moving parallel to the electric field.

For the second lens,

$$\Delta \alpha_2 = \frac{-eV_0}{2E} \frac{wz}{v \cos^3 \eta} \sin(\Phi + \theta) \quad 4.18$$

Here there is focussing as the ion usually passes through this lens in a decreasing field.

If the ion is leading the accelerating potential by an angle θ , the equations 4.17 and 4.18 become

$$\Delta \alpha_1 = \frac{eV_0}{2E} \frac{wz}{v \cos^3 \eta} \sin(\Phi + \theta) \quad 4.19$$

$$\Delta \alpha_2 = \frac{-eV_0}{2E} \frac{wz}{v \cos^3 \eta} \sin(\Phi - \theta) \quad 4.20$$

Thus in the dee gap at large orbit radius, the focussing effect is that of two separated lenses, one converging and one diverging. The powers of the lenses depend on the out of phase angle of the ion.

As the ion travels round in orbit and crosses a succession of dee gaps, it will pass through a sequence of electric lenses, alternately focussing and defocussing. Since the lenses are separated, the net result will always be focussing, provided that the powers of the lenses are the same, as any textbook on optics will show. This is because the deviation of the ion path is proportional to the height above the median plane at which

the ion passes through the lens. On the average, the ion will pass through a converging lens at a greater distance from the median plane than through a diverging lens.

The extra focussing due to the ion passing through converging and diverging lenses at different heights (the alternating gradient effect) can compensate for the diverging lens having a slightly stronger power than the converging lens. Clearly there will be a critical separation for a pair of such lenses where there would be no net focussing.

As a final point we notice that if we disregard the effect of the separation of the lenses then the net deflexion of the ion path on crossing the dee gap becomes

$$\Delta \alpha = \Delta \alpha_1 + \Delta \alpha_2 = \frac{eV_0}{E} \frac{\sin \theta}{v \cos \eta} \frac{wz}{\eta} \cos \bar{\Phi} \quad 4.21$$

The effect at high energies is essentially to reduce the axial focussing by a factor $\cos \bar{\Phi}$, where $2\bar{\Phi}$ is the angular width of the dee gap at these energies. However, the ion is less readily accelerated at these energies, its rate of radial increase being also cut down by a factor $\cos \bar{\Phi}$. Thus the axial focussing over a given radial increment of the orbit of the ion will be the same as in Rose's case.

4.5. Use of Grids.

Rose has shown that the vertical focussing produced by the electric field in the dee gap of the cyclotron is very small and, for a given dee voltage, is almost independent of the shape of the dees. A physical interpretation of this can be seen with reference to Fig. 8. Here is depicted the electric field between two dees, one of which has been raised higher than the other in a hypothetical attempt to produce extra axial focussing. It can be seen that although the axial focussing forces act over the greater portion of the dee gap, they are much weaker than the defocussing forces. Rose has shown essentially that the increased distance over which the focussing forces act is counteracted by the increase in the magnitude of the defocussing forces.

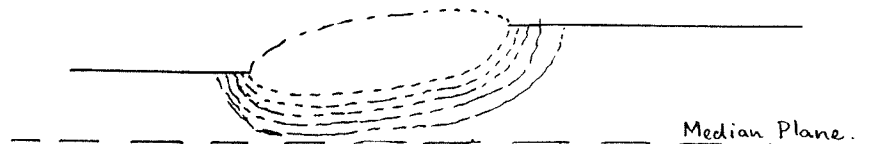


Fig 8. Dee Gap with Dees of Different Heights.

If a grid of some sort is placed across the second dee opening, then Laplace's equation becomes invalid at the grid*

* Rose. Op. cit.

Rose's treatment is now not applicable. With such a grid, the electric focussing can be increased considerably. The whole of the opening of the second dee is now at the same potential. It can be seen from the shape of the field lines in Fig. 9, that focussing now occurs at all points in the dee gap.



Fig. 9.

The idea was first used by Alvarez to produce vertical focussing in the linear accelerator and has been extended by other workers to produce extra vertical focussing in the cyclotron with varying degrees of success. (7) (8) The grids can take the form either of a set of wires stretched across the dee opening, or a graphite plate into which has been cut a set of slits. The ion beam is programmed so as to pass through the slits or between the wires. In both cases only half of each dee opening is covered by a grid. This is that half of the dee into which the ion beam enters. The presence of a grid

distorts the electric field lines at the grid slits to some extent, and this has an effect on the orbit centres of the ion beam as will be shown.

4.6. Electric Field at a Grid Slit.

There is no electric field inside a dee whose opening is covered by a grid of some sort. However, at the grid slits, or between the grid wires, there is a slight amount of intrusion of the field into the field free space. The equipotentials in the median plane at a typical slit are shown in Fig. 10a. The electric field lines are shown in Fig. 10b.

It can be seen qualitatively from the direction of the field lines in Fig. 10b that ions passing through a slit will tend to be forced away from the slit centre. Consequently, there will be a debunching of ions in the beam. The situation can be examined more closely with reference to the theory developed in Chapter 2.

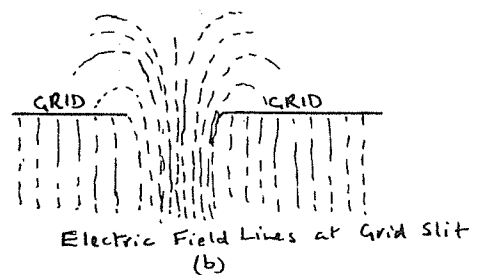
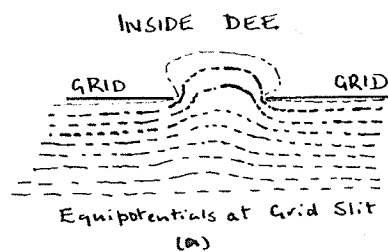
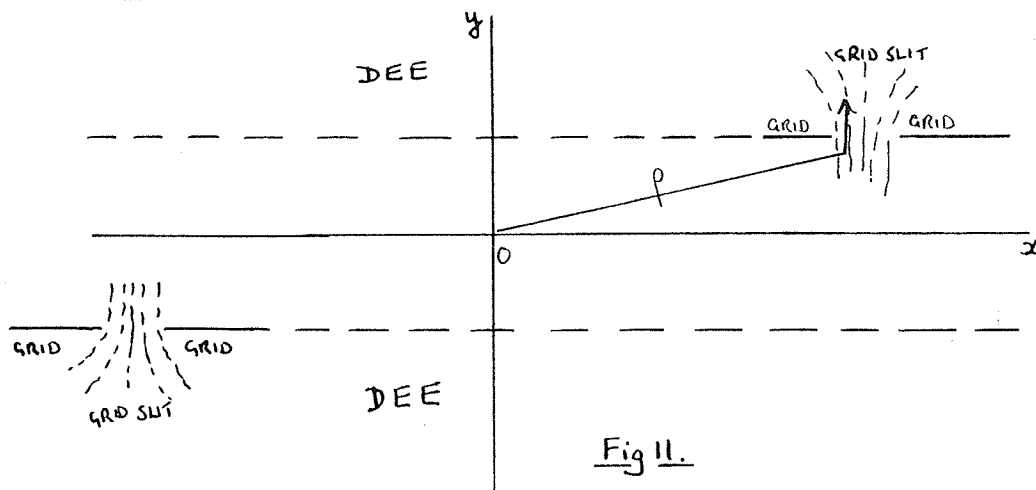


Fig. 10

Consider an ion P (Fig. 11) whose orbit centre is at the origin. As it passes through a grid slit its orbit centre will suffer displacements in the x and y directions. However, one half revolution later, it will encounter another grid slit. If the pair of grids are symmetrical about the origin, this second grid slit will be exactly the same as the first insofar as electrical effects are concerned. Then the displacements of the orbit centre produced in the x and y directions as the ion passes through the second slit will tend to annul those produced at the first slit. To a first order approximation there will be no net motion of the orbit centre over one revolution of the ion.



Next we must consider the effect of the grid slits on orbit centres not at the origin. The equipotentials at a typical grid slit are shown in Fig. 12. Consider two ions P_1 P_2 of equal energy and phase and moving in phase with the accelerating potential. Let the orbit centre of P_1 be at the origin, while

that of P_2 is on the x-axis. P_1 will be at the centre of the ion beam, and it will simplify matters if we arrange that P_1 passes down the centre of the slit. (The case where P_1 passes down the slit off-centred is rather complicated. It is merely an extension of the case where P_1 passes down the slit centre, and need not be discussed.) Let the orbit centre of P_2 be placed such that P_2 passes through the slit to the right of P_1 . (Fig. 12.)

Consider a pair of equipotentials as in section 2.3, differing in potential only by an infinitesimal amount. Using the same nomenclature as in that section, the motion of the orbit centre as its ion passes across these equipotentials is given by

$$\delta x = \frac{-\Delta\phi}{vB_0} \frac{1}{1 + \tan\omega t \tan\alpha}$$

$$\delta y = \frac{\pm \Delta\phi}{vB_0} \frac{1}{\cot\alpha + \tan\omega t}$$

There is a \pm sign in the expression for y because the x-component of the electric field changes sign across the slit centre.

For an ion passing through the slit to the right of the centre, the positive sign must be used.

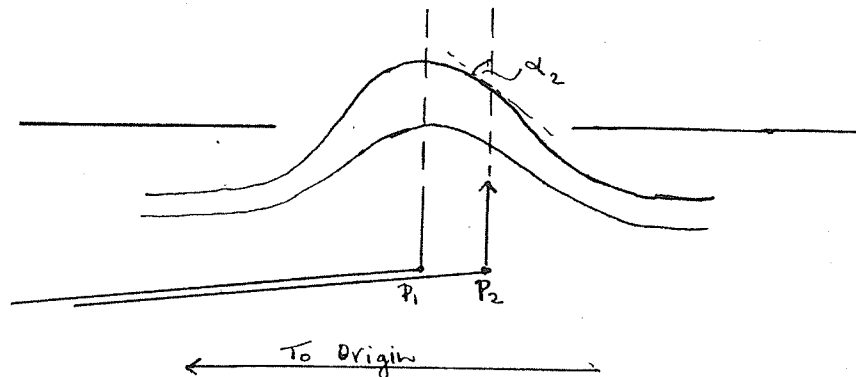


Fig 12. Equipotentials at Grid Slit.

For the ion P_1 , $\alpha_1 = 0$ so $\delta x_1 = -\frac{\Delta\phi}{vB_0}$ $\delta y_1 = 0$.

For the ion P_2 , $\alpha_2 \neq 0$ nor is ωt_2 , so

$$\delta x_2 = -\frac{\Delta\phi}{vB_0} \frac{1}{1 + \tan\omega t_2 \tan\alpha_2}, \quad \delta y_2 = \frac{\Delta\phi}{vB_0} \frac{1}{\cot\alpha_2 + \tan\omega t_2}$$

The relative motion of the orbit centre of P_2 with respect to that of P_1 is given by

$$\begin{aligned} \delta x_2 - \delta x_1 &= \frac{\Delta\phi}{vB_0} \left(1 - \frac{1}{1 + \tan\alpha_2 \tan\omega t_2} \right) \\ \delta y_2 - \delta y_1 &= \frac{\Delta\phi}{vB_0} \left(\frac{1}{\cot\alpha_2 + \tan\omega t_2} \right) \end{aligned}$$

These quantities are both positive, so the orbit centre of P_2 tends to move away from the origin in both the x and y directions at this slit.

When P_1 and P_2 pass through a similar slit at the opening to the other dee, half a revolution later, their roles are reversed. P_1 still travels through the centre of the slit, but now P_2 travels to the left of P_1 . If a similar analysis is applied to the second slit, it is found that the orbit centre of P_2 tends to approach that of P_1 along the x-axis, while it moves away from the orbit centre of P_1 in the positive y-direction. Hence, over the whole revolution it is seen that there is a continuous defocussing in the positive y-direction but no net motion in the x-direction.

The behavior of orbit centres on the y-axis is not as definite. Depending on the position of its orbit centre on the positive y-axis, an ion may pass through the first slit

totally to the right of the centre line, it may pass through both the left and right portions at some angle, or it may miss the slit altogether. If the ion definitely passes through the right hand portion of the first slit, then it will definitely pass through the left hand portion of the second slit. As before, there will be a continuous defocussing in the y-direction with no net x-motion. If the ion passes through both left and right regions of the first slit, this will occur at the second slit also. There will be an admixture of y-focussing and y-defocussing though there will still be no net x-motion. We can surmise that the net result will be a y-defocussing, as we know that there is a y-defocussing when the ion passes completely through the right hand portion of the first slit. In this case however, the y-defocussing will be smaller and will tend to zero as the orbit centre approaches the origin along the y-axis. This is as expected. The motion of the orbit centre due to its y-displacement will be of second order compared to the motion due to the x-displacement.

To obtain a complete picture of what is happening, consider a group of ions, having the same energy and phase, and whose orbit centres are spread about the origin. The region about the origin is subdivided by drawing arcs of circles from the centre and edges of each slit. The radius of these arcs is the same as that of the ion orbits. The areas enclosed by these arcs about the origin are labelled A, B, C. (Fig. 13). If an ion has its orbit centre within A, then the ion must pass

through the right hand portion of the first slit and the left hand portion of the second, as it describes its orbit. If the ion has its orbit centre within B, then it must pass through the left hand portion of the first slit and the right hand portion of the second. Ions which have their orbit centres in C pass through the left hand portion of each slit.

It can now be seen, taking into account the considerations above, that an orbit centre in A will drift in the positive y-direction with no net x-motion. An orbit centre in B will drift in the negative y-direction with no x-motion. The motion of orbit centres in C is somewhat indeterminate, but there is a tendency for the orbit centres to drift away from the origin in the x-direction, and towards the origin in the y-direction.

The passage of an ion beam through the slits of a grid therefore produces a drifting of the ion orbit centres away from the origin in the y-direction. The extra axial focussing produced in the cyclotron by the insertion of grids is obtained only at the expense of the radial stability of the ion beam.

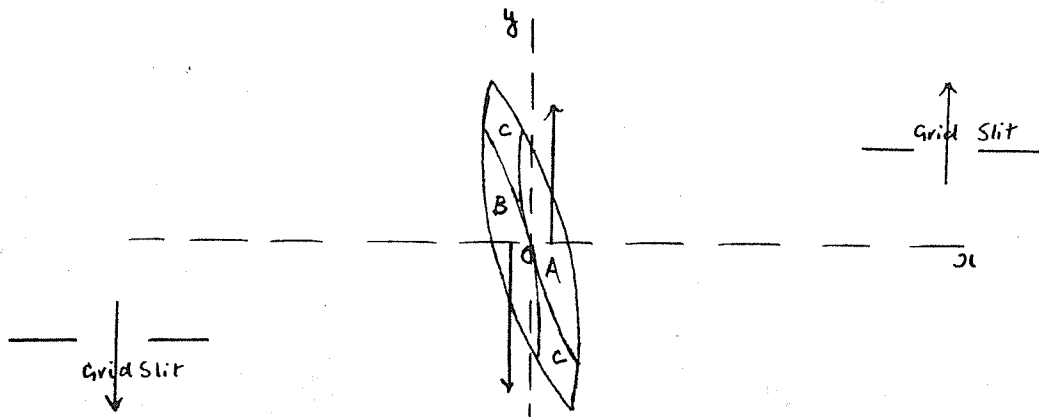


Fig 13 Areas A, B, C about Cyclotron Centre.

It might be thought that the radial instability could be rectified if the slits were arranged such that an ion which passed through them in a left hand portion - right hand portion sequence in one revolution passed through them in the opposite sequence in the next revolution. This could be done, for example, by passing the whole ion beam through the right and left halves of the slits alternately. However, this would not help matters, as the orbit centre would then be disturbed and there would still be defocussing as before. The next best thing is to arrange that the grid wires are placed at random intervals along the length of the dee. Then as the ion entered and re-entered the dees through this mesh of grid wires, there is an equal likelihood that a given ion will pass through the left hand portion of a slit as it would the right hand portion.

4.7 Transition Effects - Grid to No Grid.

The region in the cyclotron where the grid ends merits careful consideration. Here, there is a transition from grid to no-grid and the electric field becomes distorted. The equipotentials for a gridless dee intrude into the dee for some distance, but when the grid is present, the equipotentials end at the grid. So, at the boundary grid to no-grid, they curve quite sharply. The situation is depicted in Fig. 14.

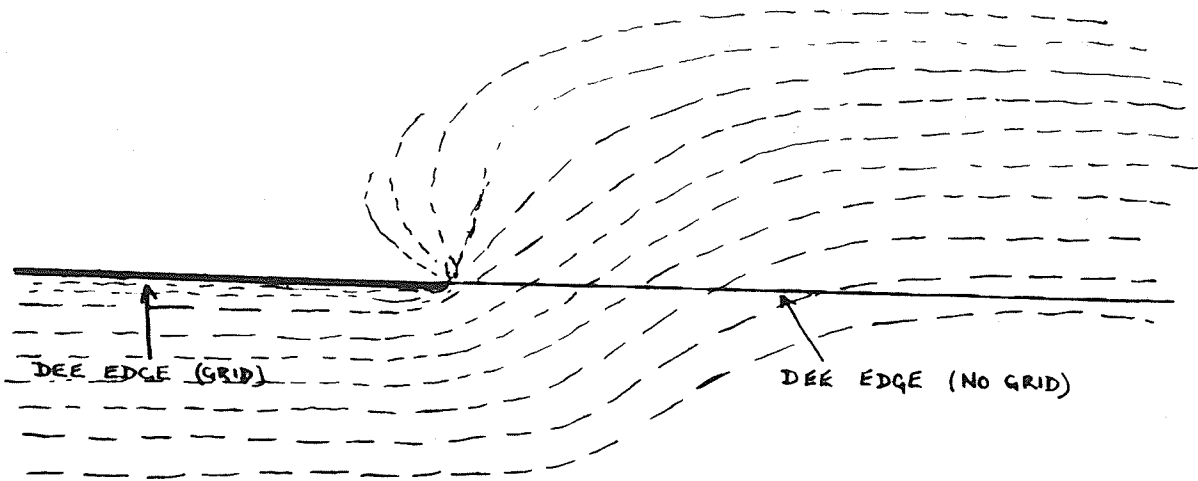


Fig 14 Equipotentials of the Electric Field near a dee edge at the boundary between grids and no grids

It is important to know what happens to the ion beam as it spirals outward through this region. We will depict the ion beam as usual by a pair of ions of equal energy and phase and whose orbit centres are at the origin and off-centred. Then we will consider what happens to the orbit centres of the pair as they pass through the region.

For an ion whose orbit centre is at the origin, the motion of the orbit centre as it passes through any part of this transition field is counteracted by an opposite displacement when the ion moves through the corresponding part of the transition field at the other grid edge, one half revolution later. Thus, there will be no net motion of an orbit centre at the origin. There will be a certain amount of drift for an off-centred ion orbit however, and to examine this drift, consider a pair of equipotentials in the transition field whose potential difference is infinitesimal. (Fig. 15).

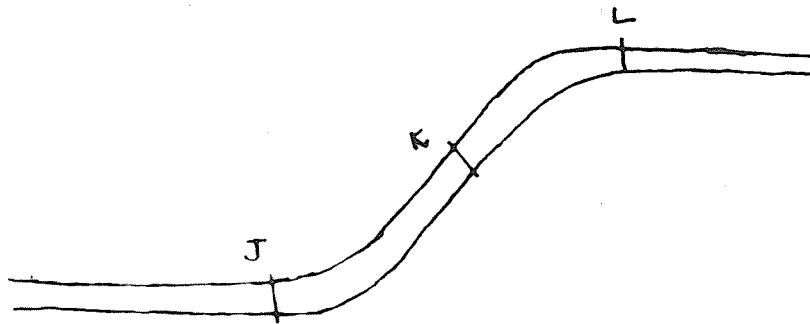


Fig. 15 A Pair of Equipotentials at the boundary grids to no grids.

There are two regions of this equipotential pair to be considered. In Fig. 15, the point K is a point of inflexion. Throughout the region JK, the curvature of the equipotentials increases with distance from the cyclotron centre, while over the region KL it is decreasing again. As the ion pair cross the equipotentials in the region JK, the situation is the same as was considered in section 2.3. The orbit centres therefore tend to drift away from the origin in the x-direction and towards the origin in the y-direction. When the ion pair enters the region of KL and we try to apply the analysis of section 2.3, we get an indeterminate result since (using the notation of section 2.3)

$\alpha_2 < \alpha_1$, and $wt_1 < wt_2$. So in this region we do not know precisely what the orbit centres are doing. However, at the region near L, the equipotentials are curling very rapidly and there is a definite drift of orbit centres towards the origin in the x-direction and away from the origin in the y-direction. So we can regard the region KL as the transition region in which the directions of the drifts of orbit centres are gradually reversed.

Thus an ion beam, spiralling outwards through the field, experiences a drift of orbit centres in one direction as it passes through the region JK and a drift in the opposite direction as it passes through the region KL. Since the radius of the orbit of the ion beam does not increase uniformly, the beam does not spend an equal amount of time in each part of the field. So these drifts will not compensate for each other, and there will be a net motion of orbit centres as the ion beam passes through the field.

This non-uniform increase in orbit radius may account for the large loss of beam intensity across the transition region grid to no grid, that has been observed. The beam might spend one revolution in the region JK and on the next revolution miss the KL region altogether. The opposite situation can also occur in which the ion beam misses the JK region and passes through the KL region only. In both cases there would be a drift in orbit centres with a resultant loss in beam intensity.

It is conceivable that the ion beam might be programmed to miss the rapid field change altogether, passing to the left of JK and to the right of KL in successive revolutions. This would be easier to arrange at low energies were the radius of the orbit increasing rapidly. It would be difficult to do it at higher energies where the turns are closer together. A safer method is to let the field fall off more slowly by spacing the grid wires further and further apart and letting them recede into the dee. (Fig. 16). The ion beam is then much more likely to move through both the JK and KL regions. It is of interest to note that this is the method which has been used in the cyclotron at Birmingham (9). It might be possible to arrange the

shape of the field lines so that the passage of the ion beam through the field produced no net effect, the drift of orbit centres in one region exactly compensating for the opposite drift in the other region. The non-uniform radial increase could also be taken into account.

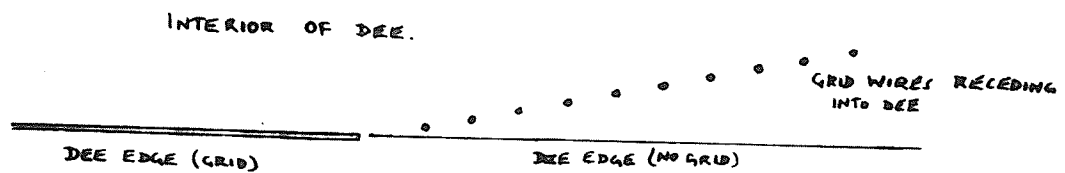


Fig. 16. Grid Wires Receding into Dee.

Chapter 5. Computer Program and Results.

5.1. Introduction.

The equations describing the motion of a charged ion moving in combined electric and magnetic fields are the familiar Lorentz equations,

$$\frac{dx}{dt} = v_x$$

$$\frac{dy}{dt} = v_y$$

$$\frac{dz}{dt} = v_z$$

$$\frac{dv_x}{dt} = \frac{e}{m} (E_x + v_y B_z - v_z B_y)$$

$$\frac{dv_y}{dt} = \frac{e}{m} (E_y + v_z B_x - v_x B_z)$$

$$\frac{dv_z}{dt} = \frac{e}{m} (E_z + v_x B_y - v_y B_x)$$

This set of six simultaneous first order differential equations was solved with a Bendix G15D Computer using a Runge-Kutta method as adapted for computers by S. Gill,⁽¹⁰⁾ Twelve iterative steps were used for each revolution of the ion. Computation was carried out until the radius of the orbit was 8-10 cm when the main flutter field began to become significant.

5.2. The Computer Program.

The computer program was based on one compiled by Dr. K. G. Standing of the University of Manitoba. Slight modi-

fications were made to this program so that the centre of curvature of the orbit could be plotted as well as the path of the ion. In the writing of the program, difficulties arising from the shape of the electric field and the smallness of the computer memory had to be overcome.

The electric field about the dees could not be described analytically owing to their square-tipped shape. A complete map of the electric field had to be stored in the memory of the computer. The field was mapped by covering it with a network of lattice points and measuring the potential and vertical field at each lattice point. This set of field measurements was then stored systematically in the computer memory. To save computer space, the fourfold symmetry of the field was taken into account. Thus only one quadrant of the field needed to be stored, although provisions were made for asymmetry over the ion source.

The major part of the computer program was taken up in calculating the electric field components at a given point in the field. To do this, the nine lattice points nearest to and surrounding the given point had to be found, using an involved but systematic question and answer technique. When these points had been found, the values of the potential at the points were obtained. The electric field components were then calculated, using Lagrange's Interpolation formula.

Another difficulty encountered was the smallness of the computer memory. It has been mentioned that to save space,

only one quadrant of the electric field was mapped, but even then, there were not enough addresses in the memory to accommodate a description of the electric field both in the median plane and out of the median plane. This difficulty was overcome by Dr. C. B. Germaine, formerly of the Actuarial Mathematics and Statistics Department of the University of Manitoba. Germaine was able to write a machine language subroutine for the computer which enabled it to break down on command a seven-digit hexadecimal word into two smaller words. One word was made up of the third to fifth digits of the original word, while the last two digits of the original word made up the second word. The three digit word was used to carry the value of the potential at a given lattice point in the field. The two digit word was used to carry the axial field strength at that point. The sign of the original seven digit word was used to indicate whether this axial field was positive or negative. Thus, for a seven digit word $\pm.abcdefg$, Germaine's subroutine broke it down into

ab	lost	(the subroutine did not provide to recover this word)
cde	potential	at a given lattice point
$\pm ef$	axial field	at the lattice point

The electric field was assumed symmetrical about the median plane and proportional to Z . This latter assumption was justified as in practice, all excursions in the Z -direction were small. The first assumption was justified as it was possible

to make the dees symmetrical about the median plane. The potentials at the various lattice points were measured in the usual manner using an electrolytic tank and model dees. The set of values obtained were punched out on tape using a flexowriter, and read into the computer memory.

When computing the orbit of an ion, the computer typed out the position and velocity coordinates of the ion together with its energy (in MeV) and phase angle. The radius of curvature and the coordinates of the centre of curvature of the orbit were also typed out. Typeouts occurred every 3-4 minutes, the phase angle increasing uniformly in increments of about 30° . Normally a complete orbit would take six to eight hours to compute.

Initially, time was not a dominant factor as plenty of computer time was available. However, this was not the case a few months later when computations were carried out for a magnetic flutter field superposed on the original uniform magnetic field.

5.3. Results for Uniform Magnetic Field.

The first computations were carried out with the ions moving in the electric field and in a uniform magnetic field. The drift of orbit centres for ions moving in various orbits could then be examined. In all cases considered, the motion of the ion was investigated only after it had completed its first revolution out from the ion source and was beginning on

the second. In practice ions emerge from the source with a slight spread of energies and in slightly different directions, so, by the time the first revolution has been completed, the ion beam has a finite width and is not monoenergetic. The subsequent spread of the ion beam was therefore investigated by computing the orbits of ions which started on their second revolutions from slightly different positions and slightly different velocities.

The following cases were considered:-

(a) the orbit of an ion which was near the centre of the beam and the centre of curvature of whose orbit was near the origin at the beginning of the second revolution. The initial coordinates of this ion are given in Table 5.1. orbit A.

(b) the ions at the edge of the ion beam at the beginning of the second revolution. These ions were considered to have the same energy as the first ion initially. The centres of curvature of their orbits were initially displaced about that of the first ion. In Table 5.1, these ions are denoted B.1, B.2, B.3, B.4. B.1, B.2 are ions which have the centre of curvature of their orbits displaced about that of the first ion in the x-direction. Orbits B.3, B.4 are initially off-centred in the y-direction.

(c) ions whose initial position coincided with that of the first ion but whose initial velocities differed. In Table 5.1, these ions are denoted C.1, C.2, C.3.

TABLE 5.1.

CASE CONSIDERED.	POSITION COORDINATES (m)			VELOCITY COORDINATES (m.s ⁻¹)		
	x	y	z	v _x	v _y	v _z
A.	0.0128			1×10^{11}	-2.3×10^6	2.3×10^4
B 1.	0.0160			1×10^{11}	-2.3×10^6	2.3×10^4
2.	0.0096			1×10^{11}	-2.3×10^6	2.3×10^4
3.	0.0128	0.0032		1×10^{11}	-2.3×10^6	2.3×10^4
4.	0.0128	-0.0032		1×10^{11}	-2.3×10^6	2.3×10^4
C 1.	0.0128			1×10^{11}	-1.66×10^6	2.3×10^4
2.	0.0128			1×10^{11}	-2.94×10^6	2.3×10^4
3.	0.0128			6.4×10^5	-2.3×10^6	2.3×10^4

At the end of this chapter, a series of graphs are shown. Graph I is a comparison of the orbits of ions A, B.1 and B.3 above. The orbits of B.2, B.4 resemble those of B.1 and B.3. The next graph, Graph II, shows a comparison of the orbits of ions A, C.1 and C.3. At a glance it is seen that the defocussing of the ion beam is quite rapid.

The drift of orbit centres for off-centred ions can be shown quite nicely by considering the motion of the average centre of curvature over each revolution of the ion. This average centre of curvature approximates very well with the orbit centre and the ion does spend part of its time in a pure magnetic field anyway. The paths of the orbit centres for various ions are depicted in Graphs III, IV, V. It is seen that,

- (a) the orbit centre of the first ion considered settles down to some fixed value.
- (b) orbit centres which are initially off-centred in the x-direction exhibit a steady drift away from the origin.
- (c) orbit centres which are initially off-centred in the y-direction exhibit a steady drift towards the origin.
- (d) for ions whose initial velocity was different from that of the first ion considered, a change in y-velocity is found equivalent to an x-displacement of the orbit centre while a change in x-velocity is found equivalent to a y-displacement of the orbit centre.

The results so far demonstrate qualitatively at least, that the theory of the drift of orbit centres in an electric

field is correct. However, there are some small discrepancies between theory and results that should be pointed out and explained. If theory is correct, there should be no drift in the y-direction for an orbit centred on the x-axis. It can be seen from Graph III that there is such a drift, though it is small and not in any definite direction. Similarly, there should be no drift in the x direction for an orbit centred on the y-axis. Yet there is such a drift, although it again is small and has no fixed direction.

These discrepancies are probably due to the fact that the orbit centre does not coincide exactly with the average centre of curvature. Over a long period of time, the difference between the two averages out to zero, and indeed, for the drift along the x-axis, the small y-component shows signs of periodically changing direction. Another factor is that the radius of curvature of an orbit is not constant over a revolution. The discrepancies introduced by this factor depend on the rate of radial increase, and how uniform the electric field is in the revolution in question. At higher energies, the discrepancy introduced by this factor will be small. A third point to consider is that initially, the orbit centre in question may not be on the x or y axis. This is more likely to be true for orbits off-centred in the y-direction; there may well be a small displacement in the x-direction here. For orbits off-centred in

TABLE 5.2.

AVERAGE ORBIT RADIUS OVER THE REVOLUTION	AVERAGE X-COORDINATE OF CENTRE OF CURVATURE	DRIFT Δx	FRACTIONAL DISPLACEMENT λ	STRENGTH OF FLUTTER FIELD REQUIRED AT THIS RADIUS.
1.96 cm	0.29 cm	-	-	0 gauss
3.15 cm	0.29 cm	0 cm	0	0 gauss
4.26 cm	0.30 cm	0.01 cm	0.06	205 gauss
5.21 cm	0.44 cm	0.14 cm	0.37	1294 gauss
6.03 cm	0.60 cm	0.16 cm	0.31	1466 gauss
6.73 cm	0.74 cm	0.14 cm	0.22	1454 gauss
7.32 cm	0.86 cm	0.12 cm	0.15	1372 gauss

TABLE 5.3.

AVERAGE ORBIT RADIUS OVER THE REVOLUTION	AVERAGE Y-COORDINATE OF CENTRE OF CURVATURE	DRIFT Δy	FRACTIONAL DISPLACEMENT λ	STRENGTH OF FLUTTER FIELD REQUIRED AT THIS RADIUS.
1.97 cm	0.31 cm	-	-	0 gauss
3.16 cm	0.30 cm	-0.01 cm	-0.04	123 gauss
4.27 cm	0.26 cm	-0.04 cm	-0.14	467 gauss
5.20 cm	0.18 cm	-0.08 cm	-0.30	953 gauss
6.04 cm	0.10 cm	-0.08 cm	-0.45	1420 gauss
6.65 cm	0.08 cm	-0.02 cm	-0.20	1437 gauss
7.40 cm	0.06 cm	-0.02 cm	-0.25	1477 gauss

the x-direction it is less likely that there is also a small y-displacement. This is because it was arranged that the initial velocity of the ion had no x-component as it crossed the Ox axis to begin its second revolution.

Quantitatively, the results seem to agree quite well with the theory. If the fractional displacement is calculated over each revolution (Tables 5.2, 5.3) it is found that it is small at small orbit radii, increases rapidly to a maximum at an orbit radius of about 5cm and thereafter diminishes. This is just how the field varies in uniformity. It is most uniform at small radii, it is most non-uniform at a radius of about 5cm, and it thereafter becomes more uniform again. The rate of drift of the orbit centres does not change much however. This is because the amount of drift over a revolution depends on the distance of the orbit centre from the origin over that revolution. As the field gets more uniform, the orbit centre is drifting further and further away from the origin so even small inhomogeneities in the electric field will produce a large amount of drift at these large radii.

Finally, it is found in the next section that the magnetic flutter field required to curb the x-drift of the orbit centres is exactly the same as that required to curb the y-drift. Thus the x-drift and the y-drift are exactly equivalent except for direction. This is as predicted by theory.

5.4. Magnetic Flutter Field Calculation.

It was shown at the end of Chapter 3 that the radial variation of the magnetic flutter field required to counteract the instability due to the electric field took the form

$$f(\rho) = \frac{2B_0}{\pi\rho^2} \int \rho \lambda(\rho) d\rho + \frac{C}{\rho^2}$$

where C is a constant and $\lambda(\rho)$ is the fractional displacement of an orbit centre per revolution due to the electric field.

From computations on the orbits of off-centred ions we can obtain an average value for λ over each revolution of the ion. Since the radius of the ion orbit does not remain constant, these average values of λ represent a range of values of the radius, rather than one particular radius. However, we can still calculate the required radial variation of the flutter field from these.

Suppose that over a range of radii ρ_1 to ρ_2 ($\rho_1 < \rho_2$) the average value of λ is λ_m . Then by regarding λ as constant over this range we can calculate the flutter field radial variation from the equation above

$$f(\rho) = \frac{B_0 \lambda_m}{\pi} + \frac{C}{\rho^2}$$

C is calculated from the magnitude of the flutter field at the beginning of the range. If the flutter field at radius ρ_1 is $f(\rho_1)$, then the radial variation becomes

$$f(\rho) = \frac{B_0 \lambda_m}{\pi} \left(1 - \frac{\rho_1^2}{\rho^2} \right) + \frac{\rho_1^2}{\rho^2} f(\rho_1).$$

From this, the magnitude of the flutter field at the end of the range $f(\rho_2)$ can be found

$$f(\rho_2) = \frac{B_0 \lambda_m}{\pi} \left(1 - \frac{\rho_1^2}{\rho_2^2} \right) + \frac{\rho_1^2}{\rho_2^2} f(\rho_1).$$

The end of one range is the beginning of the next range, with a different value for λ_m . In this way we can map out the whole radial variation, finding the magnitude of the flutter at the beginnings and ends of successive ranges. At the beginning of the very first range $f(\rho_1)$ may be taken as being equal to zero.

The values of $f(\rho)$ obtained for the various radii can now be plotted on a graph (Graph VII). The points only give an indication of the general form of the field variation required and the approximations made in obtaining them do not justify a more accurate interpolation other than connecting the points with straight lines. In practice the shape of the field variation would be simplified still further as in Graph VIII. This form has the advantage of being easily realised in practice and is also easily put into a computer program.

5.5. Results With The Magnetic Flutter Field Present.

The Graph VII depicts three radial variations for the flutter field, the first two being very similar and the third rather smaller. The first two were obtained on the basis of calculations on the drift of orbit centres in the ox and y directions (see Tables 2,3). The fact that they are similar

bears out the prediction made at the end of Chapter 2 that the x-drift and the y-drift are the same. The two radial variations are not exactly equal in Graph VII, but this is not surprising in view of the approximations made. The average between the two plots is taken to obtain the simplified version of Graph VIII.

The third plot in Graph VII is the one that was used in computations and all the results to follow are based on this flutter field. This was an earlier derivation of the required radial variation and subsequently found to be in error. Time did not permit a repeat of the computations with the more correct field variation, but the results obtained with the smaller flutter field go a long way to verify the predictions of Chapter 3.

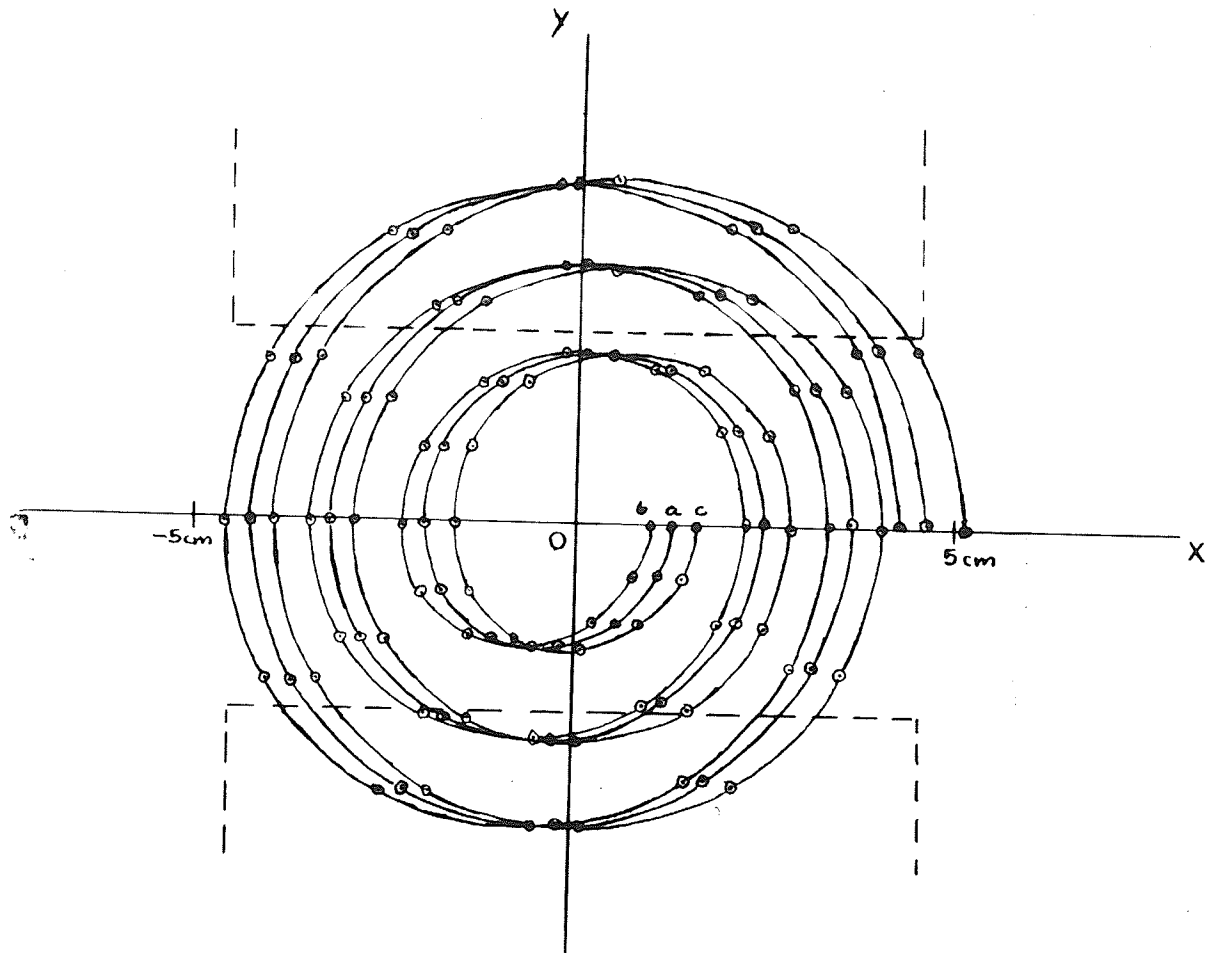
Computations were made on orbits of ions off-centred on the x and y axes and the amount of drift over each revolution calculated. The orbit was taken out to an orbit of radius of 7-8 cm, making about five or six revolutions. At this radius, the greater inhomogeneities of the electric field had been traversed and the drift at larger radii was small. The motion of the orbit centres over these revolutions is depicted in Graph VI for both the x and y directions. It is found that there is a slow drift in both the x and y directions but by comparison with the Graphs III and IV it is seen that the magnetic flutter field has cut down the drift by about fifty per cent. That there is still a drift can be attributed to the

fact that the flutter field used is smaller than that required to cut out the drift completely.

Finally, to demonstrate more vividly the action of the magnetic flutter field, Graph IX has been drawn. This graph shows the variation of the x-coordinate of the centre of curvature of an orbit which is assumed offcentred in the x-direction. The motion of the centre of curvature without the flutter field is compared with the motion of the centre of curvature when the field is present. It is readily seen that the flutter field attenuates the ^{average} Δ excursions of the centre of curvature.

Early Cyclotron Orbits.

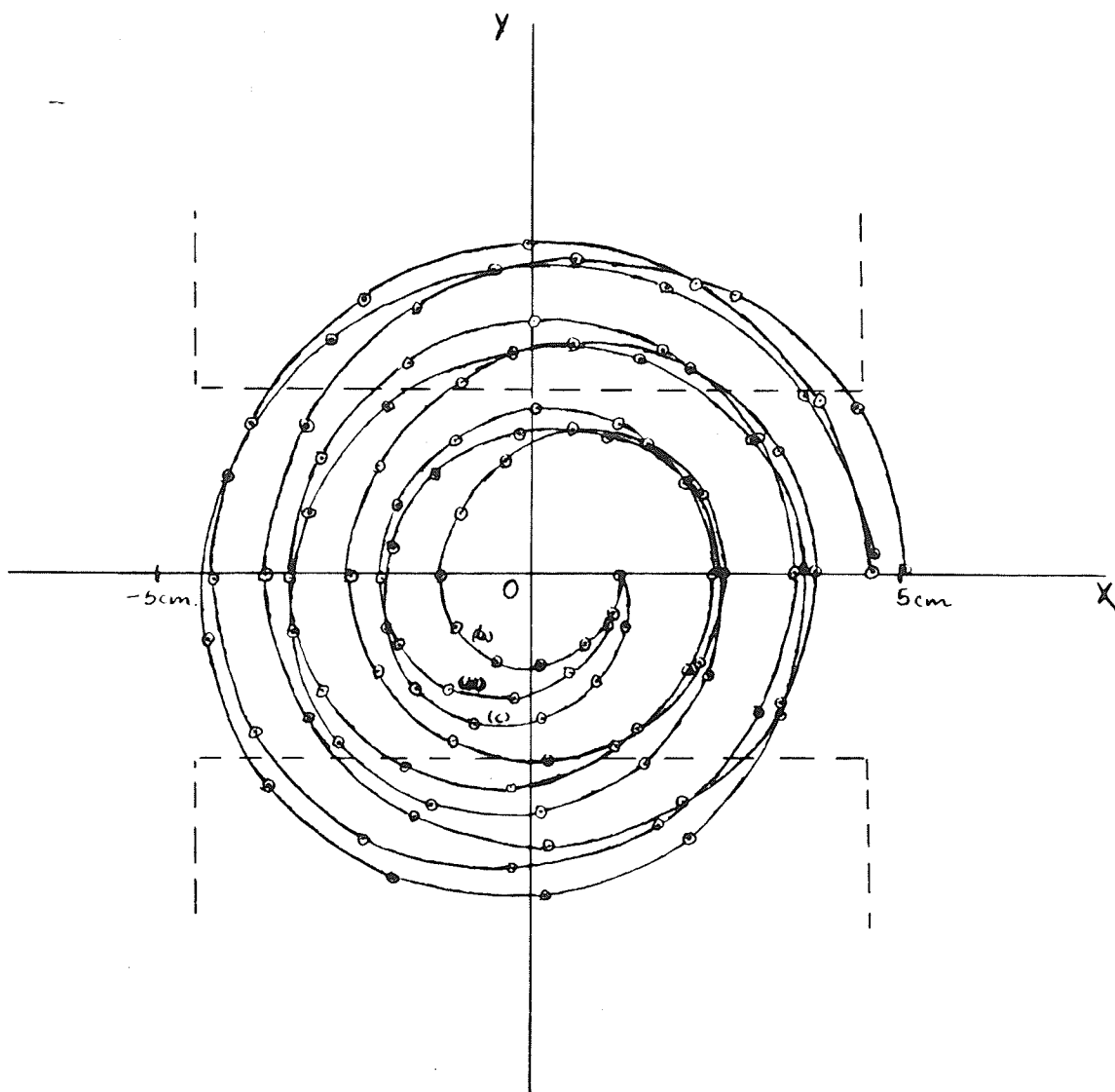
Graph I.



Orbits of ions

- a) centred at the origin after the first revolution out from the ion source
 - b), c). centred on either side of the origin ± 0.3 cm after the first revolution.
- Edges of the dees are shown dotted.

Graph II.



Orbits of ions of different velocities. All have their orbit centres near the origin after the first revolution out from the ion source.

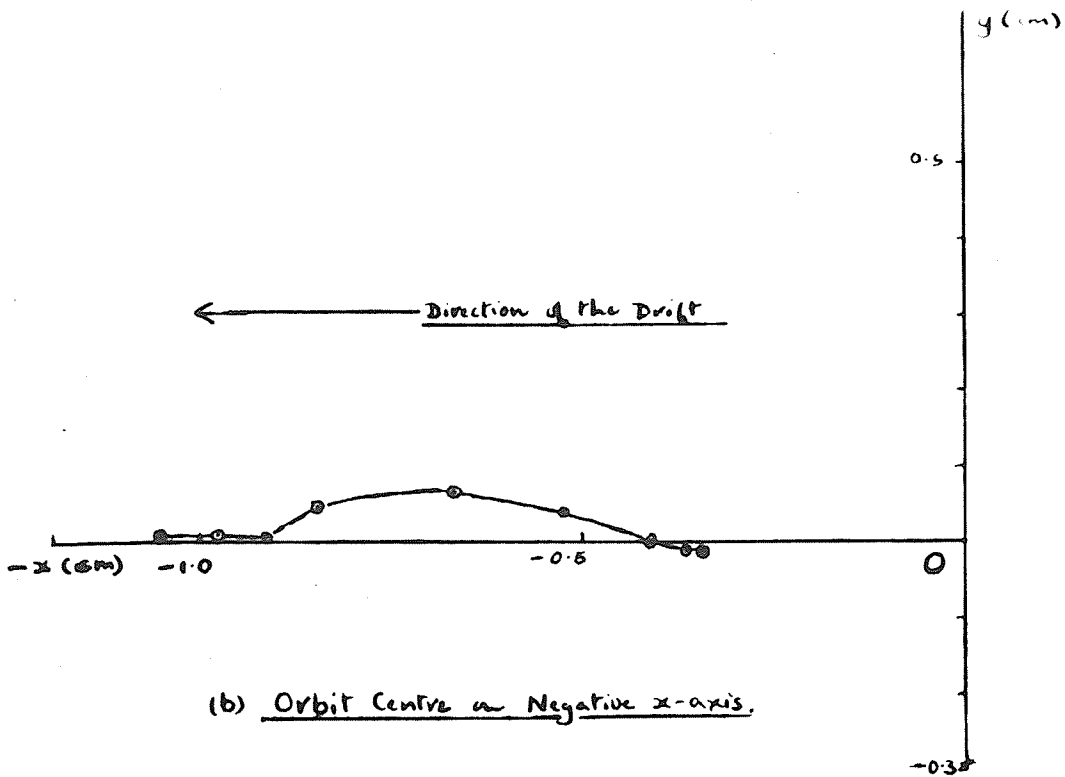
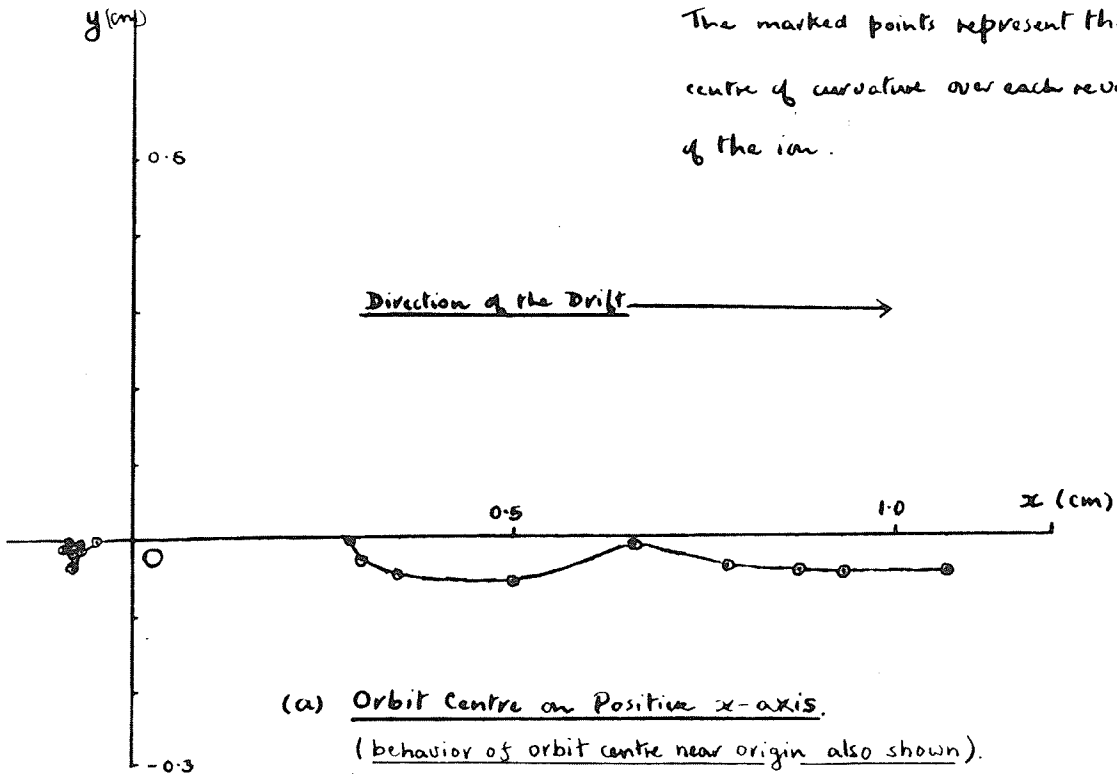
- (a) Orbit of ion which remains centred near the origin.
- (b) Orbit of ion with smaller y -velocity than (a), at the beginning of the motion.
- (c) Orbit of ion with larger x -velocity than (a) at the beginning of the motion.

Graph III

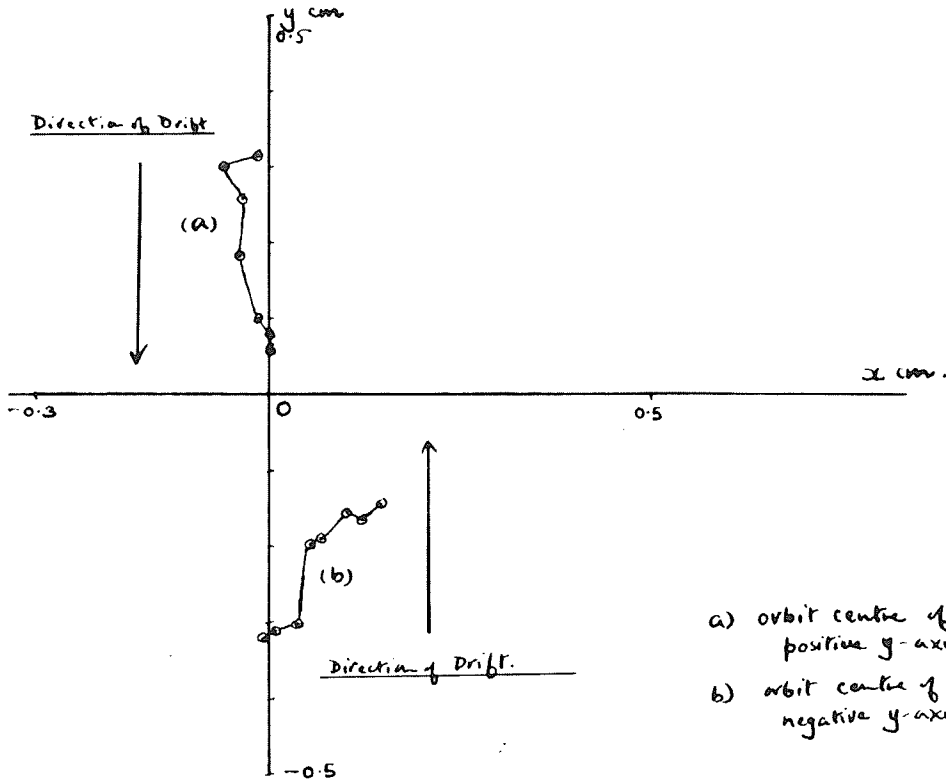
Drift of Orbit Centres on the x-axis.

(Without Flutter Field Present)

The marked points represent the average centre of curvature over each revolution of the ion.

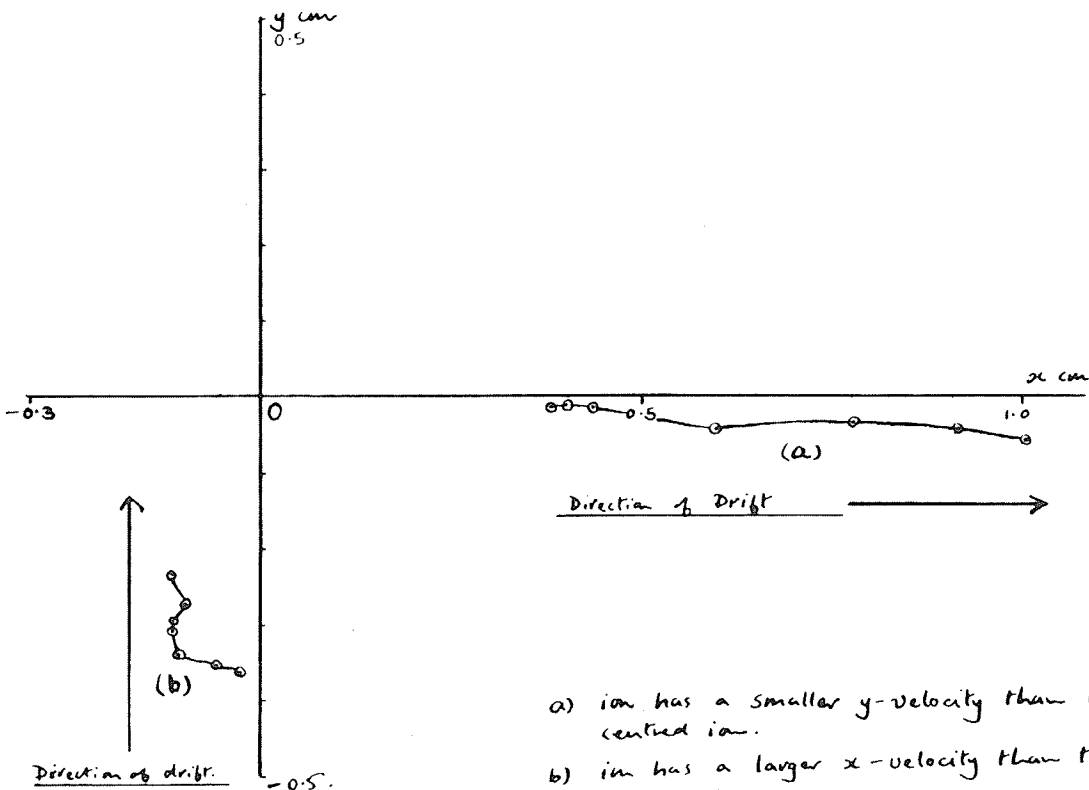


Graph IV. Drift of Orbit Centres on y-axis.



- a) orbit centre of ion is originally on positive y-axis.
- b) orbit centre of ion, originally on negative y-axis.

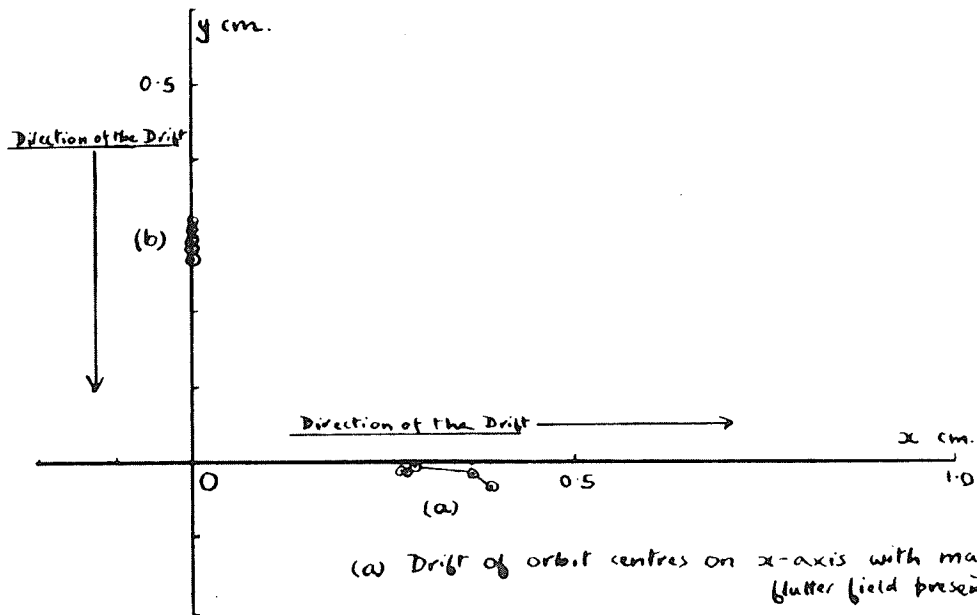
Graph V Drift of Orbit Centres of Ions with Different Velocities.



- a) ion has a smaller y-velocity than the origin-centred ion.
- b) ion has a larger x-velocity than the origin-centred ion.

Graph VI Drift of Orbit Centres on the x- and y-axes with Magnetic Flutter Field Present.

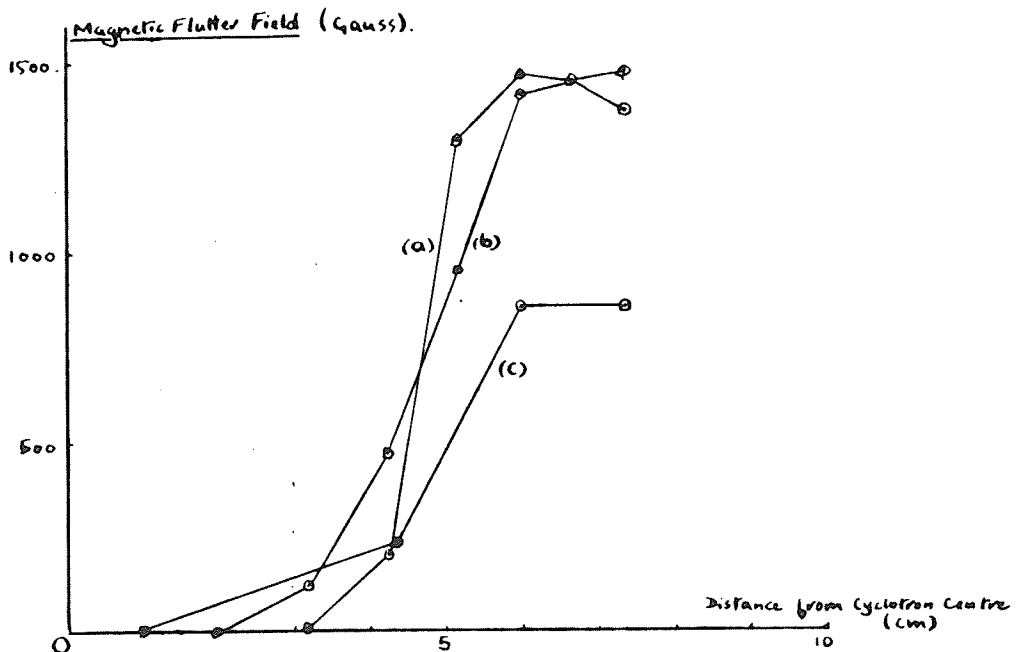
(Compare with Graphs III and IV)



(a) Drift of orbit centres on x-axis with magnetic flutter field present

(b) Drift of orbit centres on y-axis with magnetic flutter field present.

Graph VII Radial Variation of Magnetic Flutter Field.



(a) Radial Variation obtained from calculations on the x-drift.

(b) Radial Variation obtained from calculations on the y-drift.

(c) Radial Variation used in computations.

CONCLUSIONS.

The behavior of an ion beam has been investigated over its early revolutions in the University of Manitoba cyclotron. It was found that the non-uniform electric field in the cyclotron causes a drift of the orbit centres of the individual ions in the beam. A defocussing of the ion beam is thus produced. A simple theory has been set up to explain just how this drift occurs, and predictions as to the magnitude and direction of the drift have been verified by computer calculations.

A means of rectifying this instability of the electric field using a magnetic flutter field has also been discussed. It has been found that a second harmonic flutter field of sorts will do the job. This flutter field consists of four similar sectors, two hills and two valleys arranged so that the hills are orthogonal to the valleys. The whole system, when suitably orientated with respect to the electric field, produces a drift of orbit centres counter to that produced by the electric field. The size of the flutter required to balance the two drifts can be cut down considerably by imposing a radial variation on the flutter. In fact, the flutter field required need not exceed some 1500 gauss. At higher energies, the electric field becomes uniform and the flutter field is no longer required. It is found that if the flutter assumes an inverse square radial variation at this point then it will not produce a drift of

orbit centres. Thus we need not worry about the effects of the second harmonic flutter on the later motion of the beam if this inverse square radial variation is finally imposed.

Computations verify that the insertion of the flutter field does indeed cut down the drift produced by the electric field. A flutter field increasing linearly with radius and rising to 850 gauss at 5 cm radius was found to cut down the drift of orbit centres by over fifty percent. Further computations using larger flutter fields were not possible owing to shortage of time but the results indicate that the drift will be cut down completely if the flutter rises to about 1500 gauss at 5 cm radius.

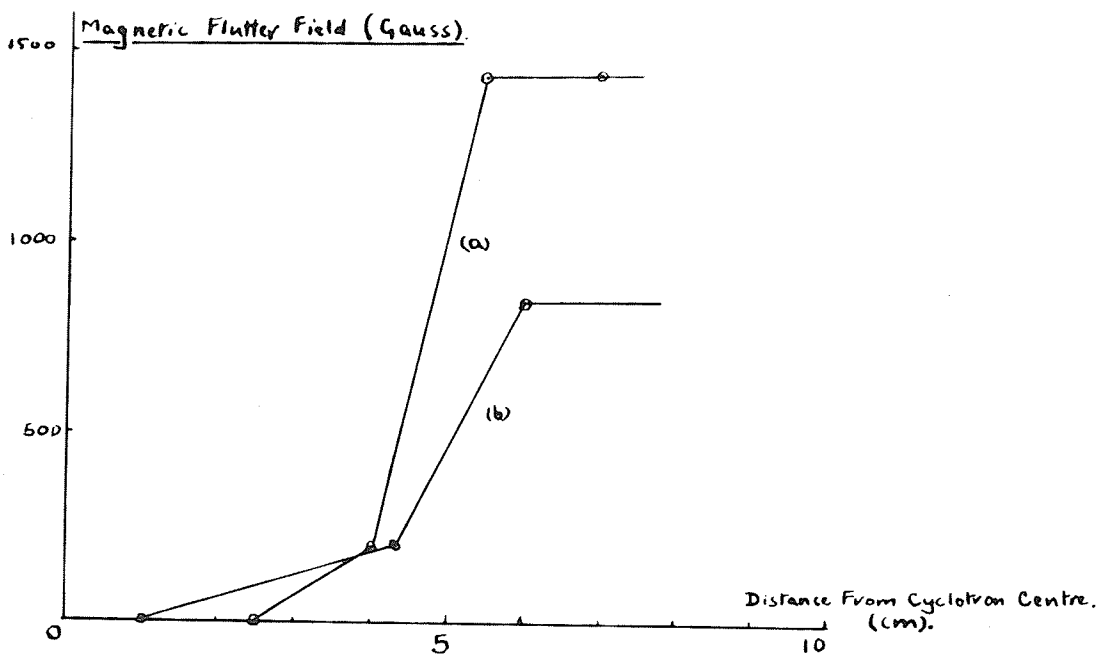
The second part of this investigation concerned the vertical or axial motion of the ion beam during its early revolutions. It has been found that the non-uniform electric field produces slightly less axial focussing than does the uniform electric field in a conventional cyclotron. However, the conclusions arrived at by Rose, Cohen and Wilson for the case of a conventional cyclotron need not be modified radically for the Manitoba machine. As before, the axial focussing is still a small effect, decreasing with energy and the field variation focussing still contributes the greatest part. The field variation focussing does now depend to some extent on the dee geometry but this is a small effect. At higher energies, the dee gap becomes very wide and the only appreciable electric fields

seen by the ion are near the edges of the dees. The ion travels for most of its time in a virtually field free region. The electric field in the dee gap, which hitherto had acted as an electric lens, now acts as two electric lenses, one focussing and one defocussing. The net deviation of the ion's path as it passes through the two lenses is a lot smaller than for a conventional cyclotron. However, taking into account the fact that the ion is also less readily accelerated as it crosses the dee gap, it is found that the amount of axial focussing for a given radial increase in orbit radius remains the same. Also, an extra focussing effect comes into play due to the lenses being separated.

Finally, the theory developed earlier for drift of orbit centres in a non-uniform electric field, was applied to the case of an electric field at a grid inserted in the dee of a cyclotron. It was found that the extra axial focussing obtained by inserting grids was obtained at the expense of the radial stability of the ion beam. As the ion beam passed through the grid slits, a drift of orbit centres occurred. This drift is along one direction only, and cannot be compensated for by using a flutter field, for example. At the point in the dee where the grid ends, there is another non-uniform electric field. Drift of orbit centres occurs here as well. This can be mitigated to some extent by making the transition from grid to no-grid less sharp. This is done in practice by increasing the spacing of the grid wires and letting them recede into the dee.

Since the drift in this transition region is symmetric, i.e., occurs along both axes, it can be compensated by a magnetic flutter field. Actually, in the Manitoba cyclotron the non-uniform field in the grid - no-grid transition region would be masked by the general non-uniformity of the field, and would be compensated by the magnetic flutter field. However, the drift at the individual grid slits cannot be compensated.

Graph VIII Simplified Radial Variations of Magnetic Flutter Field



- (a) Radial Variation averaged for the x- and y-drift.
- (b) Radial Variation used in computations.

REFERENCES

1. Thomas, L.H. "The Paths of Ions in the Cyclotron" Phys. Rev. 54: 580. (1938)
2. See for example "Principles of Cyclic Particle Accelerators", Chapter 13, J.J. Livingood (Van Nostrand, 1961).
3. MacKenzie, K.R. "The Dee-in-Valley Radio Frequency System at U.C.L.A." Sector-Focussed Cyclotrons (Sea Island). pp. 143-149 (1959)
4. Rose, M.E. "Focussing and Maximum Energy of Ions in the Cyclotron" Phys. Rev. 53: 392 (1938)
5. Wilson, R.R. "Magnetic and Electrostatic Focussing in the Cyclotron" Phys. Rev. 53: 408 (1938).
6. Cohen, B.L. "The Theory of the Fixed Frequency Cyclotron", Rev. Sci. Instr. 24:589 (1953).
7. Morton and Smith Nucl. Instr. and Methods 4:36 (1959).
8. Blosser, H.G. Bull. Amer. Phys. Soc. II. 3: 180 (1958).
9. Cox, A.J., Kidd, D.E., Powell, W.B., Reece, B.L., and Waterton, P.J. "Operation of a 40-inch Radial Ridge Cyclotron". Nucl. Instr. and Methods 18, 19: 25 (1962).
10. Gill, S. Comb. Phil. Soc. Proc. 47: 96 (1951).
11. Spitzer, L. Physics of Fully-Ionized Gases (Inter-Science Pub. 1962).

GENERAL REFERENCES

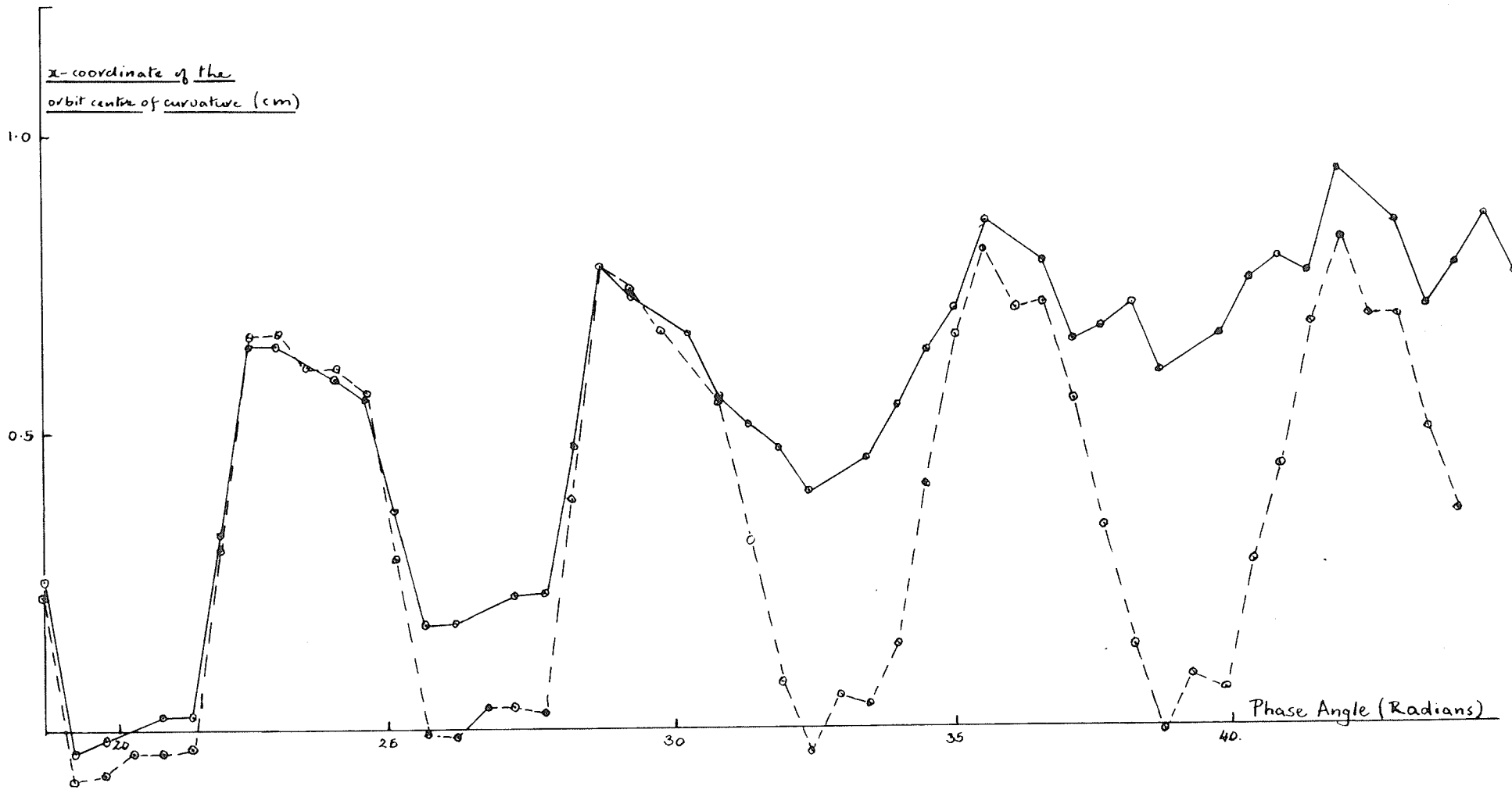
Sector-Focussed Cyclotrons. Proceedings of an Informal Conference, Sea Island, Georgia. F.T. Howard (Ed) (1959).

Principles of Cyclic Particle Accelerators. J.J. Livingood (Van Nostrand, 1961) This book contains an extensive bibliography on most aspects of particle accelerators.

Cyclotrons and Synchrocyclotrons. An article by B. L. Cohen in "Handbuch Der Physik" Volume XLIV (1959).

Physics of Fully-Ionized Gases. L. Spitzer (Inter-Science Pub. 1962)

Sector-Focussed Cyclotrons. Proceedings of an International Conference, Los Angeles, California. Nucl. Instr. and Methods. 18, 19: (1962).



GRAPH IX

Path of the x -coordinate of the centre of curvature of an off-centred orbit.

a) Without flutter field (bold plot). b) With flutter field (dotted plot).

In each case the variation throughout the third, fourth, fifth and sixth revolutions

is shown (the phase angle varies from 20 to 40 radians over these revolutions).